UNIVERSITÀ
DEGLI STUDI
DI PADOVA

Sede Amministrativa: Università degli Studi di Padova

Dipartimento di *Scienze Chimiche*

SCUOLA DI DOTTORATO DI RICERCA IN: Scienze Molecolari
INDIRIZZO: Scienze Chimiche
CICLO XXVII

Engineering of Nanocrystalline TiO_2 surfaces for photovoltaic applications

Direttore della Scuola : Ch.mo Prof. Antonino Polimeno
Coordinatore d'indirizzo: Ch.mo Prof. Antonino Polimeno
Supervisore :Ch.mo Prof. Tommaso Carofiglio

Dottorando : Enrico Frison

Index

Riassunto

La ricerca svolta nel corso della mia Tesi di Dottorato ha riguardato lo studio di una classe di celle solari a colorante organico dette Dye-Sensitized Solar Cells o più comunemente celle di Graetzel, dal nome del loro inventore. A questo scopo ho realizzato un dispositivo costituito da una cella da flusso interfacciata a uno spettrofotometro Uv-vis mediante una fibra ottica. Tale apparato ha permesso di realizzare il chemiadsorbimento di sensibilizzatori su fotoanodi di titania in flusso continuo e, contemporaneamente, di monitorarne la cinetica di adsorbimento. Sono stati presi in considerazione dei sensibilizzatori stato dell'arte, come N3 e N719, e altri sensibilizzatori prodotti nel gruppo di ricerca di riferimento per questa Tesi. Inoltre, è stato possibile studiare l'effetto congiunto di co-adsorbati come acido colico e derivati ciclodestrinici. In particolare, oltre alla βCD, è stato preparato un derivato ciclodestrinico in cui tutti gli ossidrili secondari sono stati metilati, mentre tutte le funzioni alcoliche primarie sono state ossidate ad acido carbossilico. Questi studi hanno dimostrato come il processo di adsorbimento in flusso continuo di un sensibilizzatore, da solo o in presenza di un co-adsorbato, possa essere descritto tramite una cinetica di pseudo-primo ordine. Inoltre, la tecnica in flusso continuo ha permesso controllare perfettamente l'entità del processo di sensibilizzazione realizzando diversi livelli di loading (per esempio 50%, 90%, 100%), ottenendo così delle informazioni molto interessanti sui processi coinvolti nel funzionamento delle celle fotovoltaiche e sull'effetto di co-adsorbati. Le caratterizzazioni dei dispositivi fotovoltaici sono state realizzate sia durante un periodo di otto mesi che ho trascorso presso l'Intelligent Polymer Research Institute (IPRI) dell'università di Wollongong (Australia) nel gruppo del Professor Attila Mozer, sia nell'ambito di un progetto PRIN in collaborazione con il gruppo del Professor Carlo Alberto Bignozzi e del suo collaboratore Stefano Caramori, presso l'Università di Ferrara.

Abstract

The research carried out in the course of my PhD thesis involved the study of a class of solar cells called Dye-Sensitized Solar Cells or more commonly Graetzel cells, named after their inventor. For this purpose, I have realized a device comprising a flow cell which interfaced with a UV-vis spectrophotometer through an optical fiber. This apparatus allowed to realize the chemisorption of sensitizers on photoanodes of titania in continuous flow condition and, simultaneously, to monitor the kinetics of chemisorption. The sensitizers taken into consideration were the state of the art sensitizers, such as N3 and N719, together with other organic molecules produced in the research group I belong. In addition, it was possible to study the combined effect of co-adsorbates such as cholic acid and cyclodextrin derivatives. In particular, in addition to the commercially available βCD, I prepared a ciclodextrin derivative in which all the secondary hydroxyls were methylated, while all the primary alcohol functions have been oxidized to a carboxylic acid. These studies have shown that the adsorption of a sensitizer (alone or in the presence of a co-adsorbate) under continuous flow conditions, can be described by a pseudo-first order kinetics. Furthermore, this technique allowed to fully control the extent of the sensitization process realizing different levels of loading (for example, 50%, 90%, 100%), so obtaining very interesting informations on the processes involved in the operation of photovoltaic cells and on the effect of co-adsorbates. The characterization of photovoltaic devices were carried out both during a period of eight months I spent at the Intelligent Polymer Research Institute (IPRI) - University of Wollongong (Australia) in the group of Professor Attila Mozer, and in the framework of a PRIN project in collaboration with the group of Professor Carlo Alberto Bignozzi and his coworker Stefano Caramori, at the University of Ferrara. The characteristics of photovoltaic cells sensitized with two different dyes (TFAT and ZnTMCP) were acquired varying the functionalization time of the photoanodes with cyclodextrins. No substantial improvement in performance was found, this may be due to the reduced amount of dye bonded on TiO_2, resulting in a smaller amount of charge-carriers in the semiconductor.

General aim of the thesis

Dye-Sensitized Solar Cells are intriguing devices made with intrinsically simple and widely available materials such as TiO_2, glass, Iodine, etc.. Nevertheless, DSSCs must not be mistakenly viewed as simple devices. Also, if their working principles have been studied in great detail, there are still many aspects affecting their performances, which are currently under debate. This happens also because a general rationalization of some behaviours of solar cells have not been definitively realized. For example, the sensitizer structure/efficiency relationship has to be rationalized to help the optimization of the dye. In addition, other parameters like the dye loading, the sensitization time, the use of co-asdorbates, and so on greatly affects the cell performance. In few words, building a DSSC is a challenging art.

In order to increase the knowledge on these devices, it is essential to concentrate on one step at the time. During this Thesis, I decide to focus on a keypoint in DSSC science: the interface between TiO_2/Dye/Electrolyte, namely the place where charge separation happens. In particular, I decided to study how controlled modifications of the interface between the Titanium dioxide and the electrolyte could influence the photovoltaic efficiency of a DSSC.

I used two different approaches. One of them was based on the monitoring and actively controlling the TiO_2 sensitization process, both with a dye alone or in presence of co-adsorbates. For this purpose, I decided to apply a flow technique coupled to a UV-vis spectrophotometer which allowed to quantify in real-time the dye uptake and to control its level in a reproducible way. The second approach, more chemical in nature, was based on the functionalization of TiO_2 photoanodes using cyclodextrins, which played both the role of dye-receptors and isolating layer to retard charge recombination phenomena.

1. Introduction to Dye-Sensitized Solar Cells

1.1 General overview on energy consumption and trend

Since the beginning of the human history, one of the most important contributions that made the difference in the evolution was the ability to use energy. Nowadays we are living in a world which requires always increasing amounts of energy for the daily life, let us think to computers, smartphones, tablets, or to our houses full of lights, televisions and electrical appliances.

As stated in the BP Statistical Review of World Energy for the year 2013, the "Primary Energy" consumption has increased by 2.3% (Figure 1).

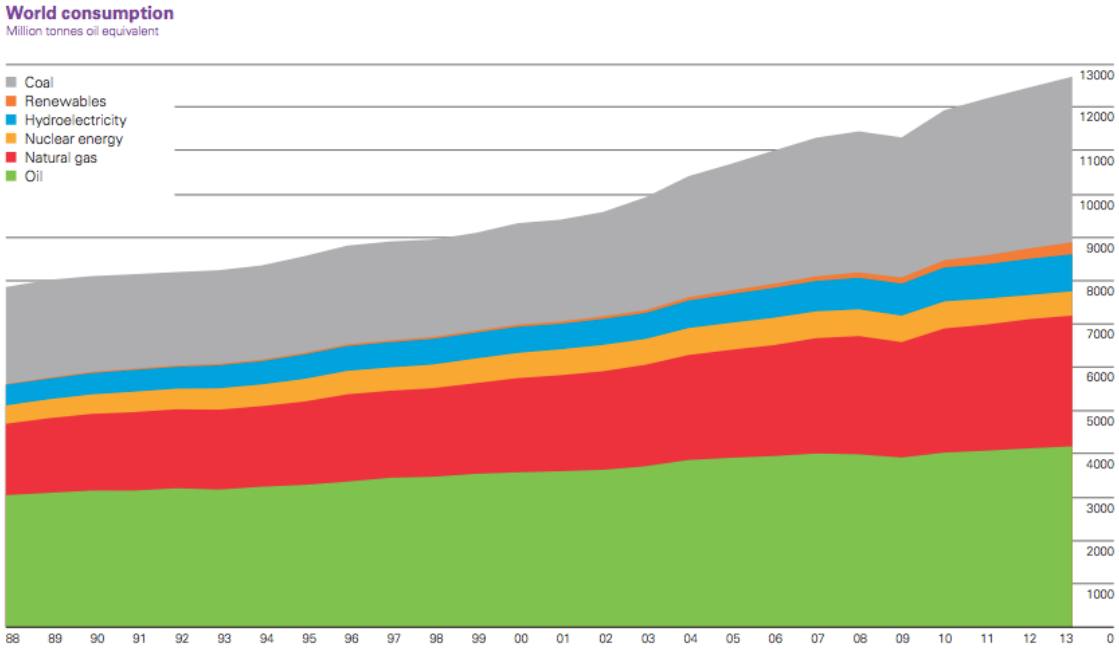

Figure 1: world energy consumption divided by energy source (Ref.1).

Energy is coming mostly from fossil fuels, such as petrol (32.9%) with a daily consumption of 1.4 million barrels, and coal, then a very large amount is extracted from natural gas. Only 2.7% of global energy consumption is obtained from renewable energy sources[1].

Most of the energy sources used until now are not renewables, this mean that their rate of consumption is higher than the rate of regeneration, and their costs increase accordingly to the efforts needed in order to find new reservoirs. Since this is clearly a process that cannot last forever, the interest in renewable energies is growing. Among

renewable energy sources we find wind power and solar power and the former is the one which showed the fastest growth in the last decade. The main technology for the conversion of solar light into electricity is based on extremely purified silicon which is then properly doped in order to modulate the charge carrier density, a highly expensive process which is one of the most important problems with the actual production techniques. In the solar industry, the prices are monitored using the so-called "Price per Watt" calculated by dividing the total cost for the installation of the solar modules for the Watt peak value that the system can produce. The trend in the last decade is that costs are decreasing although they can vary depending on the location. As an example, in 2013 the average price of solar energy for residential use in the U.S. was about $4.69/W while in Germany it was $2.05/W[2]. A wide and extensive research is going on at both and industrial and academic level, and in the last twenty years breakthrough discoveries have been achieved. One of these discoveries, which is strictly related to this thesis are the "Dye-Sensitized Solar Cells", invented by Graetzel and O'Regan in the 1991. They found that electricity can be produced with a solar cell having a completely different structure compared to the classic ones, using cheap and widely available materials, thus paving the way of a new photovoltaic not based on Silicon[3].

1.2 Dye sensitized solar cells

Dye sensitized solar cells (DSSC) also named Graetzel solar cells from the name of their inventor in the 1991 (EPFL Lausanne) represent a potentially cheaper alternative to Silicon solar cell[3]. In the latter, the absorption of the light and charge separation take places in the same phase, whereas in Graetzel cells, those phenomena happen separately. Solar radiation is harvested by a sensitizer based on Ruthenium which is anchored on the TiO_2 surface, while charge separation happens at the interface between the dye and the TiO_2 nanoparticle. In the first attempts, a thin and compact layer of titanium oxide was covered with a monolayer of sensitizer, but the light harvesting was not sufficient to obtain good electron collection, the amount of dye being very low. Nevertheless, the feasibility of the concept was demonstrated. In order to increase the amount of chemisorbed dye, the compact layer of titanium oxide was replaced with a few μm thick mesoporous layer of nanocrystalline TiO_2, thus obtaining porous electrodes with increased active surface area capable to bind large amounts of sensitizer.

1.2.1 Working principles

In general a dye-sensitized solar cell device is composed by:

- **Working electrode**: it is also called photoanodes and it is made of a mesoporous layer of nanocrystalline TiO_2 deposited onto a conductive substrate which is usually fluorine doped tin oxide (FTO).
- **Counterelectrode**: Counter electrode: it is a FTO glass covered by a thin and transparent layer of platinum catalyst;
- **Sensitizer**: : it is the dye is adsorbed onto the surface of the titanium dioxide through the entire thickness of the mesoporous layer;
- **Redox mediator**:it is an electrolyte solution, most of the time it is the redox couple I-/I3-..

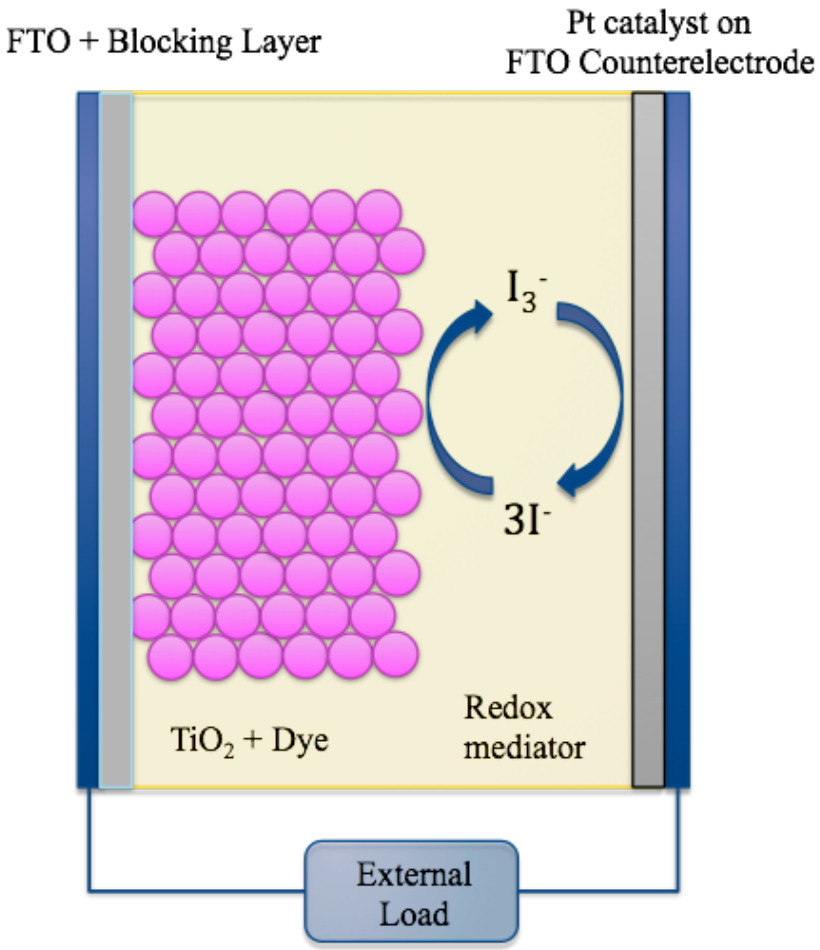

Figure 2: schematic representation of a DSSC components.

The heart of a DSSC is the photoanode made of a wide bandgap semiconductor of mesoporous titanium oxide. This layer is built starting from nanoparticles of about 20 nm diameter which are sintered at high temperature thus creating a network of interparticle connections which facilitates the diffusion of the electrons through the semiconductor. Besides TiO_2, the oxide most widely used in the allotropic form of Anatase, other oxides such as ZnO[4] and SnO[5] are actively studied.

A monolayer of sensitizer, anchored on the surface of the semiconductor by chemoadsorption, is photoexcited by the solar radiation, producing an excited species which injects an electron into the conduction band of the titanium dioxide (CB_{TiO2}) leaving the dye in its oxidized form. The injected electrons diffuse into the mesoporous layer reaching the FTO surface where they are collected and used by the external load performing the electrical work and finally reaching the counter electrode (Figure 2). The oxidized dye is then reduced to its initial state by the the electrolyte. The electrolyte is generally composed by an organic solvent in which a redox couple is dissolved, mainly

the I^-/I_3^- couple. The oxidized redox species I_3^- diffuse in the electrolyte reaching the cathode where it is reduced by the incoming electrons, thus closing the cycle. By this way, the DSSC produces electricity without varying its internal composition.

More in detail, the working principles can be summarized as follow:

Absorption of 1 electron by the sensitizer anchored on the TiO_2 and excitation of the dye;

$$S + h\nu \text{ --> } S^*$$

electron injection from the excited state of the sensitizer into the conduction band of the titanium dioxide, which leaves the dye in its oxidized state S+;

$$S^* \text{ --> } S^+ + e^-(TiO_2)$$

Injected electrons diffuse into the mesoporous semicondutor toward the FTO surface of the photoelectrode (PE) from which they are extracted performing the electrical work in the external circuit;

$$e^-(TiO_2) \text{ --> } e^-(PE)$$

the oxidized dye S+ is reduced back to its fundamental state by the Iodide present in the electrolyte, which is then oxidized to tri-iodide;

$$2S^+ + 3I^-(PE) \text{ --> } 2S + I_3^-(PE)$$

the tri-iodide I_3^- generated at the photoelectrode, diffuses toward the counter electrode where it is reduced by the electrons coming from the external load, so that the I^- is regenerated. This reaction needs to be fast, and this is why the counter electrode is covered by a thin layer of Platinum which catalyzes the reaction:

$$I_3^-(CE) + 2e^-(CE) \text{ --> } 3I^-(CE)$$

One of the most important problems that limitate the efficiency of a DSSC is the so-called recombination phenomena. One of them is when the redox mediator does not quickly reduce the oxidized dye S^+, so a recombination between the electrons injected into the TiO_2 and the S^+ dye occurs without the generation of electricity:

$$S^+ + e^-(TiO_2) \rightarrow S$$

Another recombination pathway which strongly impact on the efficiencies of DSSCs is the recombination between the injected electrons at the TiO_2 and the electrolyte that is favoured by a partial dye coverage of the surface of the semiconductor:

$$2e^-(TiO_2) + I_3^- \rightarrow 3I^-$$

This latter phenomenon causes also a depletion of the electrons present into the semiconductor which will not contribute to the generation of electric current.

Once injected, the electron can follow various kinetic paths each one characterised by its own kinetic constant. In order to obtain an effective DSSC, it is necessary that all the reactions that contribute to the current generation have a higher kinetic constant than the reactions involved in recombination parasite processes. For example, in the case of N3 dye, one of the most used and efficient ruthenium dyes, the electron injection into the conduction band of TiO_2 is an extremely fast reaction (Figure 3), that takes places in the order of picoseconds ($50*10^{-12}$ - $1.7*10^{-12}$ s), while the recombination rate between an electron in the semiconductor and the oxidized dye happens in the order of microseconds (10^{-6} s), hence one million times slower[6].

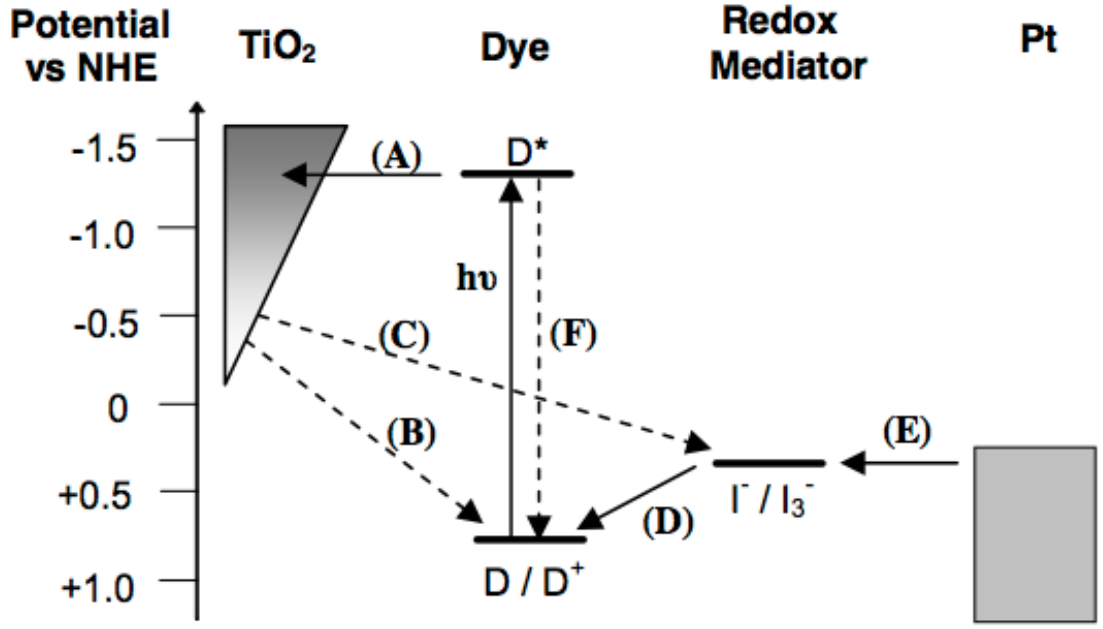

Figure 3: scheme representing the rates of the principal processes present in a dye sensitized solar cell. (J. Phys. Chem. C, 2011, 115).

1.2.2 Working electrode (Photoanode)

Generally it is made of a nanocrystalline semiconductor layer deposited onto a substrate of conductive glass which must have a low electrical resistance. For this reason, FTO is a better choice with respect to Indium Tin Oxide (ITO), because the conducibility of the latter decreases after the thermal treatments that are needed for the sinterisation of the oxide nanoparticles. Titanium dioxide is the most used semiconductor because it is widely available (it is found as a pigment in varnish, in plastic materials, in cements, etc.) it is cheap, non tossic and it has a bandgap of 3.2 eV. As a result of this, it does not absorb the visible light and appears white. Other oxides have been tested as substitute of TiO_2, such as SiO_2, ZnO, and Nb_2O. In order to deposit mesoporous layer of titanium dioxide, an aqueous paste containing TiO_2 nanoparticle with diameter of 20 nm or less, together with some additives, such as ethyl cellulose, promoting the formation of a transparent layer, is deposited on FTO using techniques such as *screen printing* or *doctor blading*. In the screen printing technique a frame of tissue with a well defined mesh is customized in order to obtain a printable area of the desired shape. The frame is then placed over the FTO substrate and an apposite TiO_2 paste is deposited on the edge of the tissue and to this point the paste is spread on the tissue keeping a constant pressure using a spatula. On the other hand, n doctor blading technique, the Titanium dioxide paste is spread by a blade that slides over a spacer, creating a uniform TiO_2 layer. Both techniques are already widely used both in laboratory and at industrial level (Dyesol, Solaronix).

An important step during the preparation of a photoanode is the sintering process at 450°C. This treatment, in addition to eliminate all additives and contaminants eventually present in the Titania paste, creates a series of electrical interconnections between the TiO_2 nanoparticles. The electron transport within the structure of the layer of Titania takes place by diffusion and it is related to the presence of sub-bandgap trap levels just below its conduction band.

There are a plethora of additional treatments that can be done on the photoanode in order to enhance DSSC efficiency, such as the deposition of a “blocking layer” before screen printing the TiO_2 paste, or a post-treatment with $TiCl_4$ followed by further sinterization for increasing the roughness factor and the total surface area, leading to a higher sensitizer loadings[7].

1.2.3 Counterelectrode (Cathode)

As in the case of the photoanode, the support for the counter electrode is a conducting FTO glass plate covered with a thin layer of platinum that acts as a catalyst for the reduction of the tri-iodide to iodide. The platinum layer can be deposited using a suitable precursor which has been formulated as a colloidal paste so it is possible to use the screen printing and the doctor blade technique already described in the case of the photoanode. Also in the case of the counter electrode, a thermal post-deposition treatment is required.

1.2.4 Electrolyte (Redox mediator)

The electrolyte is usually composed of an organic solvent (Acetonitrile, Valeronitrile, etc.) containing a redox couple. The most used is the redox couple I^-/I_3^- which, migrating by diffusion between the two electrodes, has the task of restoring the fundamental state of the sensitizer. The tri-iodide formed is, in turn, reduced to the counter electrode. The reason why the redox couple iodide/tri-iodide is the most commonly used is the value of its redox potential which is optimal for the regeneration of the dye.

The redox couple, in particular, must respond to some important characteristics for its optimal action:

1. Its redox potential must be correctly positioned with respect to that of the sensitizer;
2. it must be soluble in the solvent and posses a good diffusion coefficient;
3. it must not absorb the light radiation in the spectral region in which the dye operates;
4. it must be stable and chemically inert with respect to the other components of the DSSC.

The most common electrolyte contains iodine, iodides and different additives dissolved in organic solvents (*e.g.* acetonitrile). The most performant electrolytes contain also other additive, in the form of salts, such as Lithium (Li^+), tetrabutylammonium (TBA^+), or organic ions such as the imidazole (Im^+). These additives affect both the energy levels of the Titania and the conductivity of the solution. Other additives widely used

are the 4-*tert*-butylpyridine (TBP) and the guanidine thiocyanate (GuSCN). The addition of TBP produces an increase in the open circuit potential as a consequence of a displacement of the conduction band potential toward higher energies as well as an increasing of the electron lifetime. This effect was attributed to the coordination of the additive on the surface of the Titania that acts as a sealer of some of the possible recombination sites. Also, it seems that the TBP plays a role in decreasing the dissociation of the groups SCN- from the dye, protecting it from degradation.

Graetzel reported that the GuSCN could shield the repulsive effect between the various N3 molecules, improving the deposition of a more compact monolayer which turns out to be beneficial for an increase of the photovoltage.

In the last few years research has focused on the development of iodine free electrolyte in order to increase the lifetime of the devices. In this respect, Co(II/III)tris(bipyridyl) based redox electrolyte has proven to be a good candidate to the replacement of iodine as redox mediator[8]. In particular, it gives good results with porphyrin dyes[9] while, for Ruthenium based sensitizers, iodine still seems to be a must for optimal performances.

1.2.5 Sensitizers

A dye, to be a good sensitizer in a DSSC, must possess various requirements:

1. it must adsorb on a wide range of wavelenghts;
2. the energy level of the excited state must lay at higher energies than the conduction band of TiO_2 and the fundamental state must lay at lower energies compared to the potential of the redox couple of electron mediator;
3. electron injection must be fast in order to make negligible the recombination reactions;
4. It must also posses some functional groups that make possible the chemisorption on Titanium dioxide (usually -COOH), to have a good chemical and photochemical stability and a fairly good solubility in a solvent convenient for the sensitization process.

Up to now, some of the best results have been obtained with Ruthenium based dyes, especially the so-called N3 and N719. Their chemical structure and the correspondent absorption spectra are reported in Figure 4:

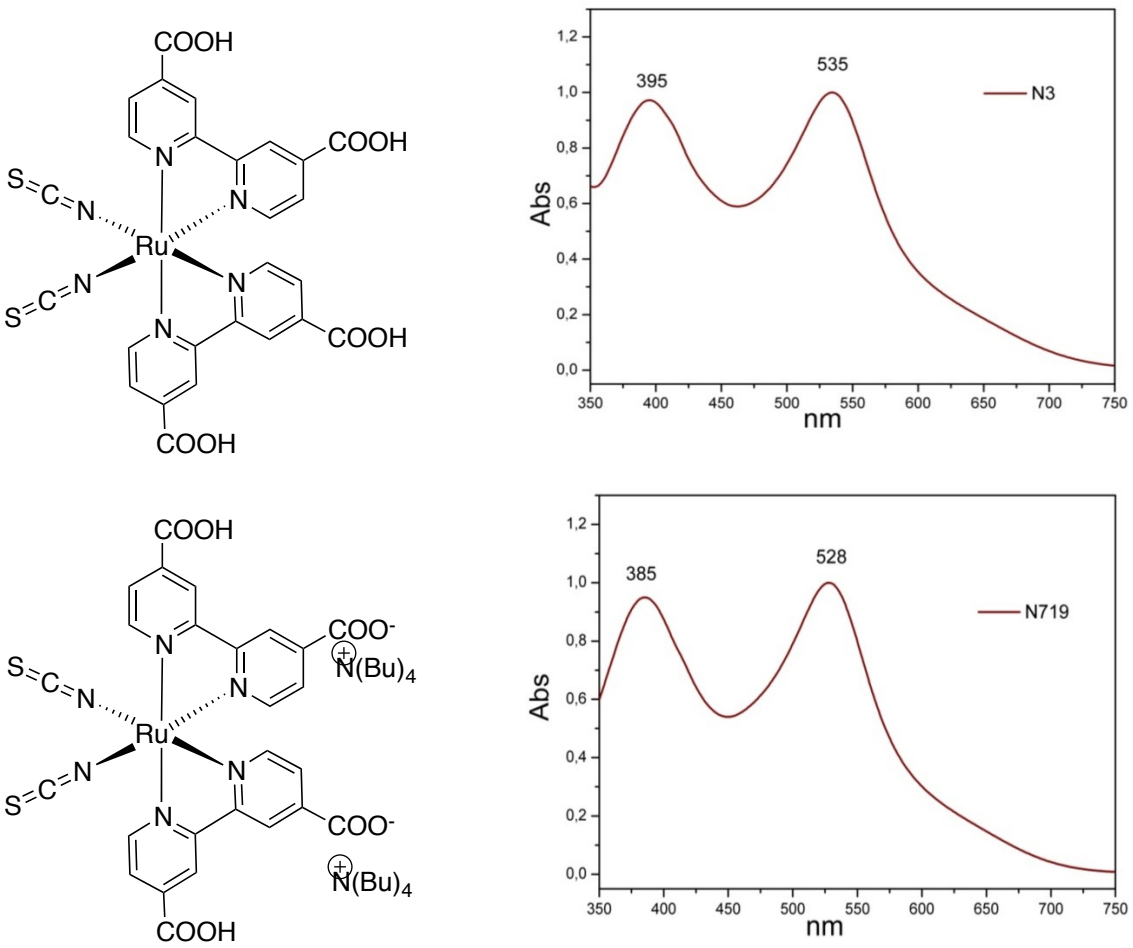

Figure 4: structure and absorption spectra in EtOH of N3 (on the top) and of N719 (on the bottom).

The excitation of the Ruthenium complex results in a transfer of charge from the metal to the ligand. In particular, the HOMO of the complex is localized primarily in the vicinity of central atom, while the LUMO is located toward the ligands directly linked to the Titanium dioxide, partially overlapping with the conduction band of the TiO^2. This arrangement of the orbitals offers a reasonable explanation of the speed with which the electrons are injected, usually in the picosecond range (10^{-12} s) and is also called "*Ultra-fast injection*". A correct matching of a series of processes with different kinetic rates is essential for a good performance of the device.

One of the main disadvantages of the Graetzel cells that may hamper its marketing is the use of ruthenium, which is a relatively rare and expensive metal.

Therefore, there is a constant research toward alternative sensitizers which do not involve the use of rare metals. Among the most studied "metal-free" organic dyes we found porphyrins bearing different subsituents[10], which adsorb onto the Titanium dioxide with the same mechanism of the ruthenium complexes.

An advantage of this class of compounds is the high molar absorption coefficient, associated with generally narrow absorption bands. In the last few years, the efficiencies recorded for these class of compounds have noteworthy increased. The best score has been reported in 2011 by Yella who obtained an efficiency of 12% using a co-sensitized DSSC containing both a porphyrin (YD2-o-C8) and a squarain (C123)[9].

1.2.6 Methods for decreasing recombination processes

In an assembled DSSC there are several recombination paths and various strategies have been developed in order to minimize them. These strategies are mainly based on photoanodes treatments, optimization of the sensitizer structure, and the use of co-adsorbates.

The surface of the FTO anode, where the mesoporous layer is deposited, is in direct contact with the electrolyte thus short-circuiting the cell since the collected electrons recombine with I_3^- prior of being extracted and performing the electrical work. In order to reduce this recombination pathway, a blocking layer[11] of compact TiO_2 (few nm thick) is applied on the FTO surface (prior the TiO_2 mesoporous layer deposition) so the photoanode is isolated from the redox mediator oxidized species. A similar approach is applied to the mesoporous layer prior to sensitization, when a thin layer of TiO_2 is applied by immersion of the photoanodes in a Titanium tetrachloride ($TiCl_4$) solution followed by sinterization. Also this treatment aims to block some active recombination sites, decreasing the rate of the back-reaction between injected electrons and the electrolyte, allowing for an increased electron lifetimes of the injected electrons.

A good dye, not only has to inject efficiently electrons into TiO_2, but, especially with organic dyes, it is generally subject to proper structure modifications that lower the recombination rates. Porphyrin dyes showed that they may increase recombination rates at the interface between TiO_2 and redox mediator[12] and the effect of the substituents on the macrocycle's periphery has been extensively studied. I report here a recent example

in this field, where, an efficiency improvement was obtained by substituents optimization on a (donor - π - acceptor) porphyrin called YD2 (Figure 5). In particular, meso substituents were modified by the introduction of alkyloxy side chains obtaining the porphyrin YD-2-o-C8 that, in a co-sensitized DSSC, produced an efficiency of 12.3%[9]. This improvement was attributed to the increased blocking ability of the alkyl chains which improve the blocking effect of the dye itself.

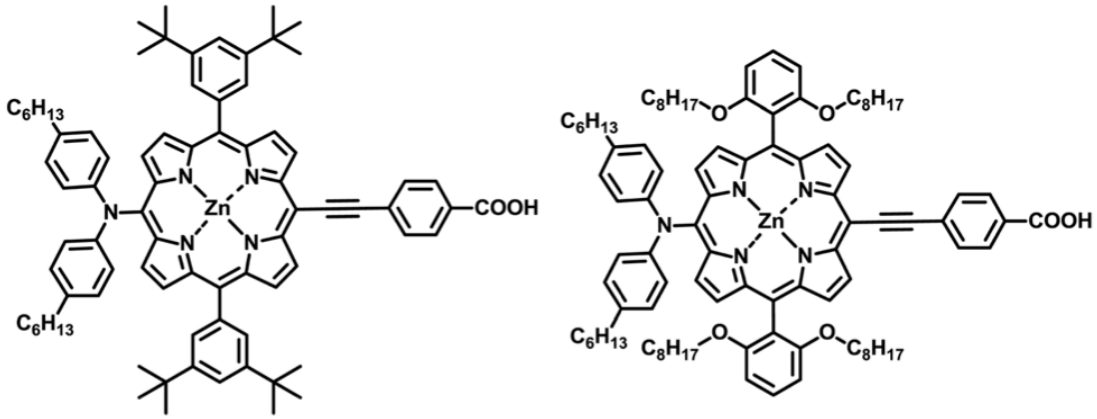

Figure 5: structure of YD-2 (left) and optimized porphyrin YD-2-o-C8 bearing alkyloxi chains on the meso substituents.

The use of additives which co-adsorb onto the Titanium dioxide together with the dye have shown to improve photovoltaic characteristic of the cell. As an example, Cholic Acid (CA), Deoxycholic Acid (DCA) and Chenodeoxycholic Acid (CDCA) are among the most commonly used co-adsorbates[13]. Also other kind of molecules such as phosphinic acid have been used with success in porphyrin sensitized solar cells[14].

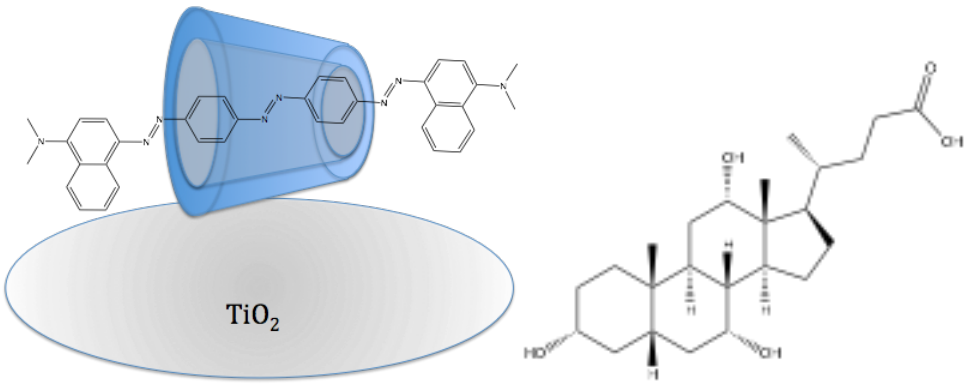

Figure 6: example of dye encapsulated in a cyclodextrin immobilized onto a TiO_2 nanoparticle (left) and structure of Cholic Acid (right) additive for the suppression of aggregation of organic dyes on the TiO_2.

These additives are mostly used with organic sensitizers with the aim of reducing their tendency to aggregate on the TiO_2 surface, a phenomenon that increases the chance of

dye recombination due to rapid self-quenching process. Other methods to reduce recombination have been reported by Ko and Graetzel (cfr. Chapter 4) based on the use of β-cyclodextrin aimed to encapsulate the organic dye thus reducing aggregation and retarding back electron transfer thanks to the blocking ability of the cyclodextrin (Figure 6).

2. Characterization techniques

2.1 Photovoltaic characterization

2.1.1 The solar spectrum

Sun represents the source that provides the light radiation and therefore the energy at the base of any photovoltaic technology. The conversion efficiency is measured on standard irradiation conditions, calculated on the basis of the average amount of this energy that strikes our planet, after path 150.000.000 km (1 astronomical unit), after crossing the atmosphere, which acts as a "filter", protecting us from the most harmful wavelengths.

The solar constant corresponds to the density of energy, radiated from the sun, that reaches a surface of 1 m^2 perpendicular to it, just outside from the atmosphere, and is equal to 1367 $W*m^{-2}$. The energy carried per unit of surface area will gradually decrease as the light radiation passes through the various layers of the atmosphere, with values that can vary between 1000 and approximately 300 $W*m^{-2}$.

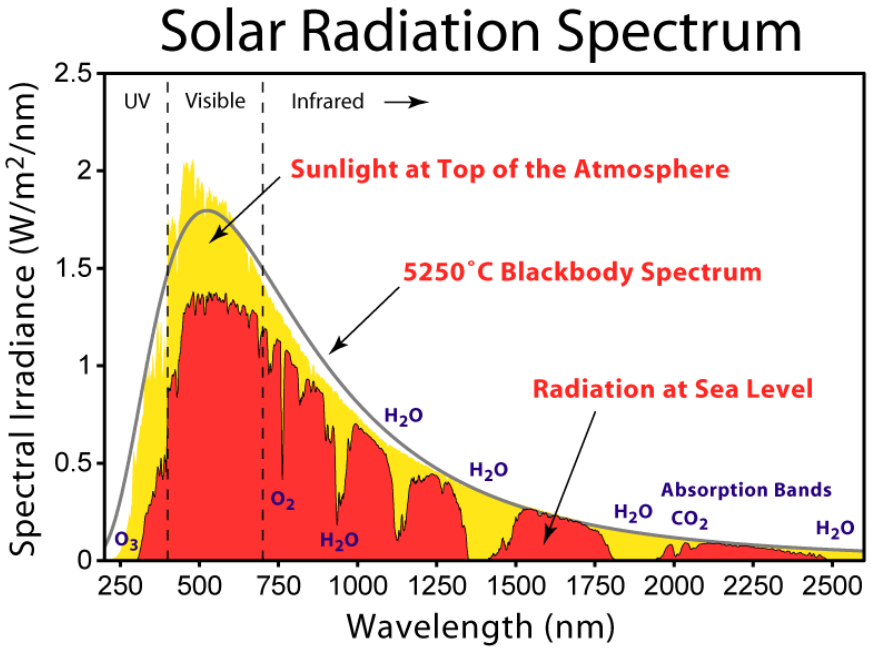

Figure 7: solar radiation spectrum. (yellow: AM0; red: AM1.5G)

Some of the incoming energy is dissipated when it crosses the atmosphere. The radiation may be scattered by clouds, water, soil, and by anything that can reflect the light. Moreover, several components such as O_2, O_3, CH_4, H_2O and CO_2 absorb some

specific wavelengths in the UV and in the infrared region. As a result of all these phenomena, the amount of energy that reaches the ground is much smaller. (Figure 7).

To quantify the intensity of the radiation as a function of the position of the sun, which relates to the thickness of atmosphere that light has to go through, it is universally used the concept of Air Mass which is the ratio between the length of the actual path of the sun's rays AM= 1/Cos Φ, where Φ is the Zenith angle (figure 8). Thus, for example, Air Mass 0 (AM 0) corresponds to the density of solar radiation over the atmosphere (1367 $W*m^{-2}$). On the other hand, Air Mass 1 (AM 1) is the density of solar radiation on terrestrial ground at noon, on a day perfectly serene with the sun at the Zenith (1000 $W*m^{-2}$). Finally, Air Mass 1.5 (AM 1.5G) corresponds to the standard conditions of the photovoltaic test for the comparison purposes between different solar cells. (T = 25 °C, radiation density of 1000 $W*m^{-2}$ and spectral distribution obtained by setting the Zenith angle Φ equal to the average inclination of the sun during the year at middle latitudes, which correspond to Φ = 48° and an elevation of 42° over the horizon).

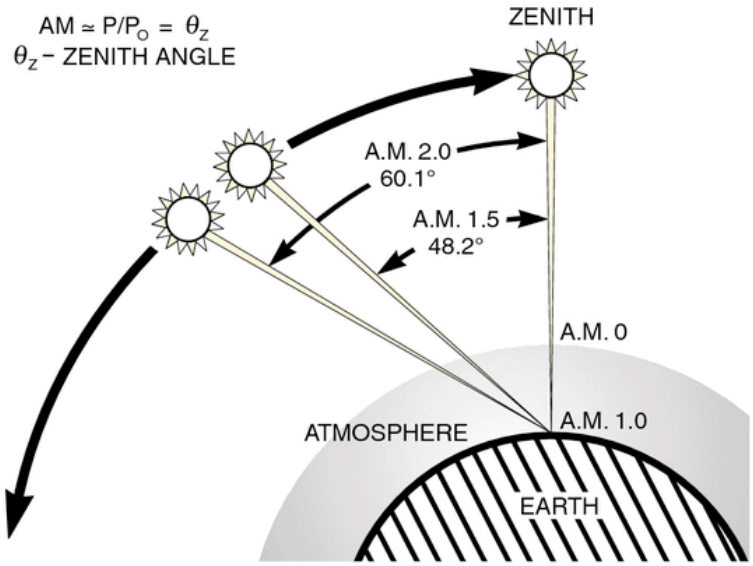

Figure 8: representation of the Zenith angle relationship with Air Mass definition.

2.1.2 Current-Voltage characterization of a solar cell

This kind of measurement is said to be in steady-state, meaning that the device has the time to equilibrate the amount of charges photogenerated with charges that recombine, so the charge density does not change resulting in a steady state condition.

The characterization of a solar cell is performed under standard irradiation conditions of 100 mW*cm^{-2} and a spectral distribution corresponding to AM1.5G conditions.

The following equation represents the mathematical equation that describes a diode which correspond to an equivalent circuit (Figure 9) of a solar cell:

$$I = I_{ph} - I_s(e^{(V+IR_s)/mV_T} - 1) - (V + IR_s)/R_{sh}$$

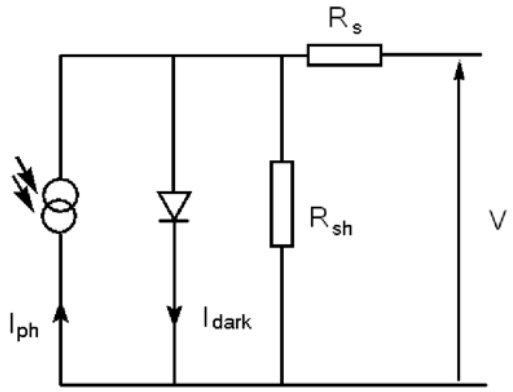

Figure 9: equivalent circuit of a solar cell.

I_{ph} is the photogenerated current when the cell is under light irradiation.

The second term represents the dark current, I_{dark}, which is measured without irradiating the cell, so I_{ph} becomes zero and dark current equals the shunt current (I_{shunt}), while I_s is the saturation current of the diode.

$$I_{dark} = I_s(e^{qV/K_BT} - 1)$$

The third term, on the right side of the equation, is the shunt resistance, I_{shunt}, and it represents the charge recombination.

$$I_{shunt} = (V + IR_s)/R_{sh}$$

R_s is the series resistance, *m* is the ideality factor, R_{shunt} is the shunt resistance associated with the correspondent shunt current.

In a ideal solar cell, R_s should be very low (ideally zero) and R_{shunt} should be very high (ideally infinite) meaning that there is no recombination and there is no dissipation of collected electrons.

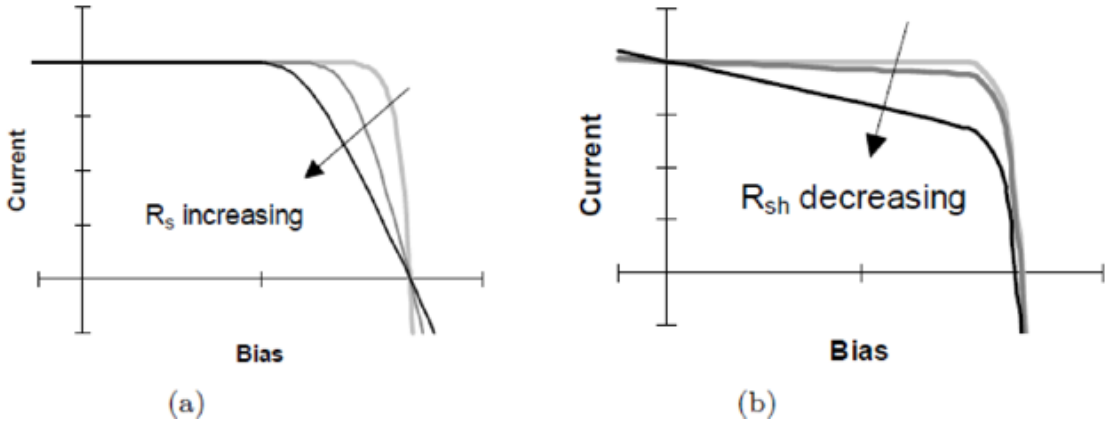

Figure 10: graphical representation of the effects of R_s and R_{shunt} on a current-voltage measurement.

In the figure 11 below is reported the output of a J-V measurements of a solar cell:

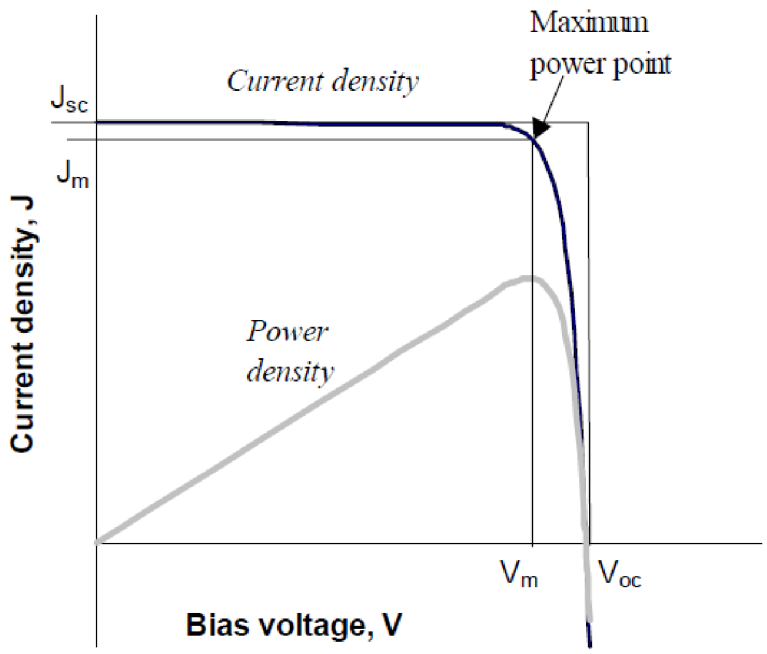

Figure 11: example of J-V output from current-voltage characterization of a solar cell. The principal values as V_{oc} and I_{sc} are reported in the picture. V_m and J_m are the voltage and current density at the maximum power point.

Fill Factor (FF) is an important parameter, correlated with the ideality of the solar cell. Practically, the more is the "squareness" and the more close to ideal is the device. The FF is calculated as:

$$FF = \frac{V_m I_m}{V_{OC} I_{SC}}$$

Finally, the efficiency of the cell is calculate using the following equation:

$$\eta = \frac{P_{\max}}{P_0} = \frac{I_m V_m}{P_0} = \frac{I_{sc} V_{oc} FF}{P_0}$$

2.1.3 Incident photon to current efficiency (IPCE)

The incident photon to current efficiency (IPCE) corresponds the so called external quantum efficiency (EQE) and it requires to be calculated the measurement of the photocurrent generation in relation to the incident light intensity at the given wavelength of irradiation (Figure 12). IPCE value is the result of the contribution of three processes such as light harvesting (LHE), electron injection and electron collection..

$$IPCE = LHE(\lambda) * \varphi_{inj} * \eta_{coll}$$

The light harvesting contribution can be determined with UV-Vis spectroscopy by measuring the absorbance of the sensitized photoanode wetted with the same solvent used in complete DSSC device. On the other hand, the injection efficiency can be measured using ultra-fast absorption spectroscopy or indirectly derived from the optical data and the IPCE spectra[14]. Collection efficiency can be described using a standard diffusion model which takes into account electron generation, transport and recombination and it tells the probability that an injected electron reaches the substrates and it is then used for the electrical work.

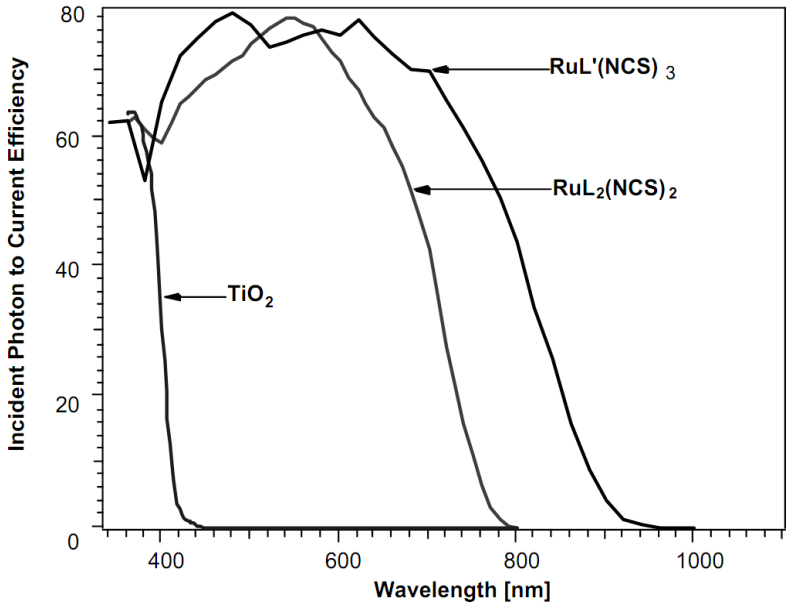

Figure 12: example of IPCE spectra for N3 and Black dye onto a TiO_2 mesoporous layer.

2.1.4 Electrochemical impedance spectroscopy

Electrochemical impedance spectroscopy is a widely used technique for studying surfaces related processes, *e.g.* corrosion, coatings, chemical reactions.

It measure the modulated current response of a system when a small AC sinusoidal modulation is superimposed to an applied DC voltage. During the measurement, a frequency scan (usually in the mHz to MHz range) of the AC component is performed ($f=\omega/2\pi$) and the current response is collected versus the frequency giving the impedance spectrum:

$$Z_{\mathrm{CELL}}(\omega) = \frac{V_{\mathrm{CELL,AC}}(\omega, t)}{i_{\mathrm{CELL,AC}}(\omega, t)}$$

This equation can be seen as the Ohm's law (R=V/I) and it describe the variation of a resistance with the frequency, which is actually what an electrochemical impedance measurement does.

These measurements give useful insights on the frequency range of some of the processes involved in the device operation. In order to simplify the mathematical background which is required for a comprehensive study and adjustment of the theoretical model to different experimental conditions, an equivalent circuit can be used

in order to describe the physical processes which are taking place in the cell. Typical components are resistors (R), capacitors (C), inductors (L) which can be combined in a number of different equivalent circuits showing the same frequency response as the cell. As an example, a charge transfer through a surface can be modelled as a parallel combination of a resistor and capacitor. The real challenge is to find the equivalent circuit that best matches the processes in the cells and fitting the measured data with it.

Since not all the components are frequency dependant, this allows to easily extrapolate some data simply looking at the graphic. A pure resistor, for example, has a value that does not change with the frequency, and this is why the Nyquist plot in Figure 13 below does not begin in the origin of the axis, but it is shifted of an R_s value. When frequency dependent elements come into play, the typical semicircles appear and from their real part (Z') and frequency of the maximum point, some data such as electron lifetime (which is related to recombination with the electrolyte), electron density in the TiO_2 and charge transfer resistance (Rct) can be determined.

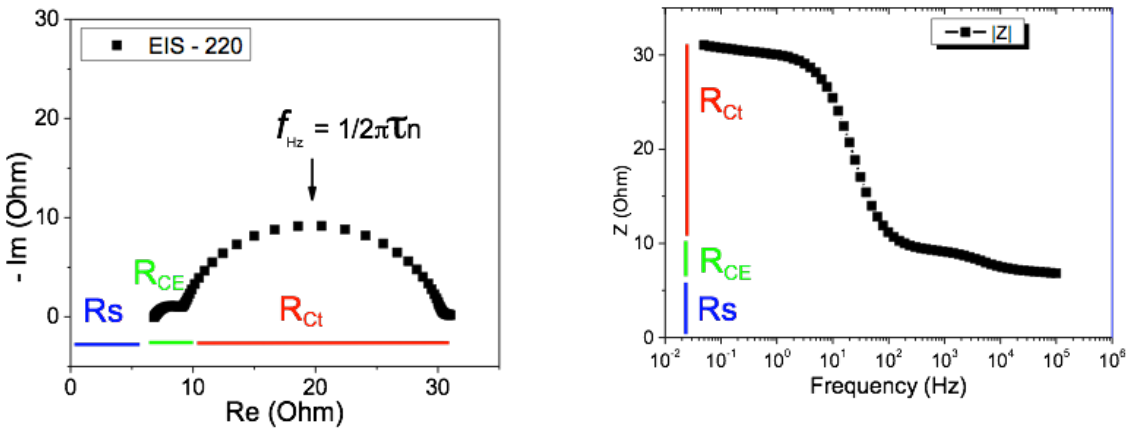

Figure 13: Nyquist (left) and Bode(right) plots of a flow sensitized solar cell used in this work. In the picture I highlighted some important resistance values associated with the DSSC (Rs, Rce, Rct) and the equation which relate the frequency associated at each point with the electron lifetime.

The real part of the impedance is represented on the abscissa axis of the Nyquist plot and its unit is the Ohm, since it measures a resistance, while the y-axis shows the imaginary part of the impedance which is the contribution arising from the frequency dependent processes.

From EIS, the series resistance R_s, sum of all the ohmic, frequency indipendent, resistances of the cell is obtained. Moreover, fitting the data corresponding to the TiO_2 layer charge transfer reaction it is possible to obtain the charge transfer resistance (R_{ct})

which also gives information on the recombination process. Once R_s and R_{ct} are determined, the characteristic frequency for the corresponding process is calculated.

2.1.5 Intensity modulated photovoltage and photocurrent spectroscopy

In an intensity modulated photovoltage spectroscopy experiment, a modulation is applied to a light source within a certain frequency range. The modulated response of the DSSC is measured through a potentiostat. In IMVS the device is set at the open circuit potential depending on the light intensity used during the measurement and the modulated voltage response to the modulated light is recorded. Finally, according to IMPS, the cell is set in short circuit conditions while under illumination, and the current response to the modulated light is acquired as a transfer function F* (Figure 14):

$$F^*_{\mathrm{IMVS,CELL}}(\omega) = \frac{-V_{\mathrm{CELL,AC}}(\omega, t)}{q_e \Phi_{\mathrm{AC}}(\omega, t)}$$

$$F^*_{\mathrm{IMPS,CELL}}(\omega) = \frac{i_{\mathrm{CELL,AC}}(\omega, t)}{q_e \Phi_{\mathrm{AC}}(\omega, t)}$$

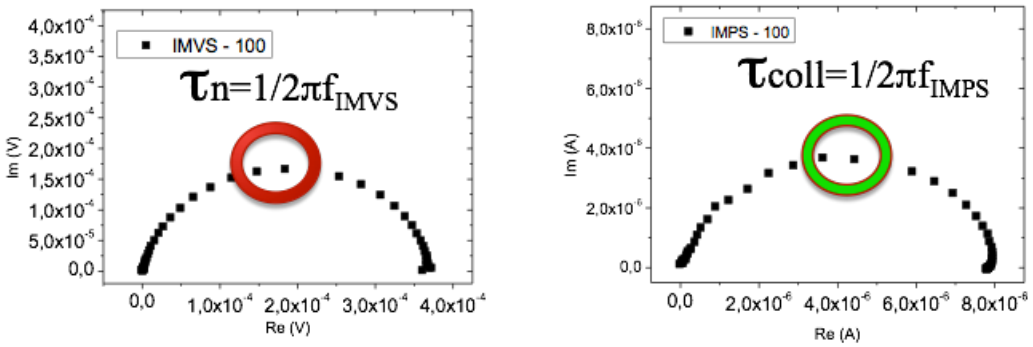

Figure 14: Example of IMVS and IMPS plot from the measurement at a defined light intensity of a flow sensitized photo-anode. The cyrcle highlight the characteristic frequency which can be raleted to the electron lifetime (IMVS) and to the collection time (IMPS).

2.2 Flow sensitization methods

2.2.1 On-line monitoring of N3 ed N719 uptake on TiO_2 photoanodes

In the previous years I developped a flow technique which allowed the real time monitoring of the dye uptake and I used it in collaboration with the University of Brescia for monitoring the dye uptake of N3 and N719 Ruthenium dyes[15]. This method allowed the calculation of some kinetic constants for the adsorption of these dyes onto the surface of TiO_2 which in this case was found to be of "pseudo-first" order in the first part of the dye adsorption, switching then to a "zero order" process not dependent from the dye concentration.

The instrumental setup is made of a fluidic part used for fluxing the dye solutions, integrated with an optical part for the spectrophotometric acquisition of the UV-Vis spectra. A TiO_2 photoanode is assembled in a "flow cell" with conneting lens for the optic fiber connections for acquisition of the UV-Vis spectra (Figure 15). Since the TiO_2 layer is completely transparent and the layer of fluxed dye is extremely thin, we can monitor the absorbance through the photoanode without any further complication.

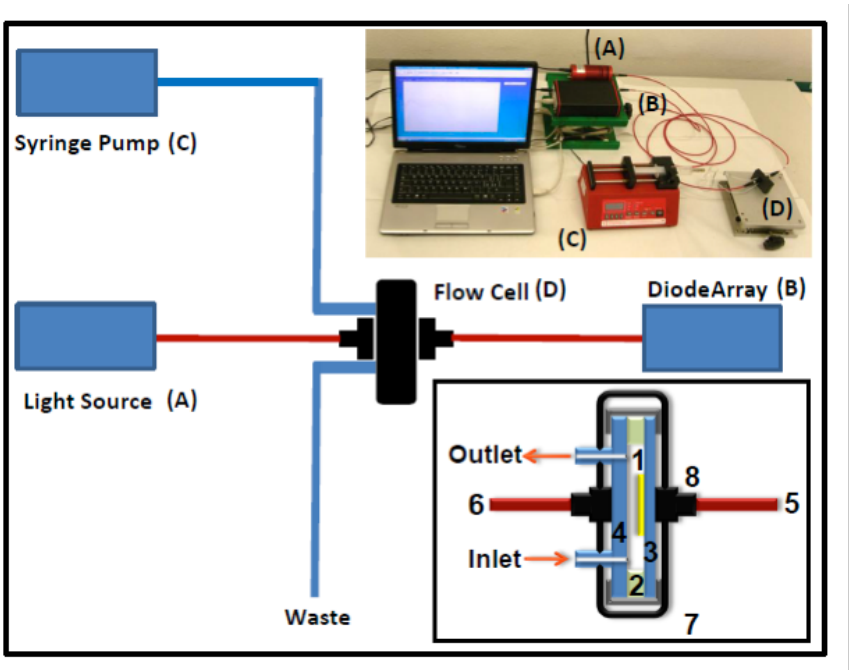

Figure 15: Diagram of the "flow cell" with the UV-VIS monitoring system. In the inset you can see a detail of the "flow cell": 1) layer of TiO2 ; 2) spacer; 3) conducting glass FTO; 4) head to flow; 5) optical fiber connected with spectrophotometer; 6) optical fiber connected to the source of light; 7) "black box" that houses the cell to be flow and protects from external light; 8) collimating lenses for the fiber optic connection.

A syringe pump is used to flush the ethanol, with the purpose of conditioning the TiO2 layer with the solvent before the sensitization process, and to remove the excess of dye not linked to the Titanium dioxide after the dye loading. The flow rate of the dye solution is set to 200 µl*min-1. By this way, the layer of TiO2 is always in contact with fresh solution of dye eliminating any problems due to concentration gradients that could arise in the methods of sensitization by dipping. As a result, the dye can be considered in a steady state and that simplify the mathematical treatment of the experimental data to extract kinetic constants of the process.

The first contribution is well described by a kinetic equation of pseudo-first order:

$$T + D \xrightarrow{k_1} TD$$

$$\frac{\partial[TD]}{\partial t} = k_1[T]\cdot[D] = k_1'[T] = k_1'([T_0]-[TD])$$

$$[TD] = [T_0]\left(1 - e^{-k_1' t}\right)$$

in which [T] indicates the number of sites available on the surface of the Titanium dioxide for the binding of the dye, while [D] and [TD] represent the concentrations of dye in solution and bound onto the TiO_2, respectively.

Since the concentration of the dye in the fluxed solution can be considered to be constant during the experiment, its value can be integrated into the k_1 to obtain a "pseudo-first" order kinetic constant for the absorption of the dye, k_1'.

The free sites on TiO_2 [T], are correlated with the total number of sites that were initially present, [T0], and with those already occupied by sensitizer when the uptake switched from the "pseudo-first" order uptake region to the "zero" order region, [TD], by the following equation:

$$[T] = [T]_0 - [TD]$$

$$[TD] = [TD] + k_2 t$$

Where [TD]' refers to the amount of dye already bound to the TiO_2 in the moment when it passes from the area of rapid adsorption to the one in which the adsorption become slower (Figure 16).

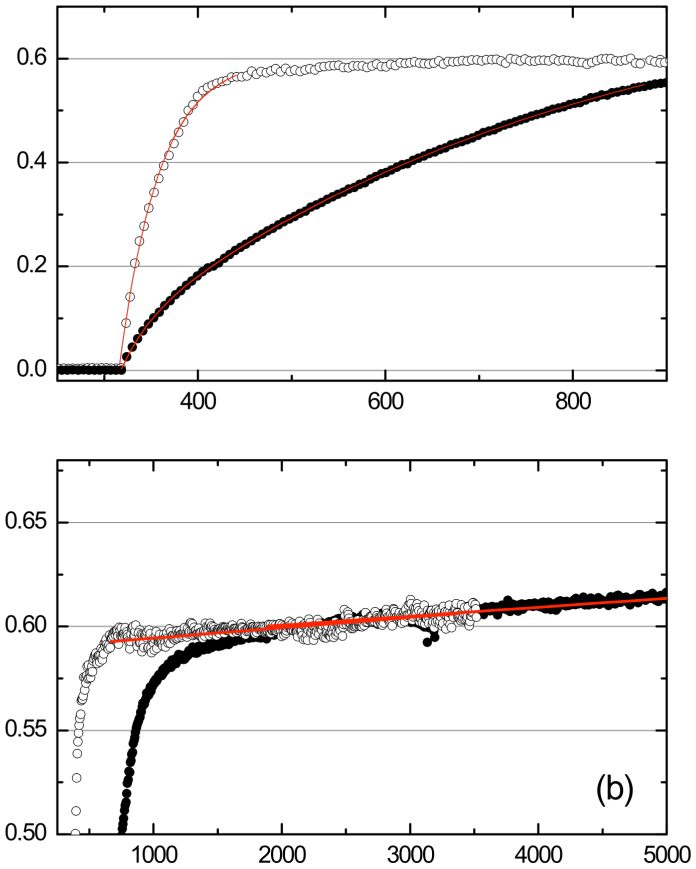

Figure 16: Fitting of the adsorption curves of N3 at two different concentrations: (a) fitting of the initial phase of uptake; (b) fitting of the area with slow kinetic regime. It was used a 0.5 mM solution and a 5.0 mm. The red lines represent the fitting of experimental data.

3. Flow Sensitization with Green Dye 2 - University of Wollongong - IPRI

3.1 Porphyrins structure and characteristics

Porphyrins are a class of macromolecules which are widespread in biological and natural systems. As an example, we can find them in chloroplasts, where they are involved in the electron transfer reactions needed for the photosynthesis. The main structural characteristic of this class of molecules is the heterocyclic π-aromatic system of 22 π-electrons which results in the presence of two characteristic bands regions in the absorption spectra of these dyes. The most intense band involve a transition from the ground state (S0) to the second excited level (S2), it is called Soret band (or B band) and is generally found around 420 nm. The second region consist of a set of four Q-bands, having about 10% of the intensity of the Soret band, that result from a S0 to S1 transition are found in the region between 500 - 700 nm[16].

Porphyrins may be used in a free base form or as metal complex, because of the size of the macrocycle which allows the insertion of several metal ions (e.g. Zn, Fe, Cu, Co, etc.), the most common ion for photophysical applications being Zn(II). When a metal is coordinate within the macrocycle, the porphyrin symmetry increase leading to a simplification reducing the number of Q-band at 2 peaks.

The great absorption characteristics together and the possibility of a relatively easy structural optimization of the molecule, are some of the reasons why this class of compound have attracted the interest as sensitizers in DSSCs[16].

3.1.1 Porphyrins as DSSC sensitizers

An extensive optimization work has been performed on porphyrins for their application on DSSC. Improvement of photovoltaic characteristic have been obtained working on substituent modification, conjugated anchoring groups, β or meso position of the linker, metallation of the porphyrin, etc. Lately, the concept of push-pull concept has also been applied to porphyrins, as in the case of YD-2-o-C8[9], obtaining a significant increase of efficiency and surpassing for the first time the highest efficiency obtained with

Ruthenium dyes. Good results in DSSC devices have been obtained also with relatively simple porphyrins, as those belonging to the so-called "Green Dye" series. It was found that a porphyrin with a β-linked malonic acid anchoring group and meso substituted with four 4-methylphenyl group reached 7.1% of efficiency despite its very simple molecular structure[10b].

Indeed an example strictly related to the following work involve the "Green Dye" porphyrin [(E) 3-(5,10,15,20-tetra(3,5- dimethylphenyl)porphyrin-2-yl)propenylidenemalonato zinc (II)] to which we refer as GD2.

GD2 has a zinc ion coordinated in the macrocyle, it brings four 3,5-dimethylphenyl meso substituents and a malonic acid linked in beta position on a pyrrol[17]. This sensitizer, on state of the arte devices, was able to give 5% efficiencie and it showed interesting characteristics (*e.g.* efficiency increase after irradiation with the solar simulator).

An extensive optimization work has been performed on porphyrins for their application on DSSC. Improvement of photovoltaic characteristic have been obtained working on substituent modification, conjugated anchoring groups, β or meso position of the linker, metallation of the porphyrin, etc. Lately, the concept of push-pull concept has also been applied to porphyrins, as in the case of YD-2-o-C8, obtaining a significant increase of efficiency and surpassing for the first time the highest efficiency obtained with Ruthenium dyes. Good results in DSSC devices have been obtained also with relatively simple porphyrins, as those belonging to the so-called "Green Dye" series. It was found that a porphyrin with a b linked malonic acid anchoring group and meso substituted with four 4-methylphenyl group reached 7.1% of efficiency despite its very simple molecular structure.

Indeed an example strictly related to the following work involve the "Green Dye" porphyrin [(E) 3-(5,10,15,20-tetra(3,5- dimethylphenyl)porphyrin-2-yl)propenylidenemalonato zinc (II)] to which we refer as GD2 (Figure 17).

GD2 has a zinc ion coordinated in the macrocyle, it brings four 3,5-dimethylphenyl meso substituents and a malonic acid linked in beta position on a pyrrol. This sensitizer, on state of the arte devices, was able to give 5% efficiencie and it showed interesting characteristics (*e.g.* efficiency increase after irradiation with the solar simulator).

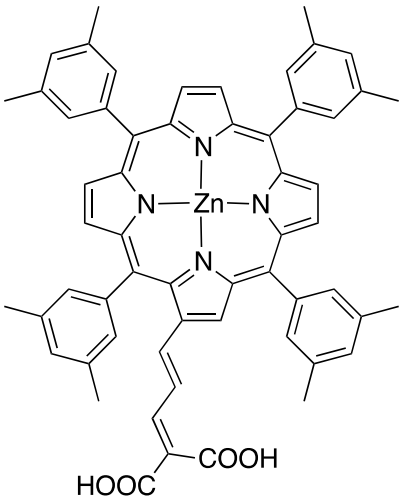

Figure 17: molecular structure of GD2 porphyrin

3.2 Co-adsorbates and surface treatments

Co-adsorbates are used in order to reduce the aggregation of the organic dyes. These molecules are generally provided with an anchoring group so that they can bind to the TiO_2 surface, creating a blocking layer that isolates the remaining free spaces on the TiO_2 from the electrolyte solution, thus helping to reduce the recombination phenomena. Biliar acids are among the most used co-adsorbates and are generally added to the dye solution at higher concentration respect to the dye. Other surface treatments have been carried out before (e.g. cyclodextrins[18]) or after sensitization (e.g. posphynic acid[14], tributyl phosphate treatment[19]) in order to optimize the DSSC's performances.

3.3 Flow technique

The Flow technique described previously in chapter 2 has been adapted for the study of GD2 adsorption on transparent 2.5 μm thick TiO_2 photoanodes. The flow cell has been re-designed in order to be used without optical fibers (Figure 18), indeed, measurements were actually performed in a completely dark room, where the only light source was a calibrated LED of the Zahner instrument. Being the whole device transparent it allowed the acquisition of the UV-Vis spectrum under flowing the dye solutions. Initially, using a syringe pump, I flowed only the solvent over the photoanode while acquiring an UV-Vis spectrum every 20 seconds, then I changed the syringe with one containing the dye solution and I continued to flux the solution until the plateau region was reached, generally within 2 hours (Figure 19). A washing with pure solvent was performed for

some photo-anodes to remove some weakly bound sensitizer eventually present. Noteworthy, the continuous monitoring allowed us to sensitize the photoanodes up to defined percentages of the total loading achievable with the in-flow technique.

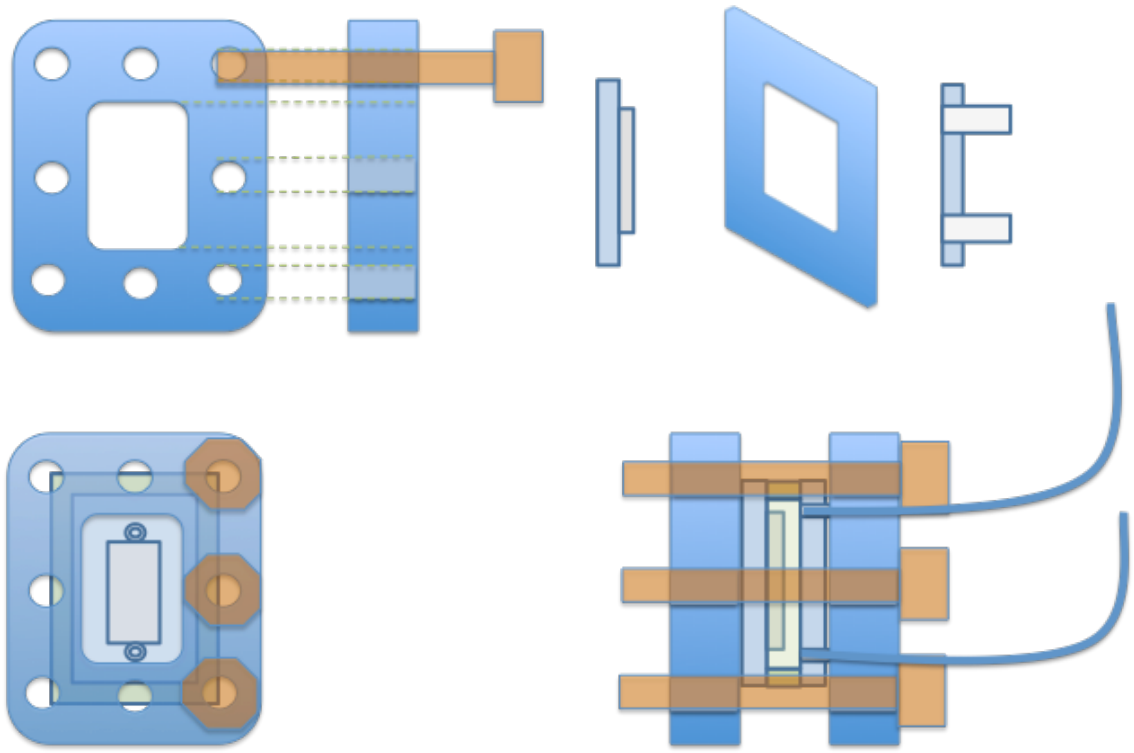

Figure 18: scheme of the flow cell bearing a central window that has been used at IPRI, adapted for the use with the Zahner instrumentation. Every part of this custom made flow device has been built and assembled at IPRI.

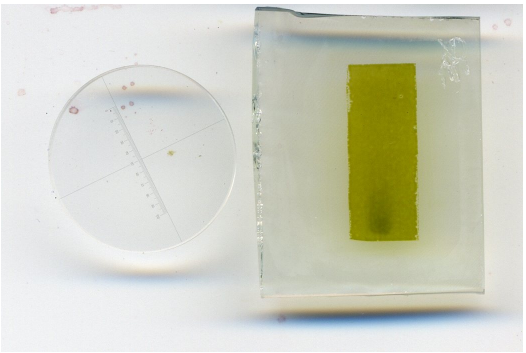

Figure 19: typical outcome obtained on a 16 x 6 mm TiO_2 photoanode after flow sensitization with GD2.

3.4 Experimental Procedure

The characterization routine for each experiment reported in the following sections was the following:

I. preparation of all the components needed for DSSC construction;

II. device assembly and sensitization;

III. J-V and IPCE characterization;

IV. electrochemical impedance spectroscopy (EIS) measurements;

V. intensity modulated photovoltage and photocurrent spectroscopy (IMVS; IMPS);

VI. data elaboration.

3.5 Results and Discussion

3.5.1 Effect of different solvents on GD2 uptake

In order to evaluate the role played by the solvent to the dye uptake process, I fluxed solutions of GD2 in Acetonitrile (ACN), Tetrahydrofurane (THF) and Ethanol (EtOH). Moreover, dye desorption was also monitored. The dye uptake profile is characterized by an initial fast uptake region followed by a plateau-like region where the absorbance does not increase over prolonged sensitization time (Figure 20).

ACN and EtOH resulted in higher absorbances of the plateau region than THF, meaning that higher amounts of dye were loaded on the devices in the same conditions. In particular, THF resulted not only in lower dye adsorption, but also in some kind of degradation of the photoanode that caused a lowering of the plateau absorbance over time, hence removal of adsorbed dye while still fluxing the sensitizer solution. It is not clear if this was due to dye desorption from the TiO_2, or from degradation of the mesoporous layer.

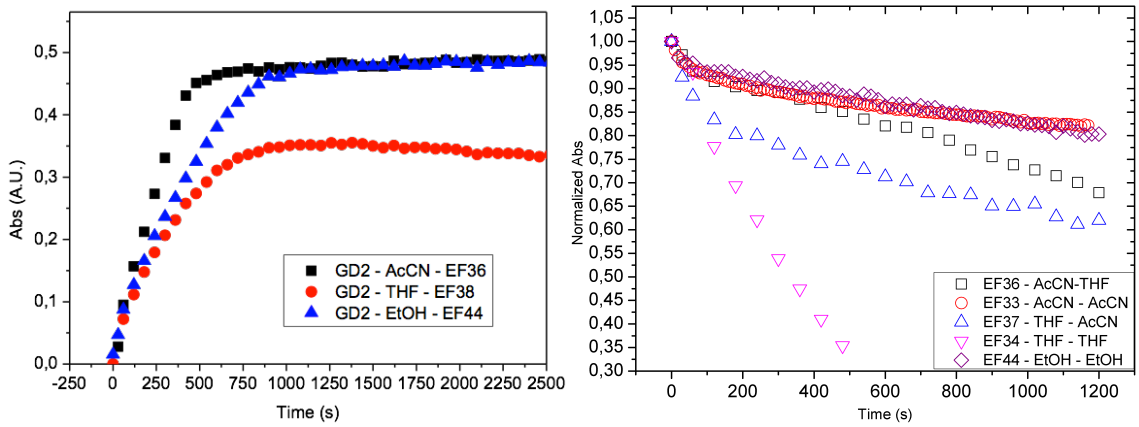

Figure 20 flow uptake profiles of GD2 sensitized photoanode (on the left), obtained using ACN (black square), EtOH (blue triangle) and THF (red circle). On the right graphic, it is reported the behaviour of the washing profiles of photoanodes rinsed with different solvents. A similar behaviour is found when rinsing EF36 and EF44 photoanodes, respectively using ACN and EtOH. All the other solvent caused faster dye desorption rates.

After sensitization was completed and the plateau region was reached, a washing procedure was applied using pure solvent while absorbance was still monitored. Significant amonunts of dye were removed during this step and their relative desorption rates resulted to be somehow related to the absorbance of the plateau region. ACN was the solvent removing the lowest amount of dye followed by EtOH. On the other hand, THF caused a rapid decrease of the absorbance of the sensitized mesoporous layer

resulting in almost complete dye desorption within the 20 minutes of rinsing, for this reason it was not possible to test the device EF34. This problem was addressed with device EF37 by carrying out a sensitization with THF, followed by rinsing with ACN. A the faster removal of the dye was still observed, if compared to ACN sensitized photo-anodes, and it may be ascribed to loosely bound sensitizer as an effect of THF.

The photoanodes sensitized using ACN as solvent performed better and, interestingly, the Voc resulted higher when THF was used for rinsing, despite the increased amounts of dye removal associated with it. The plot of the dark current suggest that lower recombination was taking place but, at the same time, a lower current density was obtained, as expected due to the lower amount of dye (Figure 21). The differences in the photovoltaic response in this case, could not be addressed exclusively to the solvent effect but also to the different amounts of dye remained attached on the TiO_2 surface after rinsing (Table 1).

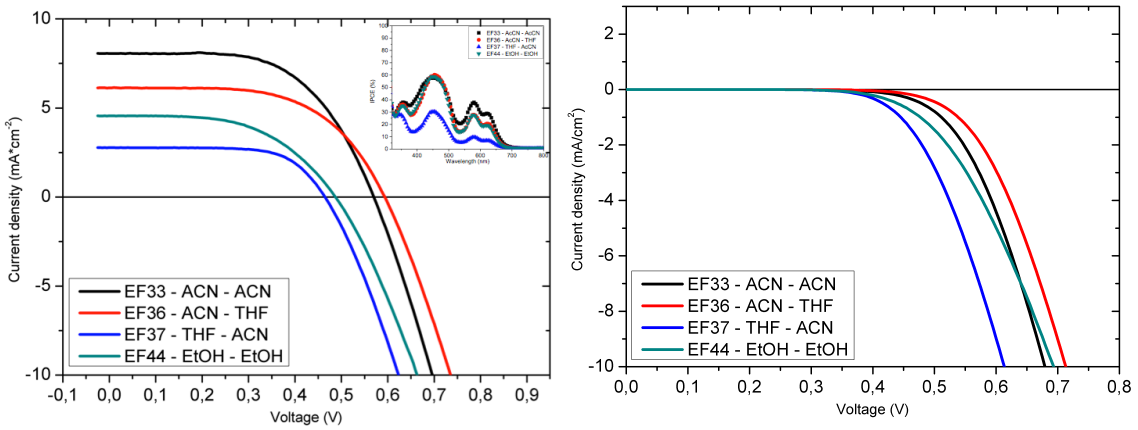

Figure 21: J-V polarization curves obtained for photoanodes which have been sensitized and subsequently rinsed using different combinations of solvents (ACN, THF, EtOH). Efficiencies are mostly related to the dye loading since each dye carries its own influence both on the dye uptake than on the dye removal.

	Voc (V)	Jsc (mA)	FF (%)	Mpp (mW/cm²)	Vpp (V)	Efficiency (%)
EF33 - ACN - ACN	570	8,06	58	2,76	385	2,76
EF36 - ACN - THF	590	6,15	60	2,17	415	2,17
EF37 - THF - ACN	460	2,80	68	0,88	355	0,87
EF44 - EtOH - EtOH	490	4,62	54	1,21	320	1,21

Table 1: the most important photovoltaic characteristics are reported in this table for the flow sensitized photoanodes followed by the rinsing procedure. Devices sensitized with GD2 in ACN and rinsed with the same solvent showed the best combination of photovoltaic characteristics (high Voc, Jsc and FF) which brings to the better performance.

3.5.2 Influence of GD2 concentration in flow-sensitized DSSCs

3.5.2.1 Sensitization using only GD2

The role of GD2 concentration on the uptake behaviour and photovoltaic characteristics of DSSCs was investigated fluxing an ethanolic sensitizer solution at different concentrations while continuous monitoring the dye uptake. The dye concentration was in the 0.05÷0.4 mM range and the experiments were repeated also in the presence of Cholic Acid as co-adsorbate. Using 0.2 mM solution we found a first region of fast dye uptake were the absorbance of the TiO_2 film increase to 0.48 within 20-25 minutes (Figure 22, yellow trace). With the 0.4 mM solution a slightly quicker adsorption was observed but the absorbance value reached at the plateau did not change from the case of 0.2 mM dye (Figure 22, blue trace). As expected, when 0.05 mM dye solution was used, the dye uptake was slower and after 20 minutes it reached about 40% of the plateau value. After 2 hours the experiment was stopped at an absorbance corresponding approximatively to 80% of the full coverage (Figure 22, trace green).

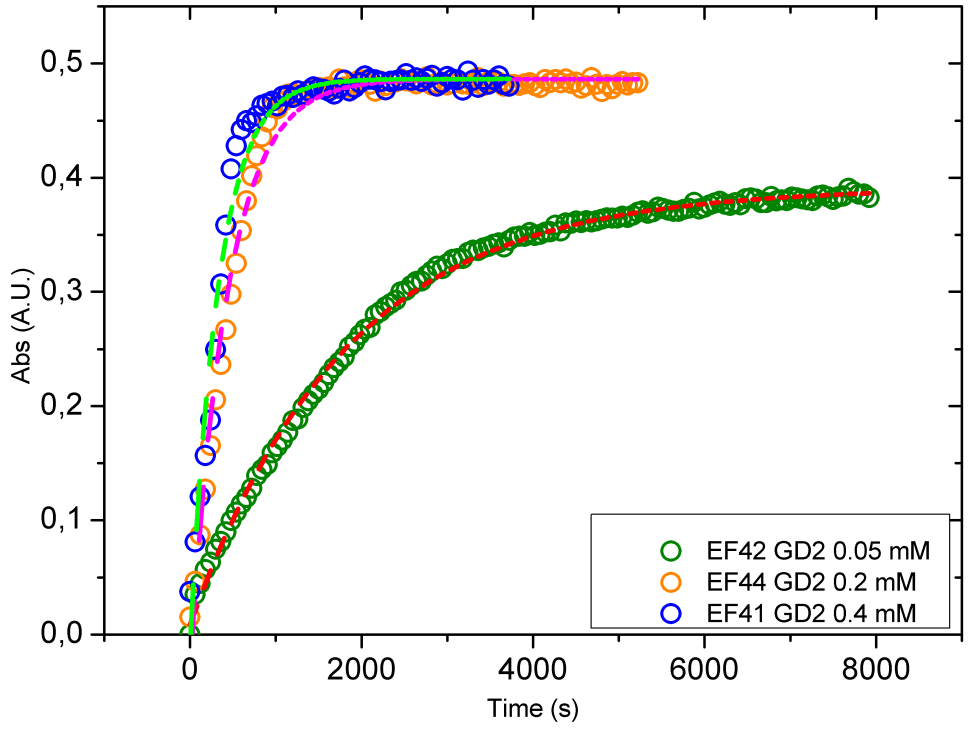

Figure 22: flow uptake profile of photoanodes sensitized using GD2 solutions in ethanol at different concentrations. (GD2 0.05; 0,2; 0,4 mM in EtOH). The dashed line represent the result of the pseudo-first order fitting which present a small deviation from the experimental data around 90% of the plateau dye loading.

This data have been fitted using a pseudo-first order kinetic equation which have been previously used to obtain kinetic data regarding the process of dye uptake of N3 and N719 dyes[15]. The fitting is in good agreement with the experimental data, while a slightly deviation occurs in the region where the slope rapidly decrease just before reaching the plateau region, around 90% of the absorbance of full covered photoanodes. A four fold increase of the dye concentration in the solution, from 0.05 to 0.2 mM, resulted in a 4.2 increase of the pseudo-first order rate constant k', in good agreement with the the kinetic model (EF42 and EF44 in Table 2). This behaviour is not maintaned when a 0.4 mM GD2 solution was used, with just 40% increase of k', this may be rationalized with the dye binding as an aggregate onto TiO_2.

DSSC name	[Dye] (mM)	k' (s^{-1})	Efficiency %	FF (%)	Voc (mV)	Jsc (mA/cm^2)
EF41	0.40	3,05E-03	1.03	47	495	4.39
EF44	0.20	2,33E-03	1.21	54	490	4.62
EF42	0.05	5,51E-04	0.70	43	480	3.35

Table 2: the value of the pseudo-first order kinetic constant is reported together with GD2 concentration. Its value shows an almost linear increase with the concentration moving from the 0.05 mM to the 0.2 mM GD2 solution in EtOH, but this linear increase is not maintained between the 0.2 and 0.4 mM solutions. All device have been rinsed with the same procedure for the same time. Photovoltaic characteristics shows that in the same conditions, the DSSC sensitized with the 0.2 mM GD2 in EtOH perform slightly better.

J-V measurements showed a lower Jsc and a raising of the shunt resistance for EF42 (0.05 mM) beginning around 0.2 V, thus meaning that strong recombination between TiO_2 and electrolyte is occurring. This is expected since the sensitization did not reached the full coverage due to the prolonged time needed for sensitization. Therefore, some areas of the semiconductor layer may have not been covered with GD2. Jsc value for EF41 (GD2 0.4mM) is slightly lower than that of EF44 (GD2 0.2mM), with evident shunt resistance for the DSSC sensitized with 0.4 mM dye solution which may suggest that higher dye concentration could promote aggregation and related recombination.

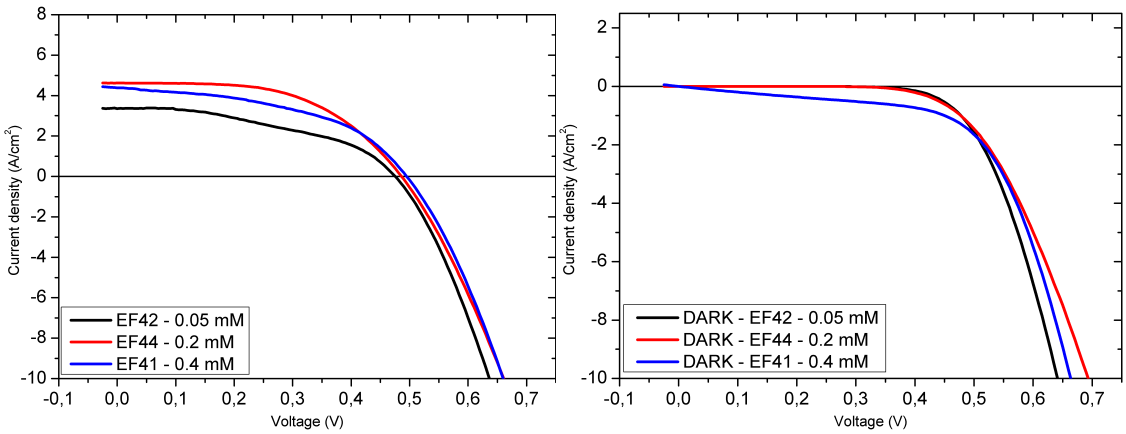

Figure 23: J-V curve of DSSCs sensitized with GD2 0.05 mM (Black line), 0.2 mM (Blue line), 0.4 mM (Red line) at increasing concentrations.

3.5.2.2 Sensitization using GD2 and Cholic Acid:

The dye uptake procedure has been repeated for different photoanodes using a solution of GD2 with the addition of Cholic Acid 2.0 mM as co-adsorbate (the 0.05 mM concentration was not studied in this case). Within 30 minutes the absorbance reached the plateau region, meaning that the maximum coverage was achieved. A slight difference in absorbance at 100% of the loading has been observed in this case because of the competition with Cholic Acid for the binding sites on TiO_2 surface, indeed the absorbance is slightly higher for device EF45 which was sensitized with the most concentrated solution (Figure 24). If compared to the photo-anodes sensitized in the absence of co-adsorbate, it is clear how the absorbance at saturation was exactly the same (Figure 24).

The fitting using the pseudo-first order kinetic equation has been executed on photo-anodes treated with GD2 + CA, considering negligible the contribution of the latter, and the results are matching the experimental data with a very good agreement. The deviation in the fitting, around 90% of full coverage, which arose when no Cholic Acid was present in the fluxed solution (Figure 22), has disappeared and, surpsisingly, the data fitting match also the data of the most concentrated solution.

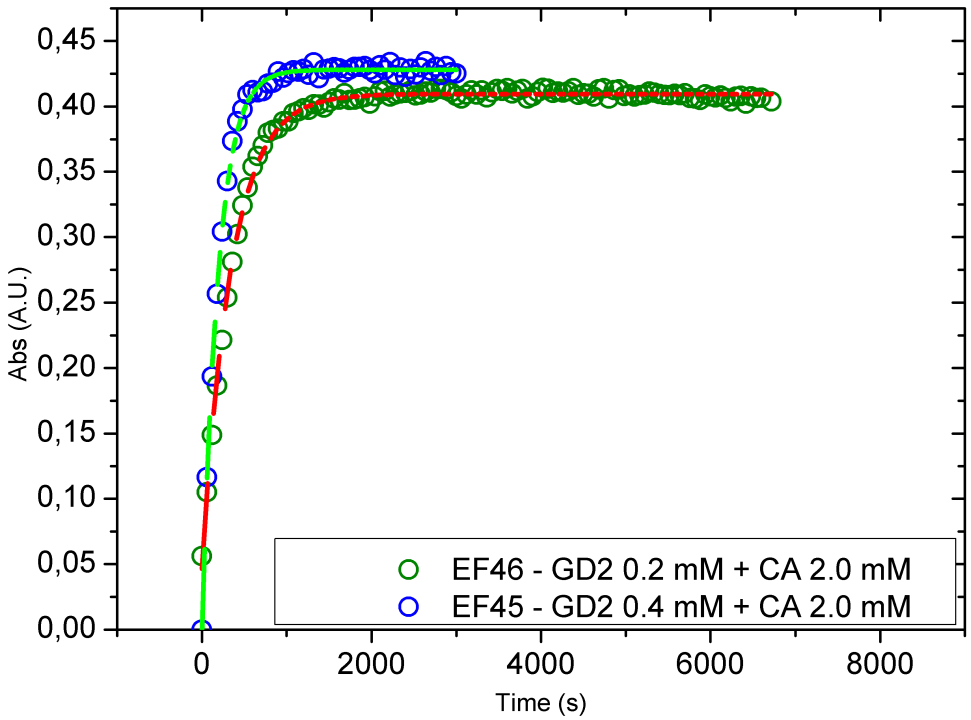

Figure 24: flow uptake profiles of photoanodes sensitized with GD2 0.2 mM and 0.4 mM in the presence of 2 mM Cholic Acid as co-adsorbate. A sligth difference in plateau absorbance is found, being higher for the most concentrated solution (as expected) because of the competion for the adsorption sites between CA and GD2. The quality of the fitting (dashed lines) with the pseudo-first order equation, is increased when 2.0 mM CA is present in the dye solution.

The pseudo-first order rate constant, is increased when Cholic Acid is present in the solution. In particular, it shows an increase of 83% when doubling the concentration of the dye, in a slight agreement with the pseudo-first order kinetic.

The overall device efficiency is higher for EF45, probably because of the higher amount of dye sticking on the photoanode which result in Jsc and Voc increase of 69% and 17% respectively (Table 3). Nevertheless, the 35% efficiency increase to 1.51%, is somehow lower than expected (2.2% keeping in consideration the 62% FF). This is clearly due to a decrease in the FF, with the cell behaving less ideally.

DSSC name	[Dye] (mM)	k' (s^{-1})	Efficiency (%)	FF (%)	Voc (mV)	Jsc (mA/cm^2)
EF46	2.0E-4	0.00291	1.12	62	502	3.611
EF45	4.0E-4	0.00531	1.51	42	585	6.142

Table 3: The 2 fold increase in GD2 concentration, when Cholic Acid is present, induced a similar increase (1.83) in the value of the kinetic rate constant k'.

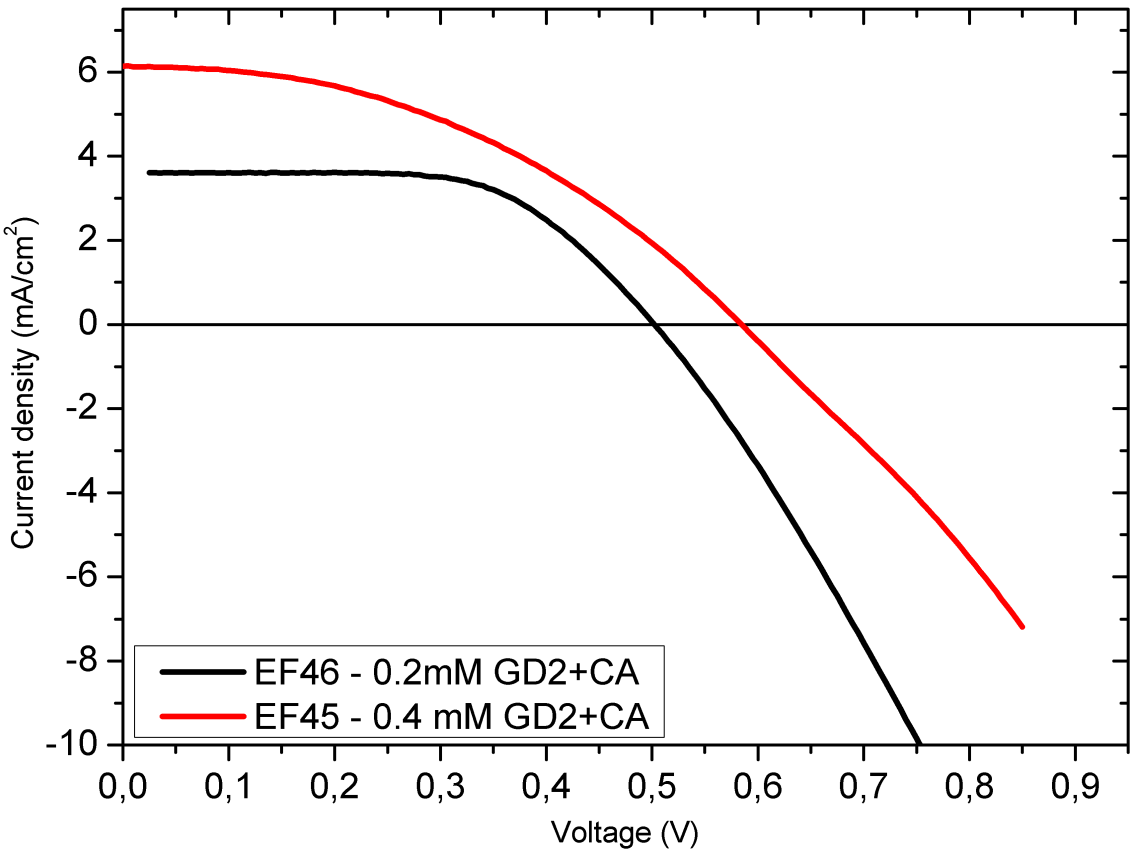

Figure 25: J-V polarization curve of photoanodes sensitized with

3.5.3 Effects of different dye loadings on GD2 sensitized DSSCs

The possibility of studying DSSCs with photo-anodes partially covered by the sensitizer was reported previously with the aim to gain a deeper understanding of what was exactly happening during the sensitization process. Althought dye loading from very diluted solutions is among the most commonly used method to obtain partially sensitized photoanodes[20], an alternative procedure is based on fully sensitizarion of the photo-anode followed by partial desorption using very diluted solutions of Sodium Hydroxide[21]. Finally, in other cases, a diluted dye solution was used in which an increasing amount of a proper inorganic salt was dissolved to compete for the adsorption sites[22]. These techniques could present some issues due to the intrinsic complexity of the DSSC environment, since these experiments are performed in different conditions with respect to the effective working environment to which the active electrode would be exposed and this could lead to changes in the response of the assembled devices.

In my work I used a flow technique that allowed the real-time monitoring of the sensitization process and I used it not only to monitor but also for gaining control over the sensitization process. It was possible to obtain several photoanodes with different sensitizer loadings just stopping to flux the dye solution at defined values of absorbance, then quickly changing the syringe and rinsing the photo-anode for a short time in order to remove weakly bond dye, without detaching considerable amounts of dye from the TiO_2.

I decided to study the characteristics of DSSCs with the following loading of GD2: loading of 50% (measured by the absorbance increase with the flow sensitization technique) in order to evaluate devices with considerable big areas of TiO_2 exposed to the electrolyte; loading of 90% which is interesting because we are close to saturation of the binding sites, finally a loading of 100% (full coverage of TiO_2) which corresponded to the plateau region in the graphic below (Figure 26). A very good matching among the partial adsorption profile is obtained among different sensitized devices, this is an indicator of good reproducibility of the data.

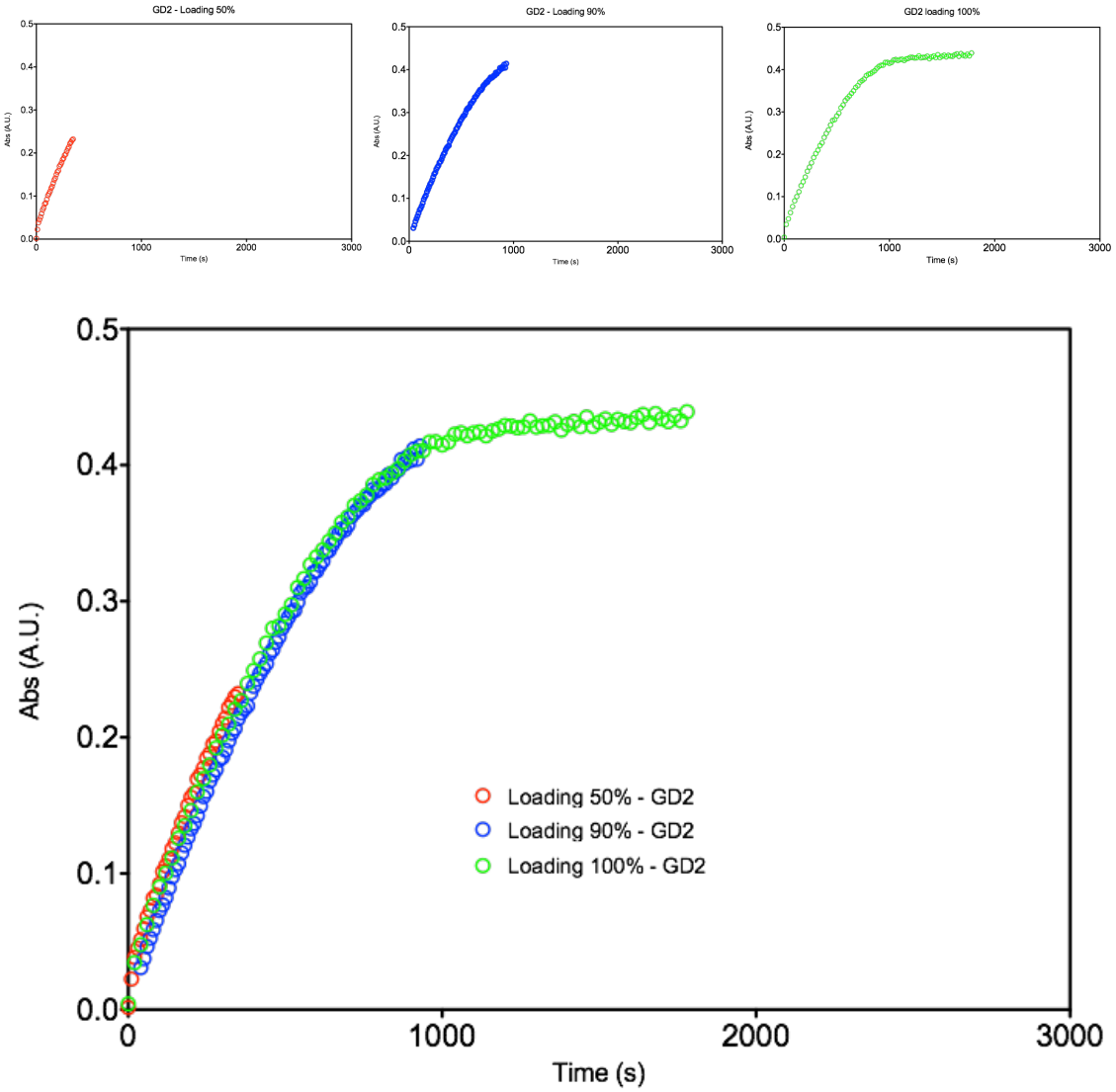

Figure 26: GD2 adsorption profiles on partially loaded photoanodes. Loading are 50%, 90% and 100% (full coverage).

After the loading process was completed, the photoanodes were dried and assembled in order to perform the complete device characterization.

The J-V of each device has been measured after 20 minutes of light soaking and the overall DSSC efficiencies have been compared.

The first evidence is that the short circuit current density (Jsc) for the half loaded device is significantly reduced. Moreover, the slope of its J-V curve suggests a decrease of the shunt resistance which is related to a higher recombination happening between the TiO_2 and electrolyte in the exposed semiconductior areas. The electrons follow the pathway that oppose less resistance, so a strategy for reducing this kind of recombination is

avoiding to leave defectual areas on the semiconductor surface in contact with the electrolyte.

To facilitate the reading of the J-V curves, I report the most important values as Jsc, Voc, FF and Efficiency in the graphic on the right (Figure 27). It is interesting to highlight how the efficiencies do not change significantly moving from dye coverage of 50% to 90% also if the Jsc current increase of about 1 mA.

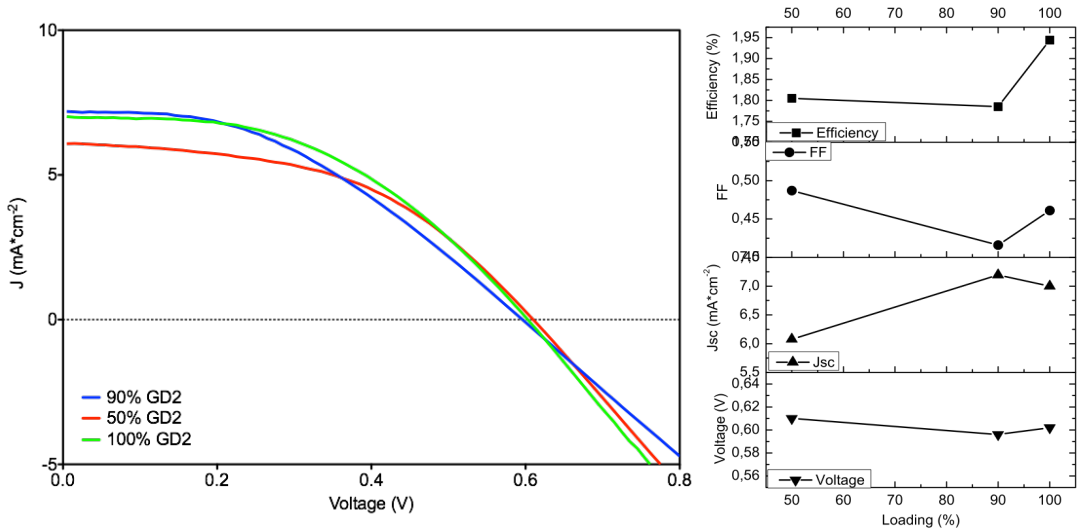

Figure 27: J-V polarization curve of photoanodes partially loaded with GD2 on the left. In the graphic on the right we found the most important photovoltaic parameters extrapolated from the J-V curves.

The IPCE spectrum (Figure 28), shows reasonably good values for this kind of sensitizer when the coverage of the surface is high, reaching 60% in the region of the Soret band between 400 - 500 nm. On the other hand, when the dye loading is 90%, IPCE slightly decreases in the region of the Q bands (550 - 650 nm) while it consistently decreases when the GD2 loading is only 50%.

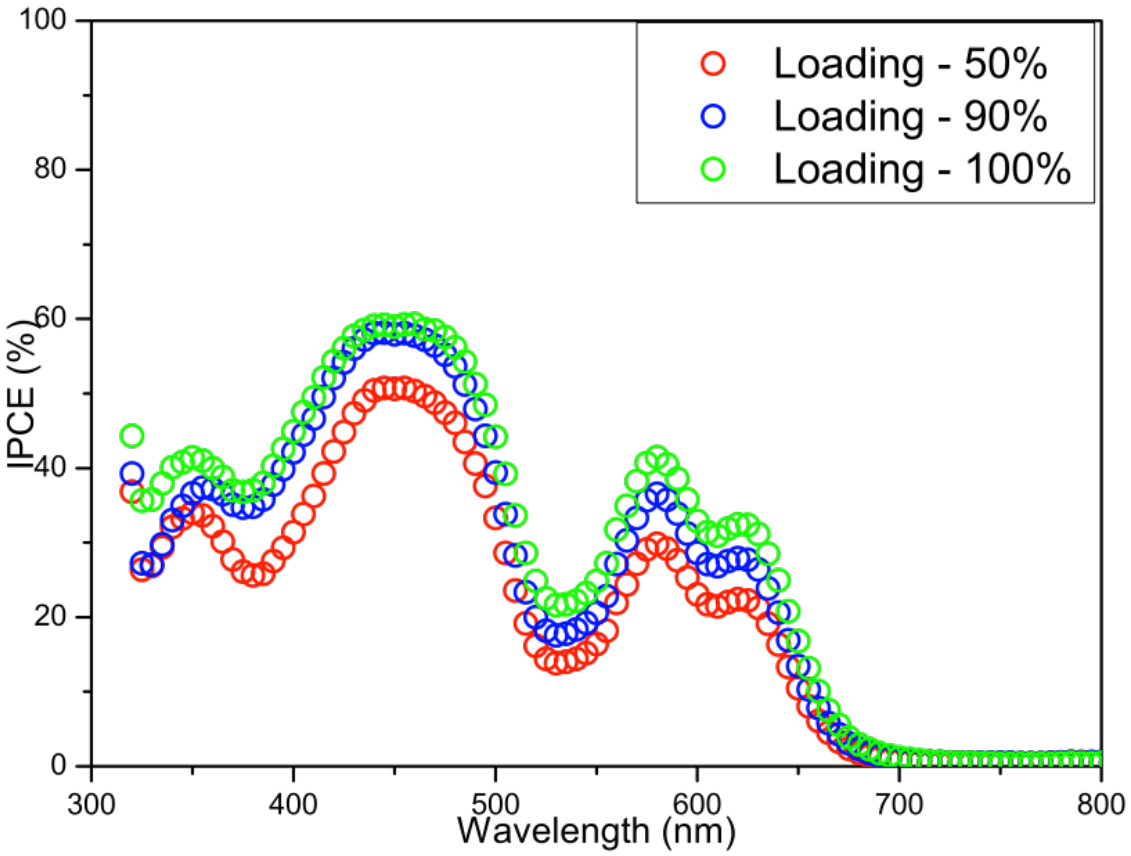

Figure 28: incident photon to current efficiency of phtoanodes EF58, EF59, EF61 loaded with 50%, 90%, 100% of only GD2 dye.

These devices have been characterized also using electrochemical impedance spectroscopy (EIS) together with intensity modulated photovoltage (IMVS) and photocurrent spectroscopy (IMPS). From the R_{ct}, which represents the recombination resistance at the interface TiO_2/Dye/Electrolyte, we see that there is no significant variation among the DSSCs loaded with different amounts of GD2, this may probably explain why there is no evident change in the V_{oc} of the devices resulting from J-V analysis. Plotting the electron lifetime (τ_n) against the electron density (ED) we found a similar behaviour for partially loaded devices (Figure 29), while the lifetime increases significantly when full coverage is achieved (GD2 - 100%). In the graphic of V_{oc} versus ED it is possible to see that, at the same voltage, the electron density in the mesoporous TiO_2 increases with the dye loading, this could be due to an increased electron injection[6b].

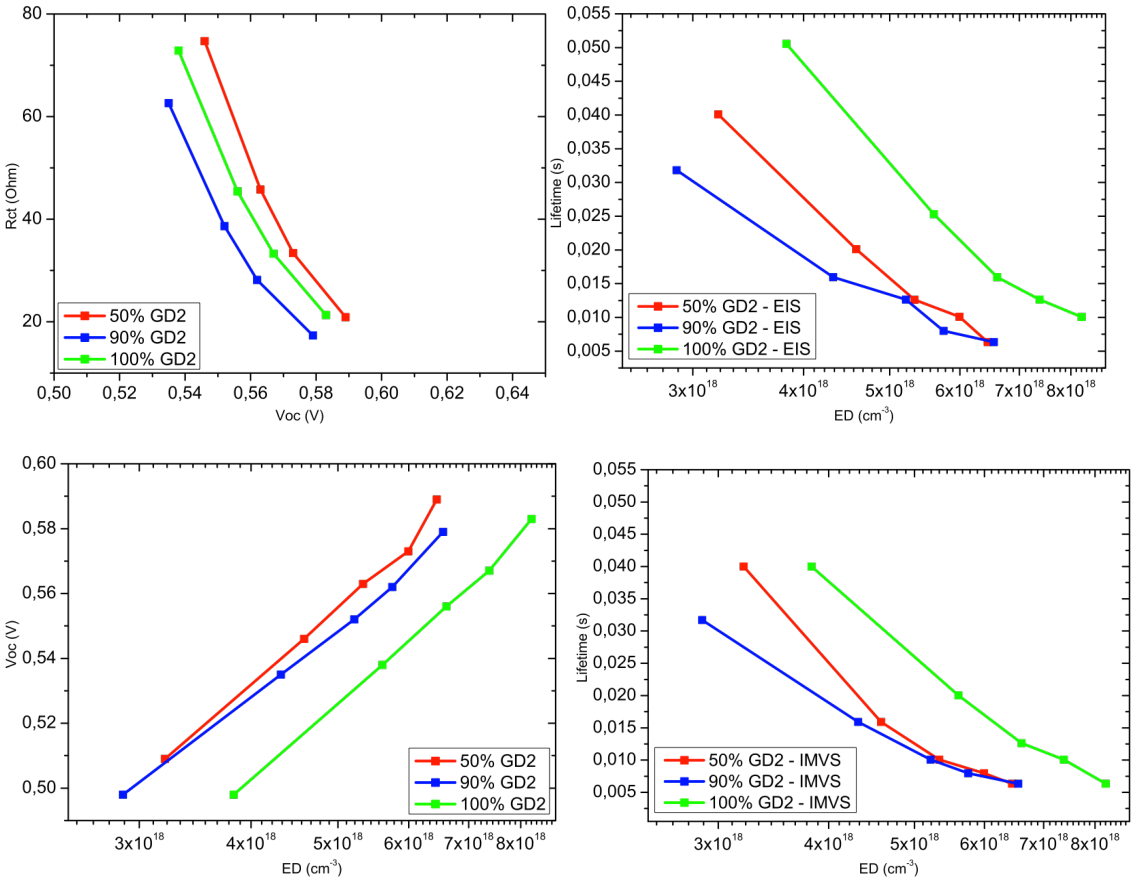

Figure 29: charge transfer R_{ct} (top left), electron lifetime obtained by EIS (top right), open circuit potential V_{oc} (bottom left), electron lifetime obtained by IMVS (bottom right).

The electron lifetimes have been obtained also from IMVS measurements which have confirmed the behaviour calculated form EIS. The results are in good agreement since the solar cells with the highest dye loading show also the highest lifetime, while the partially covered devices show similar but lower values.

3.5.4 Influence of Cholic Acid in GD2 flow sensitized DSSCs

Few studies have investigated the role of co-adsorbate during the process of sensitization and how it may affect the photovoltaic parameters, because the main interest is usually focused on the final efficiency. In addition, the real-time monitoring of the dye loading is not an easy task since the common dyeing techniques require the photoanode dipping for several hours into a sensitizer solution[23], so many of the informations on this process are lost and indirect methods are used to understand what is happening at this stage of the solar cell assembly. In order to obtain a breakthrough in efficiencies, a full knowledge should be gained on this fundamental step, and this is why the sensitization process is still under deep investigation. Althought studies of the effect of dye loading on the performance of DSSCs[24], showed that an optimal dye coverage can be finely tuned, there is a lack of informations regarding the effect of partial dye loading when co-adsorbates are present. The main idea is that the co-adsorbate could contribute to suppress the recombination with lower amounts of dye loaded on the TiO_2. In order to estimate how the presence of a simple co-adsorbate, such as Cholic Acid, affects the photovoltaic characteristics of Dye-Sensitized Solar Cells it is worth then to study the behaviour of photo-anodes loaded with different percentages of dye in the presence of Cholic Acid, one of the simplest Co-Adsorbates used in DSSCs, with the flow sensitization technique we established.

I fluxed an ethanolic solution of GD2 with Cholic Acid on different photo-anodes (Figure 30), stopping the loading at the same percentages as those obtained for the photo-anodes sensitized with only GD2 dye (paragraph 3.5.3) namely, 50%, 90% and 100% of the loading. The first evidence is that the absorbances are sligltly lower due to the competition of Cholic Acid for the adsorption sites on the TiO_2. Therefore, the percentages of loading correspond to slightly lower amounts of dye binding on the photo-anodes.

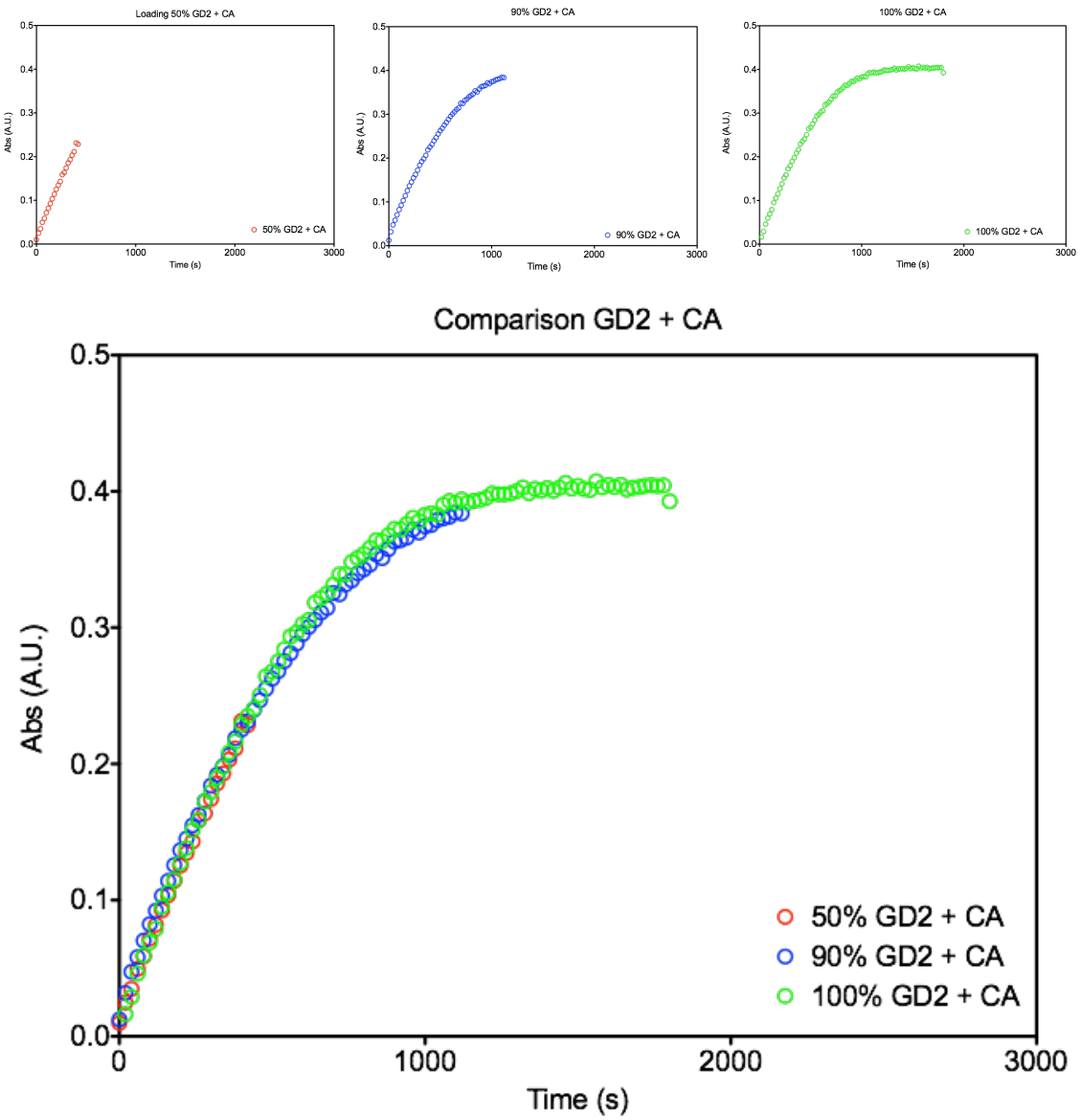

Figure 30: absorption profile of the uptake of 0.2 mM GD2 in ethanol using 2.0 mM Cholic Acid as co-adsorbate.

J-V in this case shows an higher Voc for the device with lower dye loading, suggesting that also the recombination is lower. The small deviation seen around -0.4 V in the J-V curve of 50% GD2 + CA loaded device, suggests that lower shunt resistance values should be operative. The V_{oc} values for this set of devices is similar, the difference being within 25 mV. However, this cannot exclude that slightly oscillations in the open circuit potential may be attributed to shifts in the conduction band energy of the TiO_2. The amplitude of the V_{oc} shift is in the same range observed when GD2 was loaded without using Cholic Acid, while Jsc values are generally higher with a peak value at 90% GD2 + CA loading. A marked improvement when CA is used as Co-Adsorbate in the dye solution is obtained in the Fill Factor of the cells, and this is easily seen from the increased "squareness" of the J-V curve, meaning that the cell is behaving closer to the

ideality. The efficiencies resulting from the combination of these factors are also consistently higher when CA is present in the sensitizer solution fluxed (Figure 31). An 8.4% increasing in the efficiency is obtained raising the dye loading percentage from 50 to 90% and while the efficiency difference from 90% to full coverage is negligible (+0.1%), in this narrow region there is a 6.7% increase in the Fill Factor of the cell.

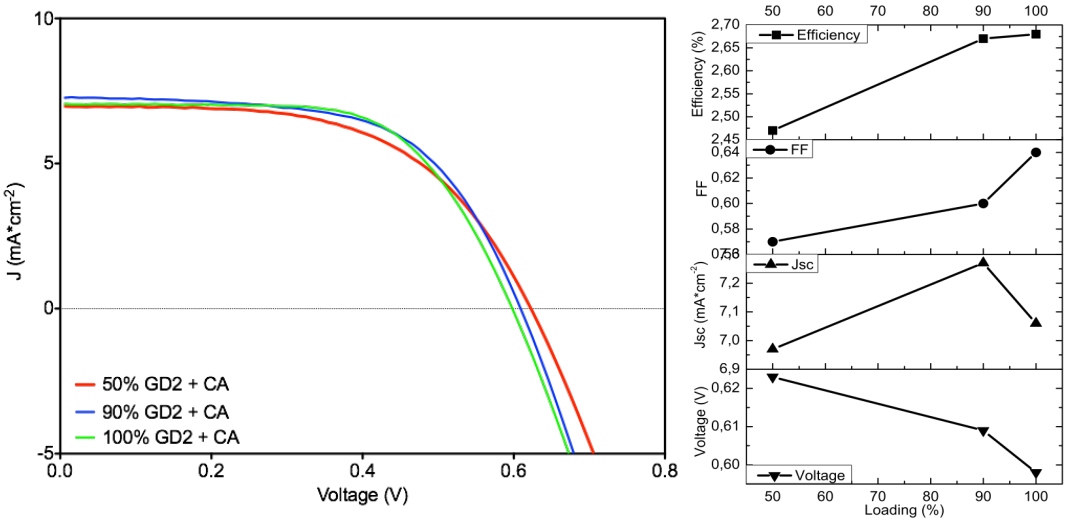

Figure 31: J-V curve of phtoanodes 50%, 90% and 100% loaded with GD2 in the presence of Cholic Acid (left). Graphic representation of most important photovoltaic characteristics (right).

The IPCE spectra shows almost no difference moving from 90% to 100% loading when Cholic Acid is added (Figure 32). This result is in agreement with efficiencies being almost the same at those levels of coverage. When the loading is 50% the IPCE values of the Q bands get significantly lower, but it is not possible to address this behaviour to a decrease in the light harvesting (LHE) or in the injection efficiency (η_{inj}) since no APCE was calculated. This slight decrease shows that IPCE is not directly correlated with the loading, since in this case the photoanode sensitization was stopped at 50% of full coverage absorbance.

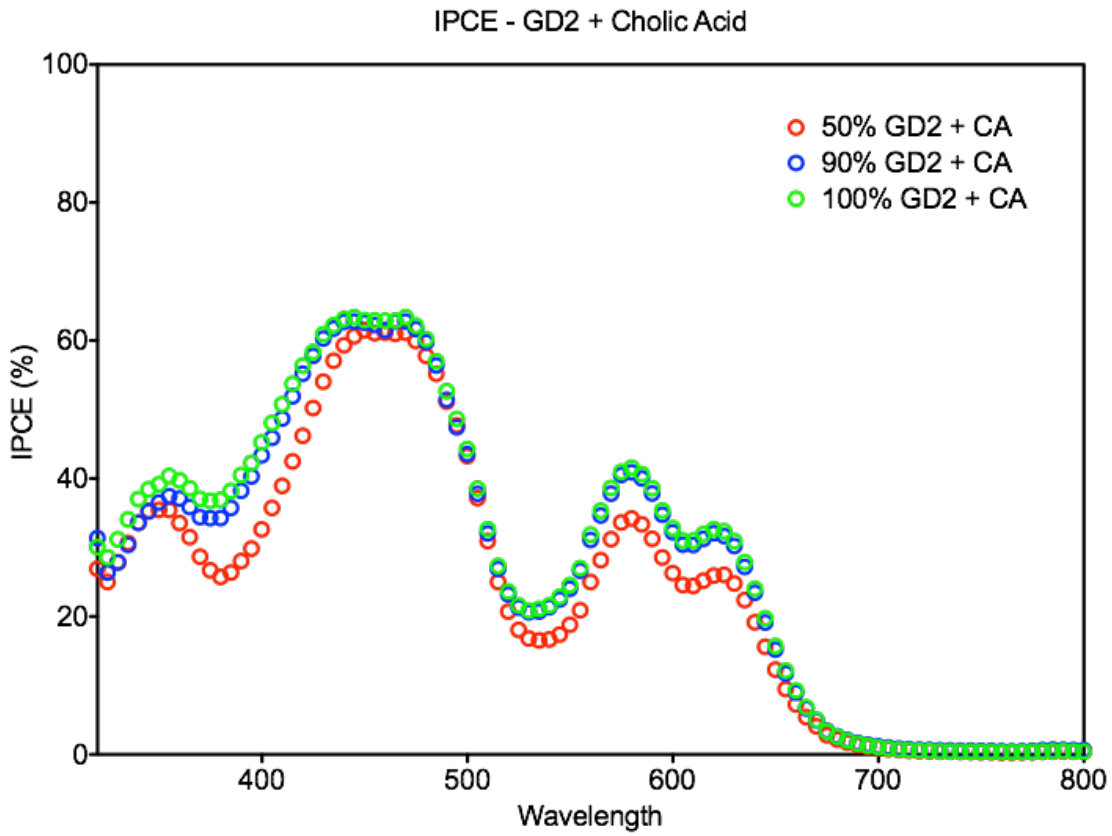

Figure 32: incident photon to current conversion efficiency of photoanodes EF57, EF64 and EF62 loaded respectively up to 50%, 90%, 100% with GD2 + CA.

The electron lifetime measured by EIS was slightly higher for device EF57, loaded to 50% with GD2 and CA, this could be due to an early blocking effect of the Cholic Acid which, being present in larger amount, sticks on the surface even at very low dye coverages, reducing the recombination that would be present if those areas would have been exposed to the electrolyte. Lifetime decreases on devices with higher dye coverage, and this result has been ascribed to the possibility that increasing amount of dye could enhance the recombination reaction[25]. This trend of the electron lifetime has been confirmed by IMVS measurements.

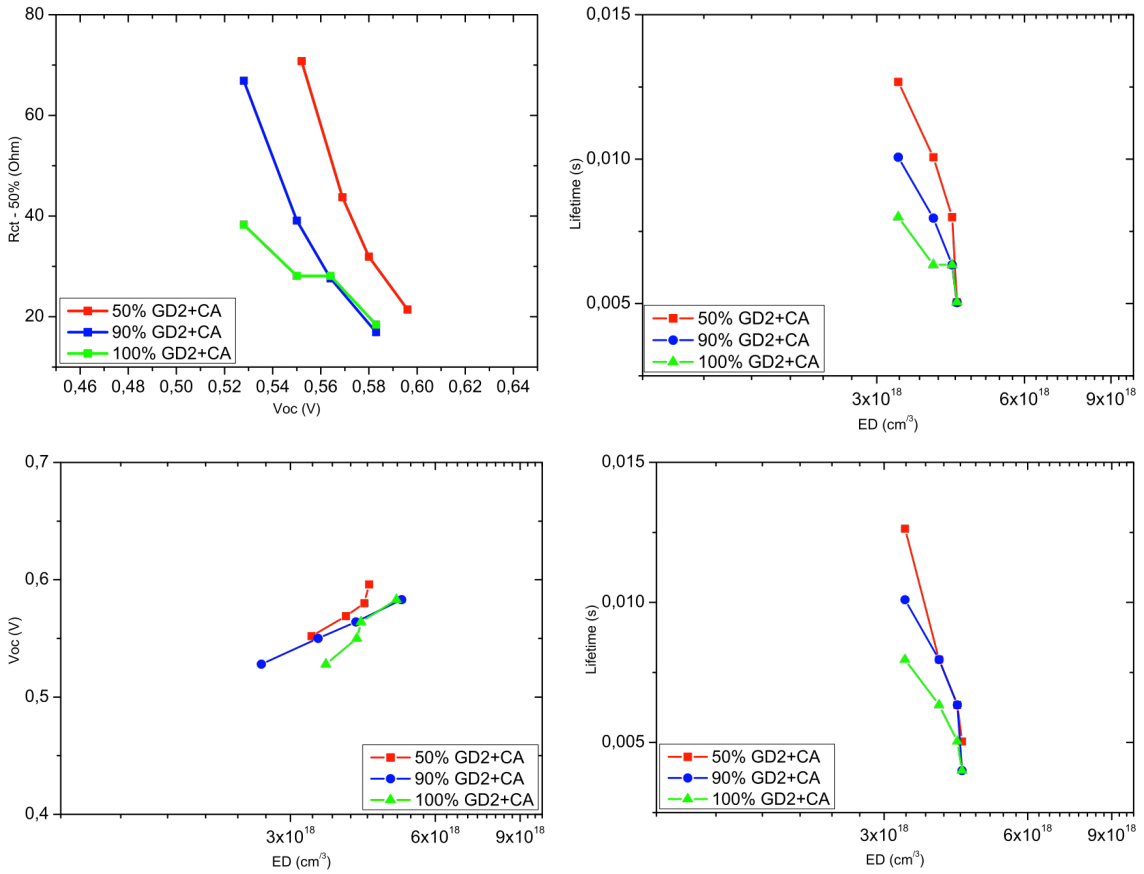

Figure 33: charge transfer recombination R_{ct} (top left), electron lifetime obtained by EIS (top right), open circuit potential V_{oc} (bottom left), lifetime obtained by IMVS (bottom right) of GD2 + CA partially loaded photoanodes.

3.6 Conclusions

In this work I described the construction and characterization of Dye-Sensitized Solar Cells, specifically optimized for dyes with high extinction coefficients, created and assembled using state of the art techniques. In particular the sensitization process was performed fluxing the dye solution over freshly prepared photo-anodes and monitoring the dye-uptake in real-time using a custom-made system which integrated a fluidic section with an optic fiber spectrophotometer. The flow technique allowed the direct investigation of several aspects involved in the sensitization process, such as: adsorption kinetics; influence of the solvent; influence of dye concentration; presence of co-adsorbates and dye loading effects. These aspects were studied with characterization techniques such as solar simulator (J-V and IPCE) and fequency dependant techniques (EIS, IMVS and IMPS). Results showed that the selection of the right solvent may improve the sensitization process and reduce the dye desorption resulting in efficiency improvements. The concentration of the sensitizer is also a critical aspect which need to

be adjusted in order to find a compromise between adsorption time and photovoltaic characteristics that influence the efficiencies. Moreover, the presence of Cholic Acid was found to improve the adsorption kinetics, which were well described as a pseudo-first order mechanism. I was also able to control the loading of the sensitizer up to different and defined levels, which allowed to study the effect of the dye coverage in flow sensitized photoanodes. In addition, the influence of Cholic Acid was studied in these conditions of partial coverage. When only GD2 is fluxed at different percentages of TiO_2 coverage, efficiencies and photovoltaic parameters were similar until 90% of loading, while a significant improvement in efficiency was obtained when full coverage was reached, probably due to the blocking layer properties of GD2. In the presence of Cholic Acid and repeating the experiments at the same dye loadings, all efficiencies were improved, meaning that its blocking properties are already important when the loading of the dye was stopped at 50%, while moving at 90% of coverage induced a consistent increasing in the efficiency of the DSSC, which remained unchanged when full coverage was obtained.

4. TiO_2 surface engineering for DSSC applications

4.1 Engineering strategies for TiO_2 functionalization

Among the strategies studied for improving the processes involved at the TiO_2/Dye interface, I decided to focus on those characterized by the engineering of the surface, an approach slightly different from the methods that have already been described in the previous chapters (e.g. co-sensitization, structure optimization, etc.). In the last few years, molecular host/guest systems has gained importance in this field. A host molecules can act as an encapsulating agent for the dye, protecting it from degradation and creating a physical barrier so that the electrolyte is not in direct contact with the semiconductor surface. Galoppini et al. demonstrated how a host/guest system might be used to shield and bind organic molecules on the TiO_2 surface by complexation. In particular, this extensive study involved several host molecules such as cyclodextrins, calixarenes, curcubiturils and hemicarcerands[26]. In some cases, the host/guest complexes were initially prepared in solution and then bound to the surface of the semiconductor. However, in most of the examples reported in the literature, the mesoporous TiO_2 layer was first treated with the host molecule then exposed to the dye molecule acting as a guest. Since this Thesis involved the use of cyclodextrin derivatives, in the next paragraph I will describe the structure and the properties of these macrocycles, together with some competent examples in the field of DSSCs.

4.2 Cyclodextrins in DSSCs

4.2.1 Structure and properties

Cycodextrins (CDs) are a class of cyclic compounds composed by six, seven and eight glucopyranose units linked by α-(1,4)-glycosidic bonds and named alpha, beta and gamma cyclodestrins, respectively. CDs are produced by enzymatic degradation of starch. Each glucopyranose bears two secondary hydroxyl groups and one primary OH functionality. These molecules have a torus shape with an hydrophobic cavity with two entrances. On the narrow side of the cyclodextrin we found the primary hydroxyl groups, while on the wider side we found the secondary hydroxyl groups (Figure 34).

As a result of this structure, the cavity is apolar while the exterior part of the molecule has a hydrophilic character. This biphilic nature is the basis of their widespread range of applications.

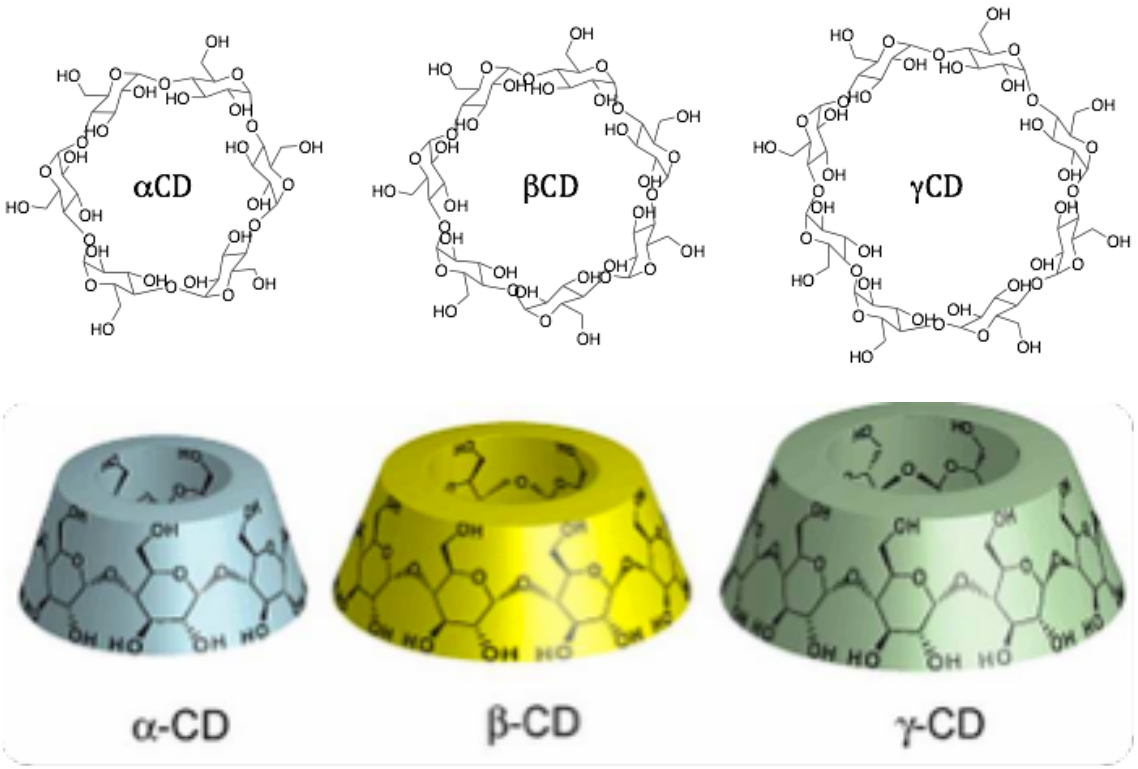

Figure 34: cyclic structure of α, β and γ cyclodextrins, respectively composed by 6, 7 and 8 glucose units.

Indeed, CDs are used to solubilize apolar molecules in aqueous environment thanks to their encapsulation within the cavity of the macrocycle (within the range of dimensions that fit with the cavity). The solubility in water is made possible by the hydrophilic surface of CDs. Due to intramolecular hydrogen bonding between OH functionalities, the CDs are quite rigid receptors. Also the differences in water solubility of the CDs can be explained on the basis of hydrogen bonding formation. α-cyclodextrin has only four hydrogen bonds and γ-cyclodextrin structure is non-planar, so that their solubilities are the highest. On the other hand, in β-cyclodextrin the hydroxyl groups are all involved in H-bonding, resulting in lower water solubility solubility and increased rigidity[27] of the cavity.

4.2.2 Examples of cyclodextrin based immobilization of dyes onto TiO_2

Haque and Durrant demonstrated that is possible to immobilize an azo dye with no affinity for TiO_2 surface by threading it through a cyclodextrin cavity attached to TiO_2 via hydroxyl interaction (Figure 35). The formation of this rotaxane host-guest compound on the surface affects the recombination rate in a DSSC. More precisely, the rate of the back electron transfer from the TiO_2 to the dye/CD complex is reduced because of the blocking effect exerted by the cyclodextrin[28].

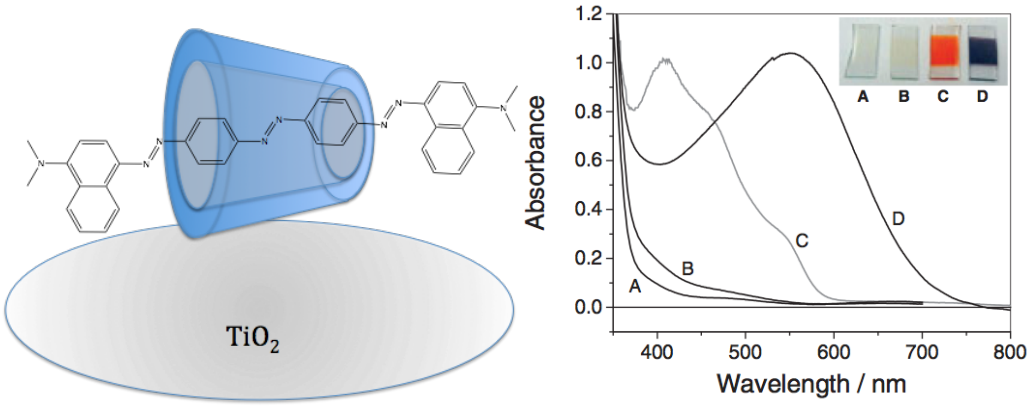

Figure 35: proposed binding mode of the azo dye-cyclodextrin complex on the surface of a titanium dioxide surface (left). In the picture on the right (Adv. Mater. 2004, 16, No. 14) letters B and D indicate the UV-Vis absorption spectra of the azo dye (B) and the rotaxane (D) on the TiO_2. The first shows no affinity for TiO_2 giving an absorption spectrum similar to TiO_2 alone (A), whereas the complex with the cyclodextrin gives an intense violet colored photoanode (D).

Toma et al. used a carboxylic acid modified cyclodextrin to chemiadsorb onto a TiO_2 mesoporous layer and successively binding a chromophore that does not possess any anchoring group in the structure (Figure 36)[18b]. The binding of the carboxy-cyclodextrin (called CMBCD in the work) is performed before the sensitization process with the dye, by dipping the photoanode in an aqueous solution of CMBCD. An iron complex with terpyridine with an intense violet colour is used as sensitizer and its characteristic colour appears only on photoanodes which have been previously functionalized with CMBCD (Figure 36a), while simple TiO_2 electrodes are colourless (Figure 36b).

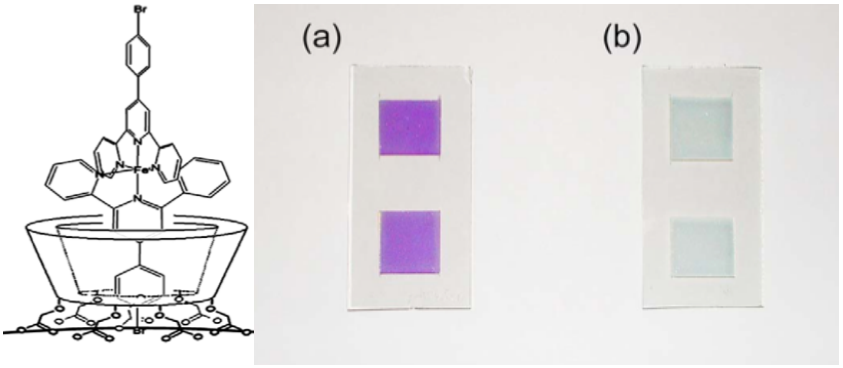

Figure 36: proposed structure for the iron terpyridine complex encapsulated into the carboxyl modified cyclodextrin on TiO_2 surface (left). Evidence of (a) chromophore binding on CMBCD functionalized photoanodes compared with (b) pristine TiO_2 layers (picture on the right). (Surface Science 600 (2006) 4591–4597)

More recently, Ko and Graetzel, investigated the influence of cyclodextrin functionalized TiO_2 photoanodes on photovoltaic parameters[18a] of DSSCs. Cyclodextrins were bound on the semiconductor surface by dipping the working electrodes into an aqueous solution of α, β or γ CD. After rinsing and drying, the photoanodes were immersed into the sensitizer solution. Efficiency measurements showed an improvement of 1.23% of the overall photovoltaic performances when βCD was used together with JK-2 dye (see table 4), this behaviour was explained as the result of dye encapsulation into the cyclodextrin cavity (Figure 37).

Dye	**Jsc ($mA*cm^{-2}$)**	**Voc (V)**	**Efficiency (%)**
JK-2	14.51	0.70	7.42
JK-2/DCA	14.85	0.73	8.01
JK-2/βCD	15.34	0.76	8.65

Table 4: reported efficiencies for TiO_2 photoanodes sensitized with JK-2, JK-2 co-adsorbed with a classical co-sensitizer as deoxycholix acid (DCA); JK-2 encapsulated into βCD. (Source of data: Angew. Chem. Int. Ed. 2009, 48, 5938 –5941).

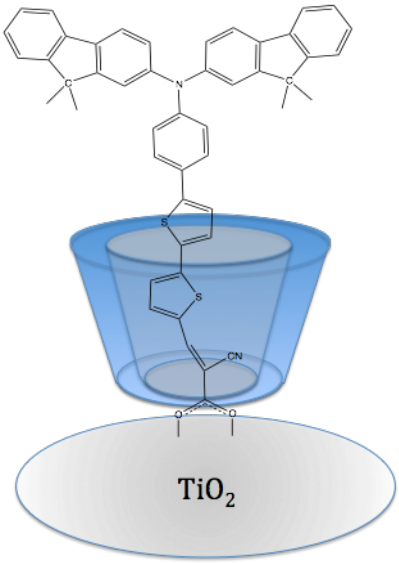

Figure 37: suggested binding mode of JK-2 encapsulated into β-CD functionalized TiO_2.

Although it has been demonstrated that the amount of cyclodextrin bound on the surface increases with the number of OH groups, the orientation of cyclodextrins on TiO_2 (i.e primary vs. secondary side) is still under debate. For example, Zhang and Yang studied the role of βCD in the degradation of some bisphenols and found that cyclodextrin bound on titanium dioxide preferentially by the secondary side, thus exposing the narrower entrance (corresponding to the primary hydroxyl side) of its apolar cavity to the solution. Moreover, they could demonstrate that uncovered regions were left on TiO_2 upon absorption of βCD since that less than a monolayer was attached. Interestingly, the cyclodextrin attached by their secondary (wider) side on the semiconductor surface were able to efficiently drive the degradation of the bisphenols that were able to enter it cavity from either the wider and the narrower side, while it was found that degradation of a bisphenol which was only able to acces the cavity by its wider side, was inhibited, giving an indirect proof of the orientation of the cyclodextrin macrocycle on the TiO_2 surface.

As far as the DSSCs are concerned, the binding of CD on TiO_2 may favour or disfavour the dye uptake depending on the orientation of the host molecule on the surface of TiO_2. As explained earlier, βCD it is supposed to bind preferentially by the secondary side, since the secondary OH groups are present in double amount with respect to primary hydroxyl groups. As a consequence of this preferential orientation, only the narrower side of the cavity is available to the complexation

with the sensitizer. Thus, a better understanding of the nature of the interface functionalized with cyclodextrin co-adsorbates is needed in order to correctly evaluate the possible variations of the photovoltaic parameters and possibly to optimize the system leading to better efficiencies and device stabilities. To this aim, I used some indirect techniques such as, contact angle, thermogravimetry, dye loading measurement by UV-Vis spectroscopy. Furthermore, I followed the sensitization process in real-time under continuous-flow conditions in order to easily track differences in the dye adsorption depending on the TiO_2 treatment.

4.3 Dye used for the study of CD functionalized photoanodes

Two dyes have been used in this study, namely TFAT (a so-called Donor-π-Acceptor dye) and ZnTMCP (a porphyrin dye).

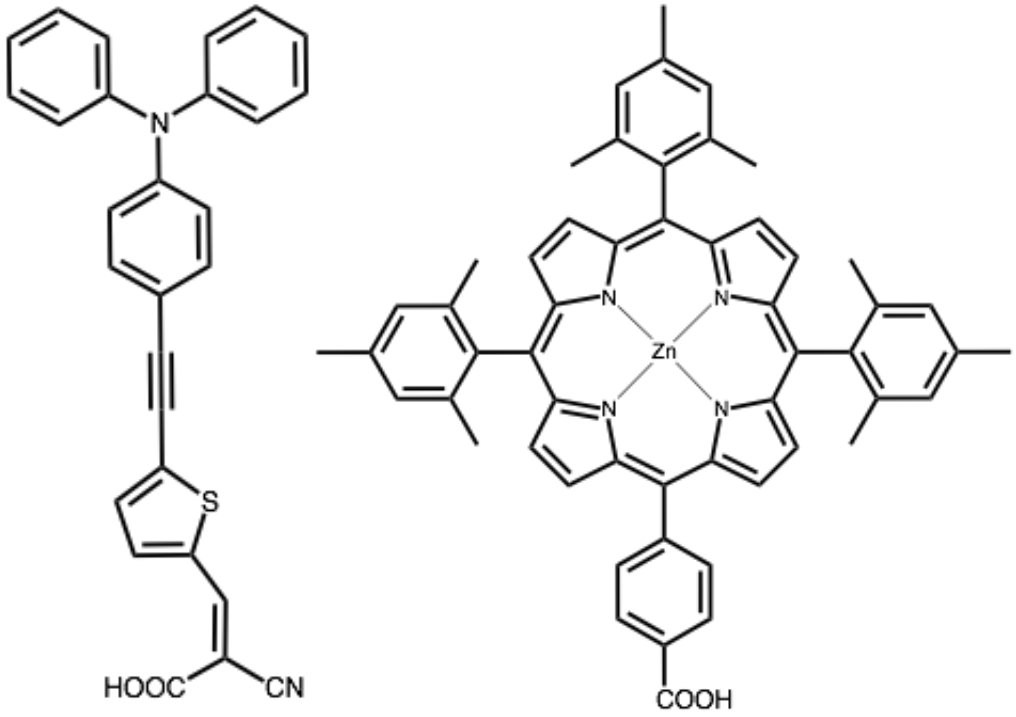

Figure 38: TFAT donor-acceptor dye (left) and ZnTMCP porphyrin dye (right) used in this study. Both dyes possess only one carboxylic acid functionality for TiO_2 chemisorption.

TFAT (2-Cyano-3-(5-((4-(diphenylamino)phenyl)ethynyl)thiophen-2-yl)acrylic acid) possess a triphenylamino moiety which act as an electron donor and it is widely used also similar dyes, generally bearing some substituents on it. The triple bond acts as conjugated π-bridge, which drives the electron density to the cyanoacrylic acceptor group bearing the carboxylic acid group. ZnTMCP (5-(4-carboxyphenyl)-10,15,20-

tris(2,4,6-methylpheny)porphyrin) belongs to the porphyrinic dye category. Due the hindering of three mesityl substituents at the *meso* positions, the rings are slightly tilted with respect to the porphyrin ring. Furthermore, the methyl groups in 2,4,6 positions of the ring help to decrease dye aggregation through steric hindrance. The fourth substituent is a benzoic acid moiety for the binding of the porphyrin onto the TiO_2 surface. ZnTMCP is also metallated by inserting a Zn^{2+} cation into the porphyrinic macrocycle (Figure 38). The photovoltaic efficiency of these simple dyes are around 5.0%[29] and 2.0%[30] for TFAT and ZnTMCP respectively. However, ZnTMCP has been tested again in 2009 by the same author in a different paper, reporting an efficiency of 4.6%. This is to clarify in what amount testing conditions may influence the efficiency measurements, resulting in a significant variability among different laboratories.

4.4 Cyclodextrins used in this work

In the following chapter I studied the adsorption behaviour and the effect on photovoltaic parameters of a simple βCD (called βCD1) and a modified cyclodextrin appositely synthesized, bearing seven COOH groups on the narrower side of the cavity and completely methylated on the secondary side, in order to drive the binding direction through the high affinity of the carboxylic groups for the TiO_2.

The synthesis of the modified β-Cyclodextrin (βCD2 - Figure 39), has been performed in four steps, involving 1) the protection of primary alcohol moiety with silyl groups (Heptakis(6-O-tert-Butylmethylsilyl)cyclomaltoheptaose), 2) exhaustive methylation of secondary hydroxyls (Heptakis(6-O-tert-Butylmethylsilyl-2,3-di-O-methyl)cyclomaltoheptaose), 3) removal of silyl protection (Heptakis(2,3-di-O-methyl)cyclomaltoheptaose) and 4) oxidation (Per(5-carboxy-5-dehydroxy-2,3-di-O-methyl)cyclomaltoheptaose) of primary hydroxyls, resulting in a β-CD with the hydroxyl groups selectively oxidized to carboxylic acids on the narrower side and fully methylated on the wider side of the CD macrocycle.

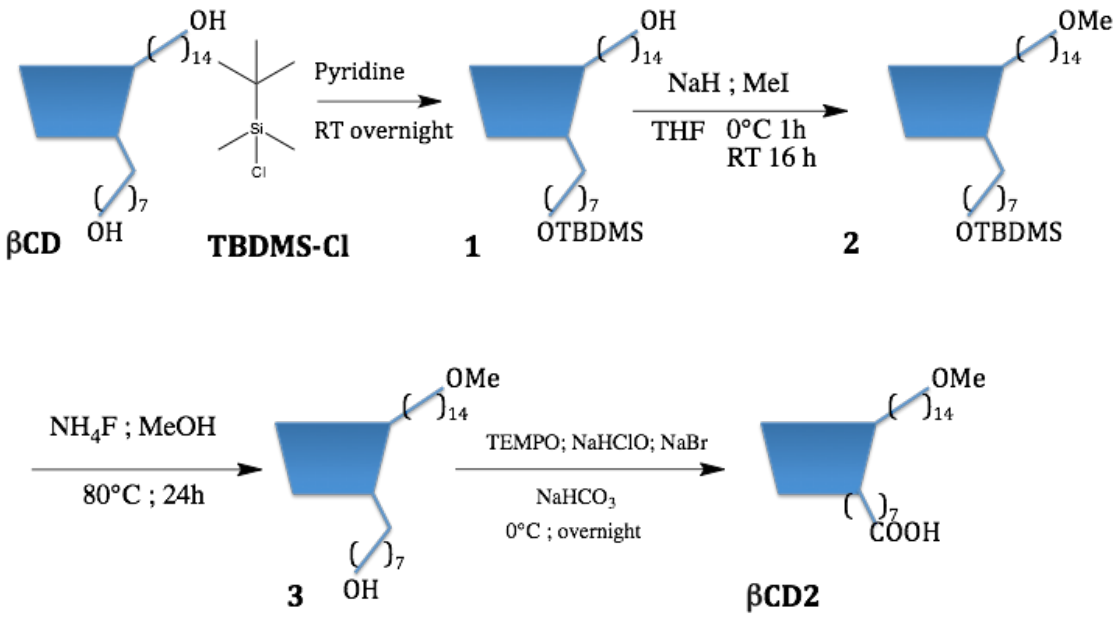

Figure 39: scheme of the four step synthesis path of βCD2.

4.4.1 Synthesis of Heptakis(6-O-tert-Butylmethylsilyl)cyclomaltoheptaose (1)

The first three steps of this procedure have been performed following a protocol reported in literature[31]. The synthesis started with the protection of the seven primary hydroxyl groups of βCD to prevent their methylation in the following synthetic step. The protecting group used was the tert-butyldimethylsilylchloride (TBDMS-Cl) which is know to selectively protect the more reactive primary hydroxy functions. The βCD sample was lyophilized to remove the crystallization water then it was dissolved in dry pyridine and temperature was lowered to 0°C by an ice bath. TBDMS-Cl was added and stirred at room temperature. When the reaction was judged complete by TLC analysis, compound 1 (Figure 39) was precipitated by addition of a large amount of water and recovered by filtration. It was purified twice by recrystallization first with CH2Cl2/ MeOH then with CH2Cl2/acetone. The final yield was 34%. The identity of the product was confirmed by MALDI-TOF showing the mass of the protected βCD as an adduct with endogenous Na+ or K+ cations. Purity of 1 was also confirmed by 1H-NMR showing the appearance of a new signal corresponding to the methyls of the TBDMS protecting group[32].

4.4.2 Synthesis of Heptakis(6-O-tert-Butylmethylsilyl-2,3-di-O-methyl)cyclomaltoheptaose (2)

The second step involved the methylation of the secondary hydroxyls of 1 with iodomethane in the presence of sodium hydride. NaH was suspended in anhydrous THF under nitrogen atmosphere in a ice bath at 0°C, then compound 1 was added to the solution. Iodomethane was added dropwise to reaction followed by heating at 40°C 30 minutes then left under stirring overnight a room temperature. Unreacted NaH was quenched carefully adding small portions of MeOH. Solvent was evaporated and the residue was resuspended in hexane and filtered to remove salts. Hexane was evaporated obtaining 2.46 g of 2 (56% yield) which was directly employed in the following step without further purification.

4.4.3 Synthesis of Heptakis(2,3-di-O-methyl)cyclomaltoheptaose (3)

Deprotection of primary hydroxyls was carried out with NH_4F in MeOH under reflux overnight. The solvent was removed under vacuum and the remaining residue was dissolved in CH_2Cl_2 and filtered on Na_2SO_4 to remove salts. After removing the solvent, compound 3 was recovered in a nearly quantitative yield (1.6 g).

4.4.4 Synthesis of Per(5-carboxy-5-dehydroxy-2,3-di-O-methyl)cyclomaltoheptaose (βCD2)

Oxidation of the primary hydroxyls of compound 3 was performed using TEMPO[33]. During the oxidation the pH of the solution was kept around 10 by adding NaOH. The reaction was left overnight under stirring. The TEMPO excess was quenched by addition of few mL of MeOH. βCD2 was purified by dialysis with a Pur-A-Lyzer membrane with a cut-off of 1000 Da. However, this purification method turned out to be detrimental for the yield. An alternative purification protocol was based on dissolving the reaction product in hot MeOH and filtering when still warm. Then the βCD2 was precipitated by addition of a large volume of acetone resulting white amorphous which slowly settled down[33]. The precipitated was filtered and dried under vacuum. In order to have all the carboxylic groups in the protonated form, a strongly acidic exchange resin (Amberlite IRA-120) was employed in aqueous conditions. In this step a large amount of product was lost due to the several workup attempts, finally producing only 200 mg on βCD2 after lyophilisation. However, this amount of βCD2 was enough to perform the experiments on TiO_2.

4.5 Results and discussion

4.5.1 Flow technique for the monitoring of TFAT and ZnTMCP dye uptake:

Using the flow technique for real-time dye uptake monitoring I sensitized different photoanodes of made of pristine TiO_2, or covered with βCD1 (βCD1/TiO_2 or βCD2 (βCD2/TiO_2). Figure 40 reports the absorbance profiles measured on 2 μm thick photoanodes. ZnTMCP uptake proceed as expected (Figure 40, purple trace), with an initial fast increase of the absorbance region followed by a plateau corresponding to saturation of surface binding sites. On the other hand, the same experiment carried out on a βCD1 treated photoanode resulted in a slower dye adsorption (Figure 40, blue trace) and a lower plateau absorbance value likely due to the fact that some of the surface sites are now occupied by the cyclodextrin moiety. Finally, when βCD2 was bound to the surface the uptake of ZnTMCP showed an extremely slow kinetic (Figure 40, red trace), reason for which the loading with the flow technique was stopped before saturation of available sites (6000 seconds).

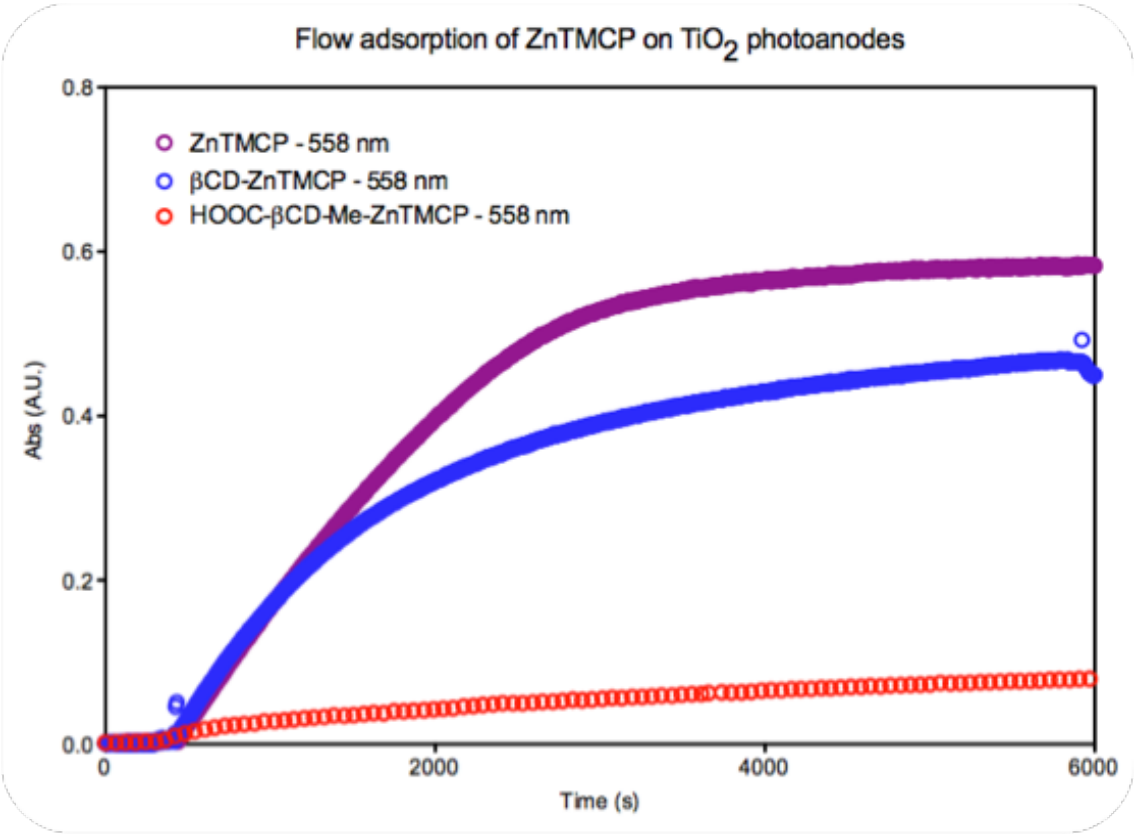

Figure 40: flow uptake of ZnTMCP on bare TiO_2 (violet), βCD1/TiO_2 (blue) and βCD2/TiO_2 (red).

The flow sensitization technique has some technical limits due to the equipment used, such as the difficulty to follow the absorbance of the TFAT dye which has an absorbance maximum around 425 nm, a region where the light intensity of the lamp is not enough, resulting in high signal to noise ratio of the spectra. In order to avoid this problem and because of increased sensitization time needed by photoanodes functionalized with βCD2 I switched to the classical sensitization method by dipping for the remaining part of this chapter.

4.5.2 Sensitization by dipping:

For studying the effects of βCD1 and βCD2 I decided to use a more classic approach based on the sensitization through a dipping procedure. In Figure 41 is reported the protocol used: a freshly prepared photoanode is immersed into a cyclodextrin solution overnight (17 h). Then, after rinsing and drying, the anode is dipped into the solution of the sensitizer and left overnight (17 h). I prepared at least three βCD1 and βCD2 functionalized photoanodes, which were subsequently sensitized with TFAT and ZnTMCP as reported in Table 5.

Solution	**Photoanodes**		
	TiO_2	**βCD1/TiO_2**	**βCD2/TiO_2**
βCD1	βCD1/TiO_2	/	/
βCD2	βCD2/TiO_2	/	/
TFAT	TFAT/TiO_2	TFAT/βCD1/TiO_2	TFAT/βCD2/TiO_2
ZnTMCP	ZnTMCP/TiO_2	ZnTMCP/βCD1/TiO_2	ZnTMCP/βCD2/TiO_2

Table 5: columns represent the photoanodes (functionalized with βCD or not) which are immersed into the corresponding solution of βCD or dye (rows in the table). Some TiO_2 electrodes are only sensitized with cyclodextrins in order to evaluate the loading.

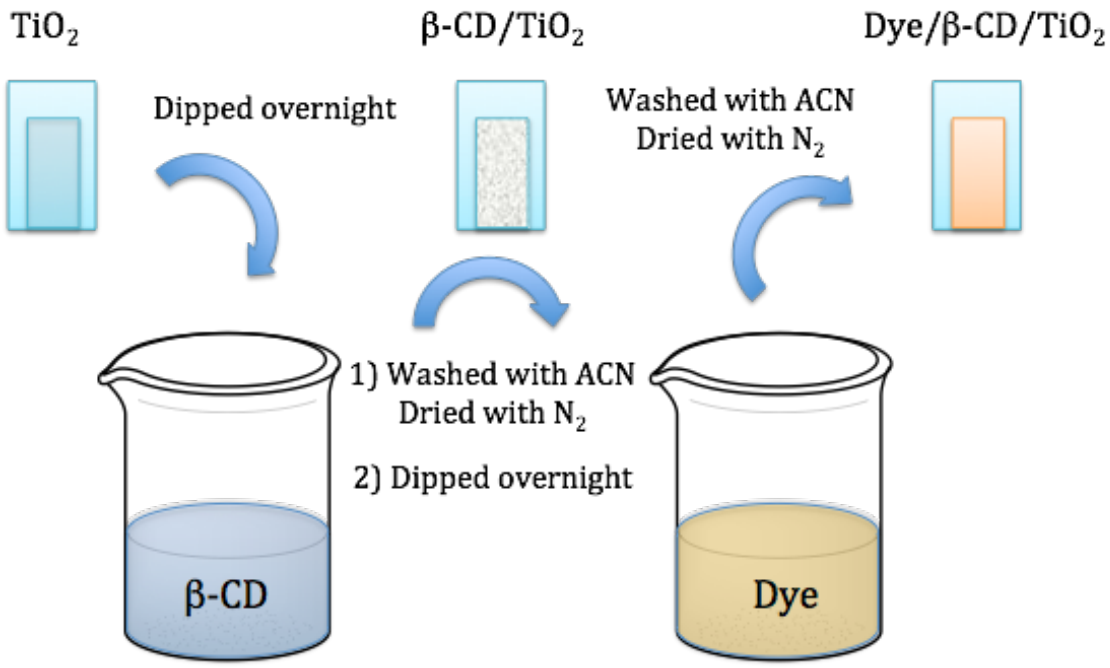

Figure 41: schematic view of the process of functionalization of TiO_2 photoanodes with cyclodextrins, followed by sensitization with the dye.

A new set of photoanodes is prepared each time that a new measurement has to be realized because it is important to perform the measurements as soon as possible in order to minimize possible degradations. In addition, most of the techniques used are destructive for the substrate.

4.5.3 Contact angle measurements:

Indirect evidence for the surface functionalization is obtained by dynamic contact angle measurements on an 8 cm^2 mesoporous oxide area. Since the TiO_2 hydrophilicity could vary upon exposure of the oxide to ultraviolet radiation, all the samples are kept in the dark before measurements. Different samples of $\beta CD1/TiO_2$, $\beta CD2/TiO_2$ and pristine TiO_2 showed similar contact angles meaning that the hydrophilicity of the surface did not significantly change (Figure 42). The highest contact angle is found when only TFAT is bound TiO_2 with the hydrophobicity of the surface decreasing on TiO_2 treated with cyclodextrins in the order $TFAT/\beta CD1/TiO_2 > TFAT/\beta CD_2/TiO_2$. A similar trend is obtained for ZnTMCP dye.

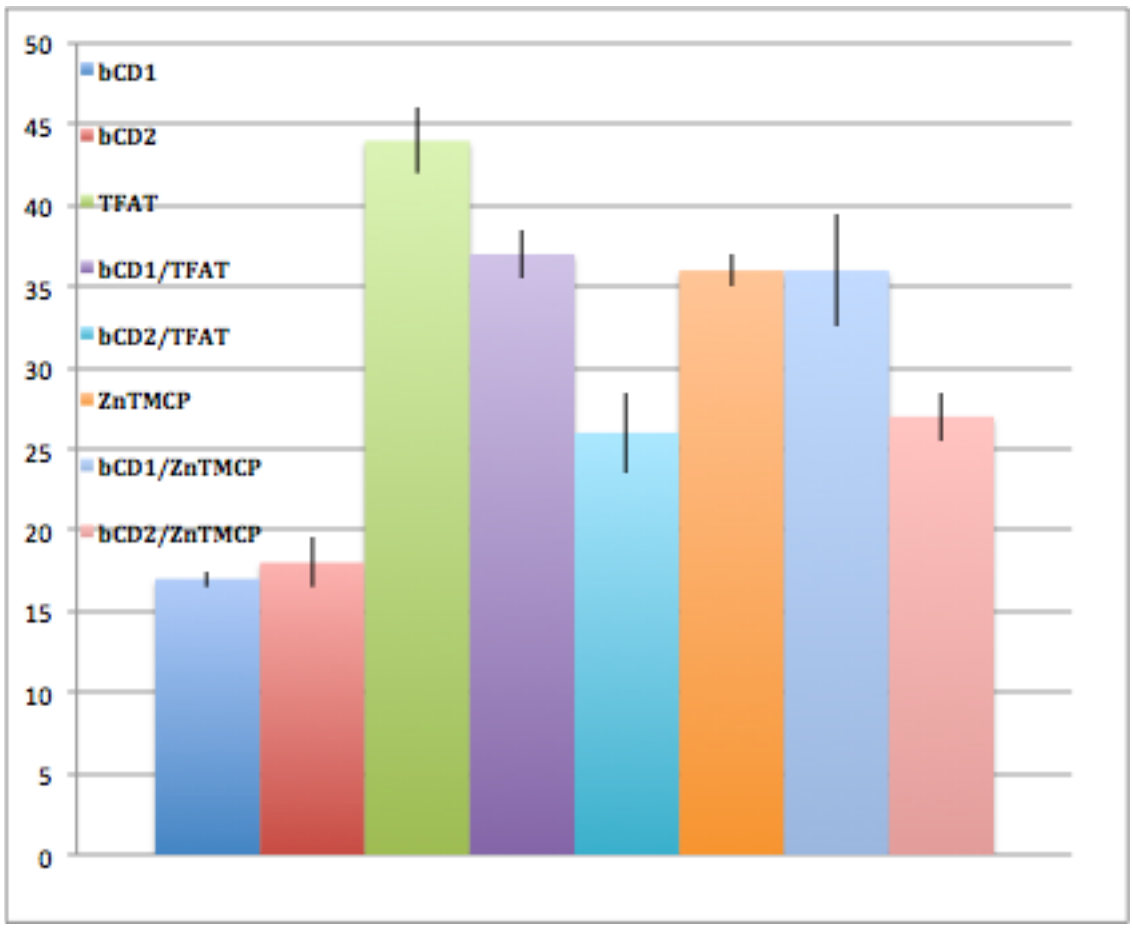

Figure 42: contact angle of photoanodes treated with βCD1 and βCD2.

4.5.4 Spectrophotometric analysis on sensitized photoanodes

Spectrophotometric analysis of sensitized photoanodes is a valuable tool for the characterization of DSSCs since it allows to acquire quantitative informations on the binding of the dye to the photoanodes. In particular, when upon absorption on TiO_2 a shift in the absorbance of the dye appears, it is even possible to gather informations on the coupling mode between the dye and the semiconductor surface. As depicted in Figure 43 the UV-Vis absorption of TiO_2 photoanodes sensitized with the dye only, present the most intense spectra with an absorption band broadened with respect to the spectra recorded in solution, possibly due to dye aggregation on the semiconductor surface. When βCD1 functionalized TiO_2 is used, the absorbance strongly decrease, meaning that a lower amount of dye can bind the surface due to the presence of the co-adsorbate12. The decreasing in absorbance is even more marked with βCD2, probably due to its higher affinity for the TiO_2.

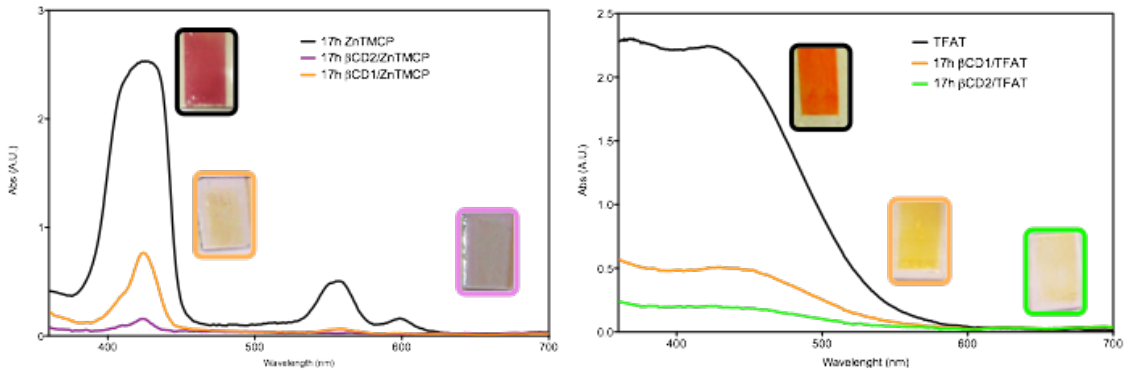

Figure 43: absorbance spectra of ZnTMCP (on the left) and TFAT (on the right) dyes on TiO_2 photoanodes. On cyclodextrin functionalized working electrodes, the overall absorbance decreases in the order βCD1/TiO_2 > βCD2/TiO_2.

4.5.6 Thermogravimetric analysis for dye loading evaluation

Dye loading on the photoanodes is estimated by thermogravimetric analysis. In the graphics of Figure 44 on the ordinate reported the moles of dye normalized to 1 mg of mesoporous TiO_2 are reported. This allows to compare more easily the amount of the different dyes bound to the photoanodes and avoid the small variations of titanium dioxide amount because of the manual preparation of the photoanodes. The trend in the dye loading follows what is expected from the spectrophotometric analysis (Figure 43) with the amount of dye that decreases when the photoanode is treated with βCD1 and βCD2. This result confirms that the co-adsorbate is firmly bound on the surface thus decreasing the number of active sites available for the dye. However, the error associated to the measurements is significantly high due to very low amounts of sample used, 10^{-3} of TiO_2 with loss of weight among 5 and 15% correspond approximately to 10^{-4} to 10^{-5} grams of organic molecules bound to the surface, a value which is near the detection limits of the instrument. On the other hand, the estimated amount of cyclodextrins is about $6*10^{-8}$ $mol*mg^{-1}_{TiO2}$ which correspond to an area formally covered by the cyclodextrins of 0.052 m^2 (based on a molecular model of the cyclodextrin). Since the TiO_2 surface area is about 0.095 $m^2*g^{-1}_{TiO2}$ (data supplied by Solaronix) an estimated coverage of 55% can be calculated, suggesting that less than a monolayer of CD is present on the titania surface. Nevertheless, this result does not preclude the possibility of lowering the recombination, hence a better device performance could be anticipated for these photoanodes after sensitization[28].

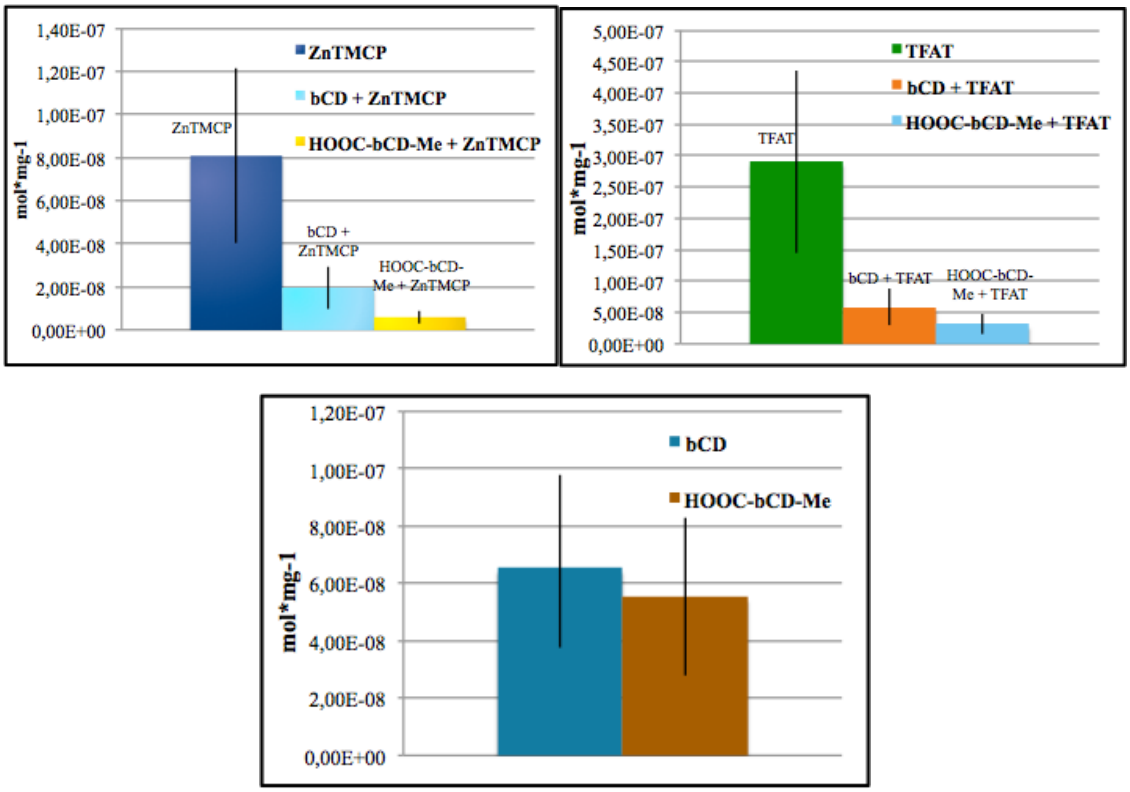

Figure 44: moles of organic molecule bound to the surface of mesoporous TiO_2. ZnTMCP (up left) and TFAT (up right) amounts of dye are showed in the graphic. Dye loading decreases when βCD1 is bound on the oxide. The lowest amount of dye uptake is found for photoanodes treated with βCD2. The amounts of cyclodextrins calculated by TGA (center bottom graphic) is similar for βCD1 and βCD2 but led to different amounts of dye bound on the photoanodes.

4.5.7 Spectrophotometric evaluation of dye loading

I measured the dye loading also by classical methods using UV-Vis spectroscopy. When a co-adsorbate is used, it is important to optimize the dye/co-adsorbate ratio, in order to lower the aggregation and to create a blocking layer on free spaces left on TiO_2 without decreasing the amount of dye that binds the titanium dioxide surface below a critical threshold to achieve good efficiencies. Since the common sensitization protocol uses the co-adsorbate dissolved into the sensitizer solution, the optimization is usually performed by dipping different photoanodes in various solutions in which the co-adsorbate concentration is systematically varied while keeping constant the dye concentration. However, in the protocol followed in this Thesis the functionalization is performed in a separated step prior to sensitization. Therefore, in order to obtain results comparable with literature, I decided to change the exposition time of the photoanodes to the cyclodextrins solution rather than the concentration of the CD solution. In addition to the photoanode sensitized for 17 h as reported previously in Table 5 as a blank experiments with no CD applied, I prepared three working electrodes exposed to

cyclodextrins solutions for 1, 2 and 5 hours. These electrodes were subsequently sensitized by dipping for 17 hours into the solution of the dye. The effective dye loading is measured by UV-vis spectroscopy after desorption of the dye in a known amount of a 0.1 M NaOH solution in THF/H2O (1:1). The dye uptake on the mesoporous oxide decreases upon increasing the functionalization time. In particular, after one hour of immersion in βCD1, its concentration is approximatively half of the dye loaded on electrode not exposed to CD (Figure 45). On βCD2 functionalized photoanodes, the amount of dye loaded is one order of magnitude lower than in the case of photoanodes treated with βCD1, confirming that the cyclodextrin modified with seven carboxylic acids on the primary side and methylated on the secondary OH groups, passivates the TiO_2 hindering the possibility of the dye to reach the active binding sites.

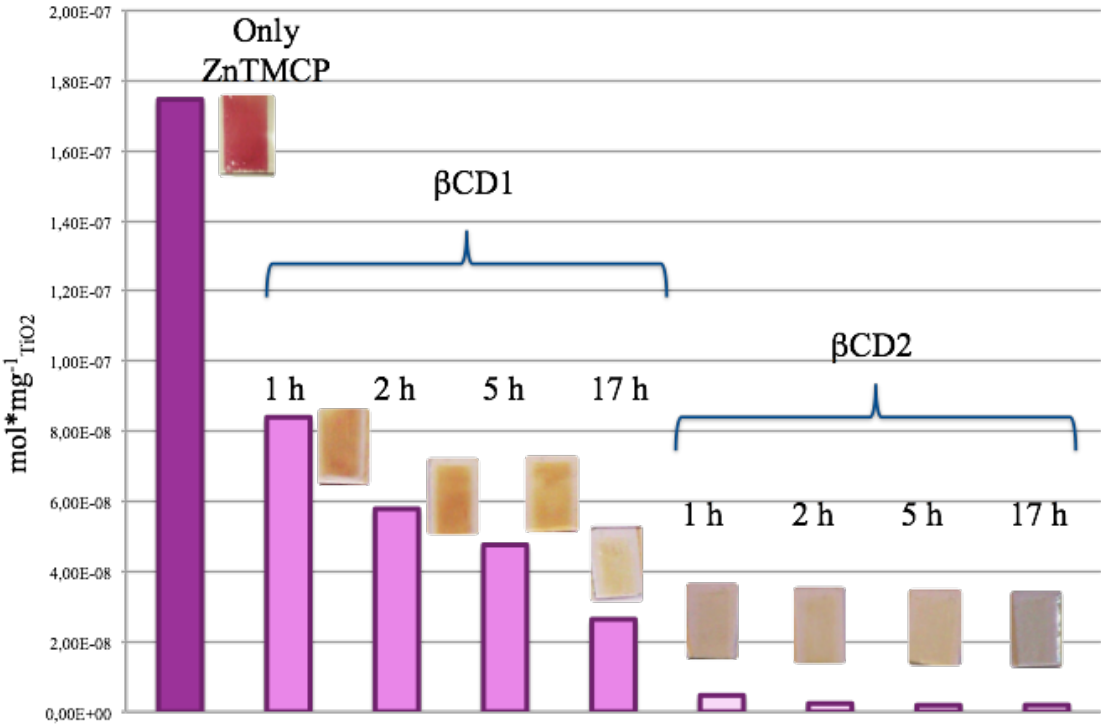

Figure 45: dye loading of ZnTMCP measured by UV-Vis spectroscopy. From left to the right we found the ZnTMCP loading obtained from TiO_2 only, βCD1 funtionalized TiO_2 (1, 2, 5 and 17 hours) and βCD2 functionalized photoanodes (1, 2, 5, 17 hours in βCD2). All the electrodes were dipped for the same time into the sensitizer solution.

The same behaviour is found when TFAT is the sensitizer (Figure 46), namely increasing the dipping time into the cyclodextrin solution, the amount of dye loaded on the surface decreases. Also, in this case all the measured values for βCD2 functionalized photoanodes are lower.

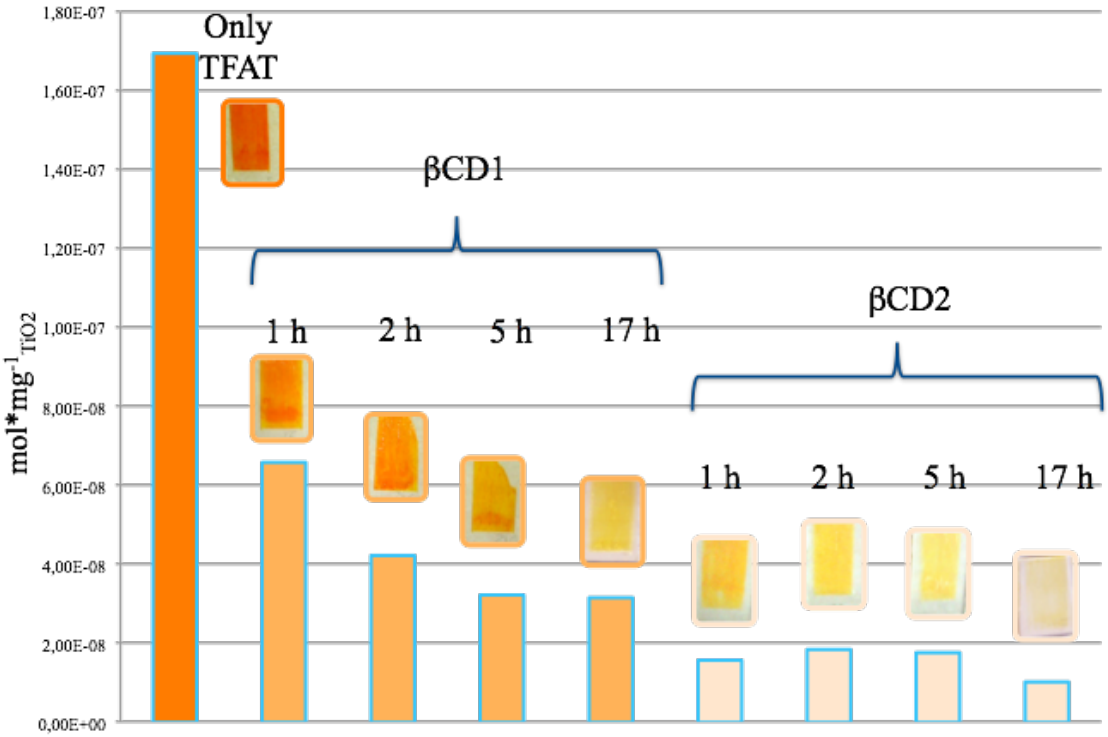

Figure 46: dye loading of TFAT measured by UV-Vis spectroscopy. From left to the right we found the TFAT loading obtained from TiO_2 only, βCD1 functionalized TiO_2 (1, 2, 5 and 17 hours) and βCD2 functionalized photoanodes (1, 2, 5, 17 hours in βCD2). All the electrodes were dipped for the same time into the sensitizer solution.

4.5.8 Photovoltaic characterization

In collaboration with the University of Ferrara (UniFE), I measured the efficiencies of the dye sensitized solar cells completely assembled (Table 6). The devices have a blocking layer, a 4 x 4 mm active area of mesoporous TiO_2 (2 μm thick), a platinated counter-electrode and a high performance electrolyte. Initially, the efficiencies were measured for the following photoanodes: TiO_2/dye, TiO_2/βCD1/dye, and TiO_2/βCD2/.

TFAT loaded photoanodes perform better than those based on porphyrinic sensitizer. In addition, for both sensitizers, the efficiency decreases when βCD1 is present and it further decrease when TiO_2 is functionalized with βCD2 (Figure 47). This effect is likely to be related to the decreased amount of dye loaded on the photoanode. It should pointed out that, the photoanode TiO_2/βCD1/ZnTMCP showed an increased efficiency with respect to both TiO_2/dye and TiO_2/βCD2/ZnTMCP. This interesting result was further investigated by EIS in order to understand its origin.

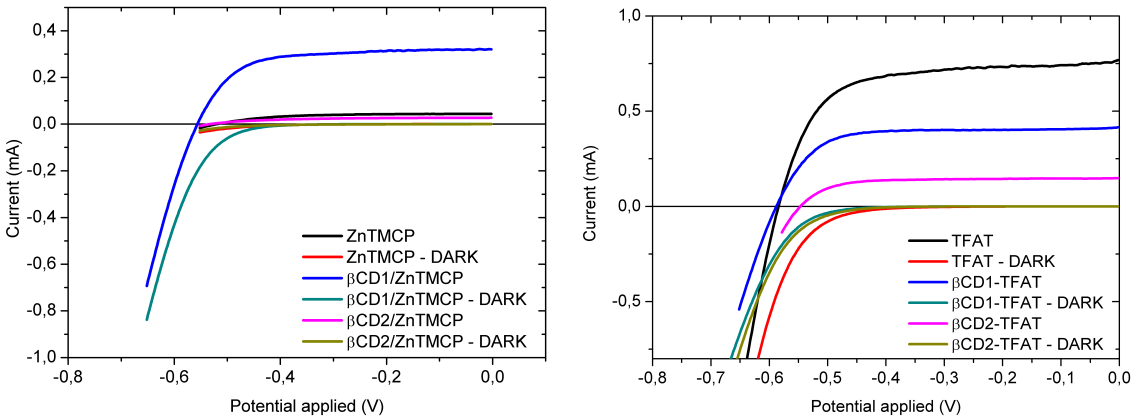

Figure 47: I-V curves TFAT (on the left) and ZnTMCP (on the right) sensitized TiO_2 and cyclodextrin functionalized photoanodes. TFAT efficiencies decrease in the order βCD1>βCD2. ZnTMCP showed an increased efficiency on the photoanode functionalized with βCD1 (blue line on the right graphic).

	V_{oc}	J_{sc}	V_{mpp}	J_{mpp}	FF	η
TFAT	-0,586	5,21	-0,469	4,46	68,5	1,31
βCD1/TFAT	-0,601	3,02	-0,493	2,63	71,5	0,81
βCD2/TFAT	-0,576	1,63	-0,483	1,36	70,0	0,41
ZnTMCP	-0,522	0,30	-0,361	0,24	56,2	0,06
βCD1/ZnTMCP	-0,557	2,01	-0,444	1,68	66,6	0,47
βCD2/ZnTMCP	-0,532	0,18	-0,383	0,13	51,4	0,03

Table 6: photovoltaic parameters of DSSC reported in Figure 47. For TFAT, while Voc and FF are comparable, Jsc significantly decreases on cyclodextrin treated photoanodes.

Electrochemical impedance spectroscopy have been measured on these devices at the Voc potential under irradiation at 100 $mW*cm^{-2}$ and the results show that a longer electron lifetime is obtained with βCD1 functionalized photoanode (Figure 48). That means that once injected, the electron has more time for diffusing through the TiO_2 interface and to be collected at the FTO surface. Despite this, the efficiency is low which is probably due to the lower dye loading.

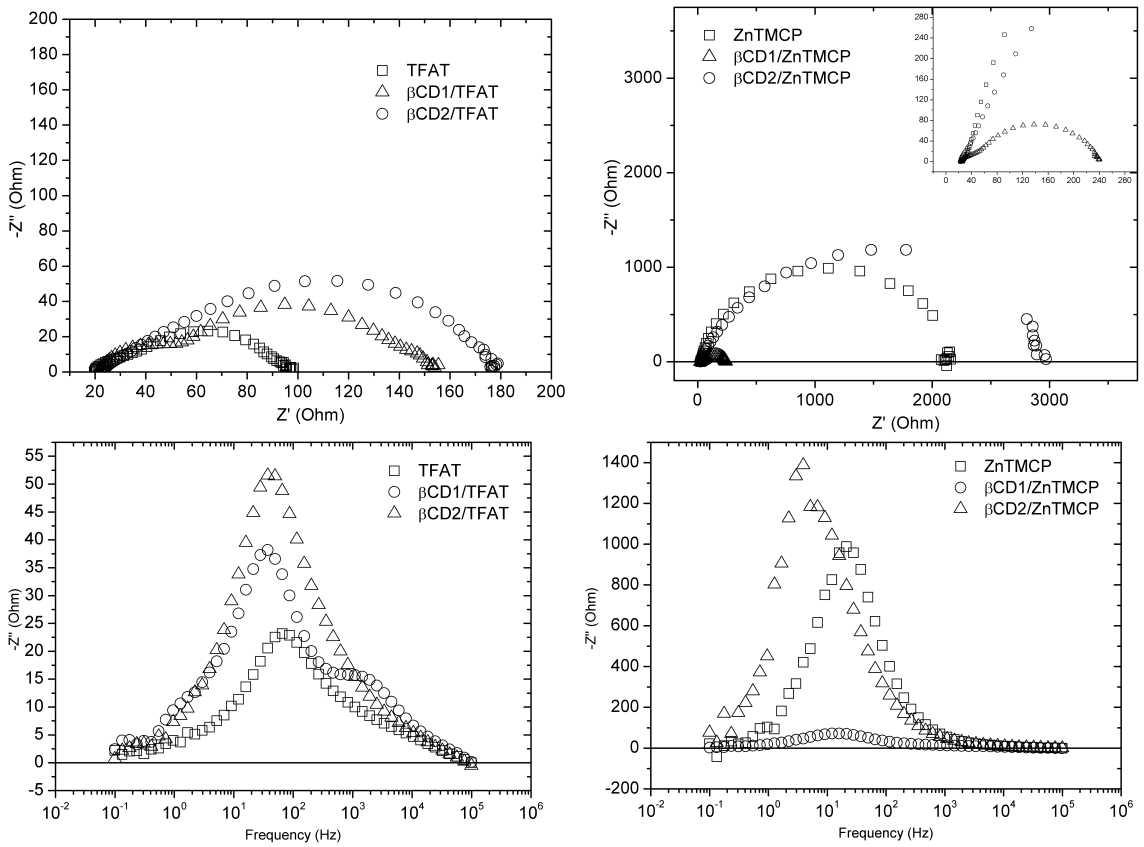

Figure 48: Nyquist plots of the impedance measured forTFAT (left) and ZnTMCP (right) photoanodes. The frequency of the peak of the imaginary parts versus frequency plot is used to find the characteristic frequency of the interface process under study (charge transfer resistance between TiO_2 and electrolyte). On the right plots, for ZnTMCP on βCD2/ZnTMCP photoanodes, an anomalous behaviour is observed which could be the origin of the lower efficiencies of the correspondent cells.

After the first sets of measurements, further J-V polarization curves have been performed. The aim of these measurements was to understand if the dipping time into cyclodextrin solution can be optimized in order to improve the photovoltaic performances. In addition, to rule out the possibility that the differences observed for ZnTMCP photoanodes were actually due to poor counter-electrodes quality, I decided to use commercially available Platinated photoanodes (Dyesol). Given the stronger affinity of βCD2 for the TiO_2, which lead to a lower amount of dye loading (i.e. lower efficiencies), a shorter functionalization time was used for βCD2 respect to βCD1 (Table 7).

Cyclodextrin	βCD1 or βCD2 Functionalization Time	TFAT or ZnTMCP sensitization time
βCD1	30 min	17 hours
βCD1	60 min	17 hours
βCD1	120 min	17 hours

Cyclodextrin	βCD1 or βCD2 Functionalization Time	TFAT or ZnTMCP sensitization time
βCD2	10 min	17 hours
βCD2	30 min	17 hours
βCD2	60 min	17 hours

Table 7: second set of measurements obtained from photoanodes which have been functionalized with cyclodextrins for shorter times. The sensitization time is kept of the same length as previous J-V characterizations for comparison purposes.

When TFAT is treated with βCD1 a significative increase in efficiency is observed for both sensitization times of 60 and 120 minutes (table 8). This is essentially due to an increased current, which together with the increase in the Voc suggest a decrease in the recombination. This effect is not present in any other of the cell measured. In particular when βCD2 is used together with ZnTMCP, very low open circuit voltages have been measured, suggesting higher recombination rates.

	Voc (V)	**Jsc ($mA*cm^{-2}$)**	**FF (%)**	**η (%)**
17 h - βCD1/TFAT	0,549	1,166	68,8	0,28
30 min - βCD1/TFAT	0,534	0,940	66,9	0,21
60 min - βCD1/TFAT	0,578	1,901	71,9	0,49
120 min - βCD1/TFAT	0,581	1,864	73,7	0,50
17 h - βCD2/TFAT	0,433	0,116	59,3	0,02
10 min - βCD2/TFAT	0,528	0,507	69,4	0,12
30 min - βCD/TFAT	0,52	0,369	66,6	0,08
60 min - βCD/TFAT	0,518	0,326	69,3	0,07
	Voc (V)	**Jsc ($mA*cm^{-2}$)**	**FF (%)**	**η (%)**
17 h - βCD1/ZnTMCP	0,46	0,153	60,8	0,027
30 min - βCD1/ZnTMCP	0,492	0,467	60,9	0,087
60 min - βCD1/ZnTMCP	0,46	0,164	52,7	0,025

120 min - βCD1/ZnTMCP	0,442	0,222	57,8	0,035
17 h - βCD2/ZnTMCP	0,328	0,034	50,4	0,004
10 min - βCD2/ZnTMCP	0,403	0,093	53,7	0,013
30 min - βCD2/ZnTMCP	0,393	0,065	53,5	0,008
60 min - βCD2/ZnTMCP	0,397	0,091	54,8	0,012

Table 8: photovoltaic parameters of photoandes treated with βCD1 and βCD2 for shorter times. On the left column it is reported the dipping time into the cyclodextrin solution together with the co-sensitizer/dye combination of the correspondent photoanode. The dashed line divides DSSC functionalized with βCD1 from those assembled using βCD2.

4.6 Conclusions:

In this chapter I investigated the effect of a beta cyclodextrin and a carboxy methyl modified cyclodextrin as co-adsorbates. Based on some papers which showed how cyclodextrins may be used as molecular insulators decreasing the back reaction rate after electron injection into the TiO_2 semiconductor, I tried to apply the same principle to TiO_2 photoanodes using a TFAT and a porphyrin dye. The dye uptakes have been monitored in flow, and very different behaviours were found when phtoanodes were treated with cyclodextrins.

The amount of dye bound on the mesoporous oxide decreases upon increasing the exposure times to the cyclodextrin solutions and this fact has been confirmed both by spectrophotometric methods and by using thermogravimetry analysis. This latter technique has been especially useful since it allowed to estimate the magnitude of cyclodextrin bound to the photoanodes, a measurement not feasible with UV-Vis since CDs do not have useful cromophores. Photovoltaic efficiencies have been measured on a first set of photoanodes where co-adsorbate and sensitizer where loaded by dipping the photoanode overnight into their solutions, and efficiencies decreased following the decrease in absorbance directly measured from the sensitized photoanodes. Some photoanodes were then functionalized for shorter times into the cyclodextrins solutions, looking for an optimal ratio co-adsorbate/dye. Moreover, those devices have been assembled using commercial counterelectrodes in order to minimize variability due to the platinum catalyst deposition. Devices assembled with the commercial platinated counterelectrodes showed decreased efficiencies with respect to those used previously

which were platinated using a screen printing Pt paste formulation. Nevertheless, being produced using automated machinery, their response on assembled DSSCs should assure more reproducibility. The second set of measurements showed that a slight performance improvement seems to be present on βCD1/TFAT photoanode for βCD1 functionalization times of 60 and 120 minutes. These results should be considered preliminary, since there is an ongoing collaboration related to a PRIN project.

5. Final conclusions

The work performed in this Thesis aimed to study how controlled modifications of the interface between the Titanium dioxide and the electrolyte could influence the photovoltaic performances of a Dye-Sensitized Solar Cell.

Two different approaches were used: the first, described in Chapter 3, was based on the active control of TiO_2 sensitization with GD2 porphyrin in combination with Cholic Acid as co-adsorbate. The second, reported in Chapter 4, was based on the functionalization of photoanodes using cyclodextrin derivatives and two organic dyes (TFAT and ZnTMCP). Here the main results obtained are summarized.

Chapter 3

From the monitoring of the flow uptake of GD2 using different solvents. I found that ACN and EtOH are the best choice for the sensitization process, whereas THF resulted to be detrimental from both the dye uptake level and from photovoltaic efficiency point of view. From the fitting of the uptake profile when GD2 dye was fluxed alone, I found that the chemisorption process can be described by a pseudo-first order kinetic. In addition, by studing the effect of the increasing the dye concentration in the range 0.05÷0.4 mM, it was found that the rate of uptake did not increased linearly due to dye-dye aggregation phenomena. This latter hypothesis ei salso supported by a decreasing of efficiency when the concentration of the dye was the highest examined, that is 0.4 mM. The same study was also carried out in the presence of 2.0 mM Cholic acid. Also in this case the dye uptake was described by a pseudo-first order kinetic. Furthermore, the increasing of the uptake rate as the concentration of the dye increased was closer to the linearity, and the photovoltaic efficiency was higher for the most concentrated solution of GD2 (0.4 mM) suggesting that the co-sensitizer was actively acting against dye-dye aggregation phenomena.

One of the advantages resulting from the sensitization/monitoring under flow conditions is the possibility to load a know amount of dye, a strategical approach for gathering information on the DSSC properties. Thus, TiO_2 photoanodes have been loaded to 50%, 90% and 100% levels of GD2 and GD2 + CA (0.2 mM in dye and 2.0mM in co-adsorbate). Using only GD2, I found that efficiency follows the expected trend, that is

increasing up to 2% when 100% dye loading is reached. EIS and IMVS measurements allowed to ascribe this beneficial effect to an increasing of the lifetime of injected electrons as result of the blocking effect of the dye molecule itself.

On the other hand, when GD2 is used in combination with CA, photovoltaic efficiency reaches it's maximum value already at 50% of dye loading, supporting a strong blocking effect of the Cholic Acid on TiO_2 surface. Finally, raising the dye coverage to 90% increased the efficiency to the same level as for full coverage (100%).

Chapter 4:

βCD2 was synthesized starting from βCD1 using a 4 step procedure. The influence of the chemisorption on TiO_2 surface with βCD1 and βCD2 was studied in order to understand how they affect the photovoltaic parameters. Two organic dyes have been used in combination with differently functionalized photoanodes, namely TFAT and ZnTMCP.

The monitoring of dye uptake in the presence of cyclodextrins resulted strongly affected by the nature of the cyclodextrin used. In particular, the cyclodextrin carrying seven carboxylic groups on the primary side, βCD2, passivated completely the photoanode so that the sensitization proces of very slow. For this reason, I decided to study the effect of cyclodextrin co-adsorbates by the traditional way based on dipping rather than using a flow protocol. Since hte cyclodextrins do not posses useful chromophores, I had to find indirect ways for confirm and quantify the absorption of these macrocycles on photoanodes. An useful technique appeared to be the measurement of the contact angle. Indeed, functionalized and sensitized photoanodes show different contact angle values due to the change in the hydrophylicity of the surface after treatments with the dye and co-adsorbate molecules. In particular, as expected when the sensitizer was bound to the TiO2 the contact angle increased, because the surface became more hydrophobic. In addition, UV-Vis absorption spectroscopy (monitoring the dye) showed lower absorbance values for cyclodextrin treated photoanodes, with a trend which followed what was initially found by flow monitoring.

Also TGA analysis permitted to estimate of the amount of dyes loaded on surface of the semiconductor, and to extrapolate the loading the cyclodextrin co-adsorbate., From TGA measurements, a surface coverage of 55% for βCD1 was calculated.

Dye loading determined by UV-Vis spectroscopy showed how increasing the dipping time of TiO_2 photoanodes into the cyclodextrin solution, prior to sensitization, decreased the amount of dye bound to the surface. Prolonged dipping times resulted detrimental for the performances of the DSSC, whereas a slight increasing in efficinecy was observed for exposition times to the CS solution shorter than 60 minutes. This effect is still under study as part of a PRIN project.

5. Experimental Part

5.1 Procedures for Dye-Sensitized Solar Cells assembly and characterization - UoW/IPRI

5.1.1 Conductive glass cutting and cleaning

A 3 mm thick Fluorine doped Tin oxide glass sheet (8 Ohm/cm^2; Nippon Sheet Glass) with dimensions of 100 x 100 mm is scored following a 25 x 25 mm scheme, using a modified tile cutter, then pieces are cutted using pliers. Some of these will be drilled, then every FTO piece is cleaned following a standard procedure.

The fresly cutted FTO pieces are transferred into a jar and sonicated for 20 minutes using the following solvents:

1. Soapy water, then rinsed with distilled water;
2. Acetone;
3. Ethanol.
4. Once the cleaning is completed they can be stored under ethanol from which they will be removed immediatly prior to use.

5.1.2 Counter-electrode preparation

The FTO intended to be used as counter-electrode is drilled using a Dremmel provided with a diamond tip (1 mm in diameter), then it is cleaned as reported previously. A drop of 10 mM Platinic Acid (H_2PtCl_6, 38% Pt, Sigma Aldrich) precursor in ethanol is deposited on the conductive side of the electrode and allowed to spread in order to cover the whole area. The CE is then heated at 400°C for 30 minutes.

5.1.3 Photoanode preparation

The FTO electrodes are located over a programmable hot plate and heated to 400°C. A TiO_2 precursor solution (Titanium diisopropoxide bis(acetylacetonate)), TAA, 75% in isopropanol is diluted 1:9 (vol.) with ethanol and the freshly prepared solution is

sprayed on the conductive side of the FTO electrodes. The heating is mantained for 30 minutes, then they are allowed to cool.

A TiO_2 mesoporous layer is screen-printed on the photoanodes using a commercially available TiO_2 paste (Dyesol - DSL-18NR-T) using a screen (dimensions of the printed area is 16 x 6 mm) with 90T mesh, obtaining an average thickness of 2.5 μm. The working electrodes are then placed on the programmable hot plate and sintered following a programmed temperature ramp (Table 9), followed by cooling at room temperature:

	Step 1	Step 2	Step 3	Step 4	Step 5
Ramp (min)	10	15	5	5	5
Temperature (°C)	150	325	375	450	500
Duration (min)	10	5	5	30	15

Table 9: ramp temperature for TiO_2 sinterization

A 0.02 M of acqueous $TiCl_4$ solution is prepared by dilution from a 2.0 M solution and the sintered photoanodes are dipped into it and kept at 70°C for 30 minutes. The solution is allowed to cool, the electrodes are removed and washed with plenty of distilled water first, then with ethanol and finally dried with a gentle stream of compressed air. The $TiCl_4$ treated photoanodes are sintered again at 500°C for 15 minutes and then cooled to 110°C untill prior to utilization. If electrodes are stored, they need to be thermally treated at 450°C for 30 minutes before use.

5.1.4 Flow sensitization

The working electrode is assembled in a custom made "flow cell" which allows to flux a thin layer of sensitizer solution over the photoanode while acquiring the absorbance versus time of sensitization.

The flow cell is made by two rectangular bricks, with thickness of 1 cm, of high density polyethilene (HDPE) with a central window for allowing the acquisition of the UV-Vis spectrum, held together by metallic screws. A polymer spacer (DuPontTM - Kalrez®;

thickness 0.5 mm) is laser cutted with the same dimensions of the working electrodes with a central window in order to do not cover the TiO_2 active area. It is then centered over the photoanode and a fluidic head is placed on top, creating a sealed cavity over the mesoporous oxide with PTFE tubings connections for the sensitizer flow (Figure 49). The photoanode in this configuration is then carefully sandwhiched between 2 HDPE supports and fixed with screws, paying attention to do not tight it too much in order to prevent breakage of the glass.

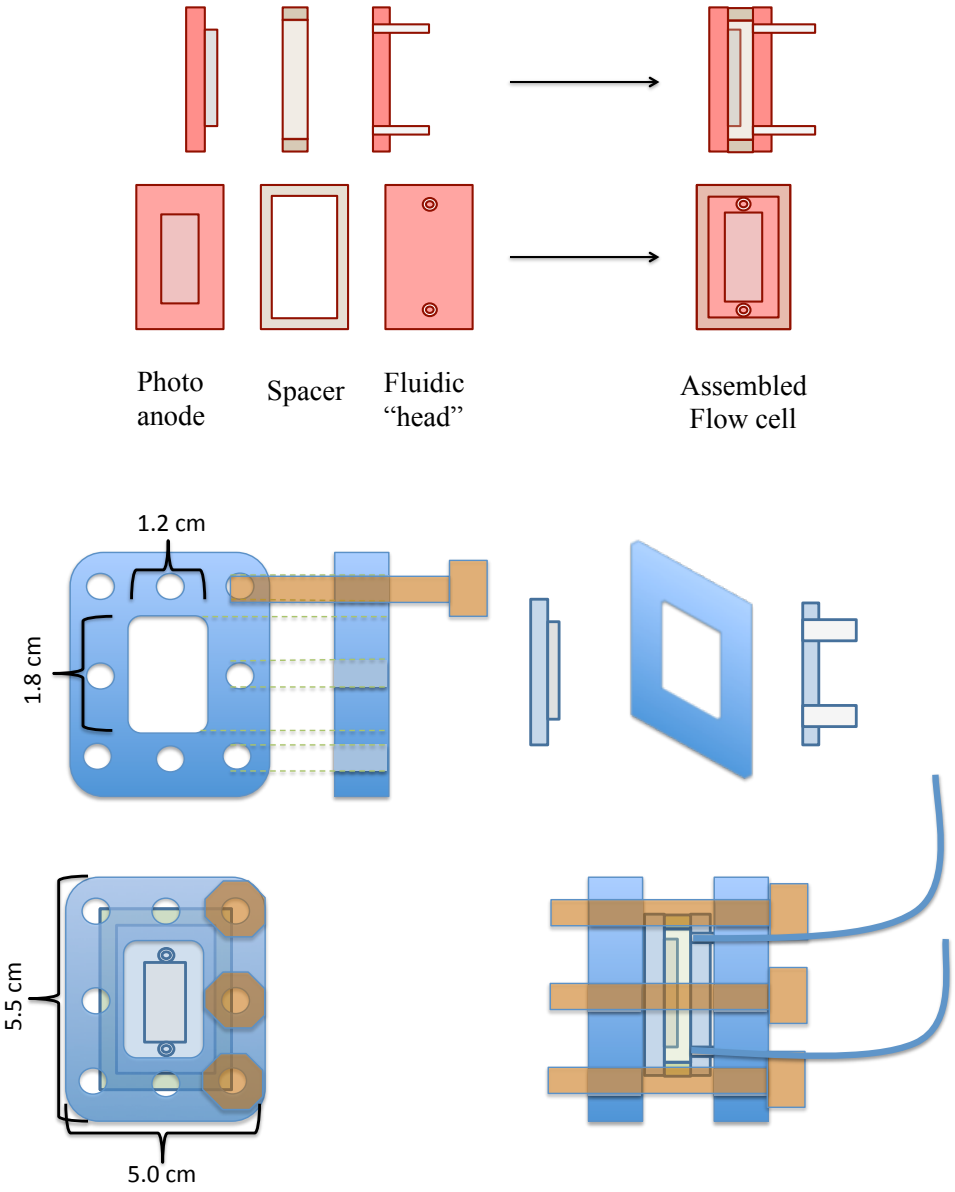

Figure 49: flow cell structure (top); Plastic support for the flow cell (bottom).

The PTFE tubings (Sylicone Tubings - Model 340 1521) are connected to a gas tight syringe (SGE gas tight glass syringe - 25 mL - Model: SYR-GL-25LL-S) mounted on a syringe pump (New Era Pump Systems - Model: NE-300 Infusion Pump). For the UV-

Vis absorption acquisition, a Zahner potentiostat (IM6) was used to control a calibrated white LED light source with a diffusing lens was mounted on an optic fiber connected to the UV-Vis spectrophotometer (International Light - Model: ILT900 - Software: Spectrilight III) and aligned with the caibrated light (Figure 50). The flow cell window with the transparent TiO_2 layer, ready to be sensitized, is carefully placed in the middle of the light pathway, between light source and detector.

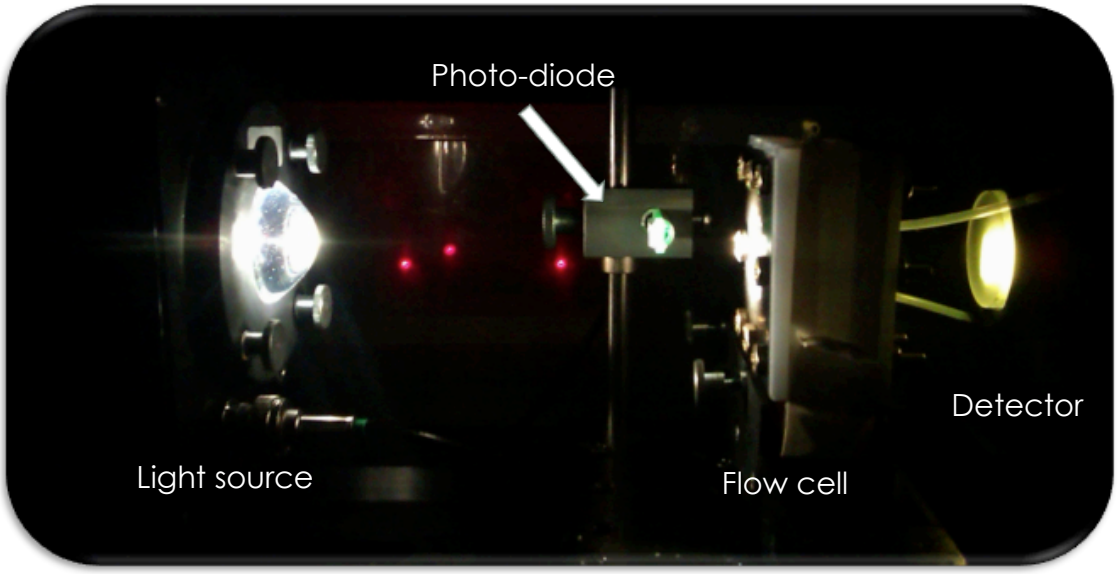

Figure 50: flow setup in working conditions into the dark room.

Measurements are performed in a completely dark room, where the LED is only light source. Full spectrum is acquired every 20 seconds, then the maximum absorbance value of the Q-bands (568 nm) is used for successive calculations. After data acquisition is started, only solvent is fluxed, with a rate of 200 μL/min, for several minutes and the baseline is recorded. The syringe is changed with another one containing the desired sensitizer solution and the flux is carried on as required by the specific experiment. In some cases a long rinsing procedure is applied after the dye uptake is completed, hence the syringe is changed again and only solvent is flowed for 20 minutes, while in all the other cases the freshly sensitized photoanode was quickly rinsed fluxing pure solvent for 30 seconds.

5.1.5 Electrolyte preparation

An high performace electrolyte based on Acetonitrile/Valeronitrile, optimized for porphyrin sensitizers is used (Table 10). The electrolyte is then kept under inert atmosphere (Argon) in glove box.

Component	Concentration
Acetonitrile/Valeronitrile	85/15 Vol.%
Iodine (I_2)	0.05 M
4-tertbutylpyridine (4tBP)	0.5 M
1.2-dimethyl-3-propylimidazolium iodide (DMPII)	0.6 M
Lithium Iodide	0.1 M

Table 10: high performances electrolyte composition

5.1.6 Device assembly and electrolyte backfilling

For assembling the freshly prepared photoanode together with its counterelectrode, a 25 μm thick Surlyn® polymer sheet, which act also as spacer, is used. The polymer sheet is placed on the photoanode paying attention to do not cover the TiO_2 active area, then the counter-electrode is placed on top of Surlyn assuring that the previously drilled hole is within the spacer. The device is sealed using a hot press, which applies a calibrated pressure while heating was provided with a Peltier cell from the counter-electrode side.

The partially assembled device was transferred into a custom made plastic box connected to a programmable vacuum pump, the counter-electrode must be facing up and about 50 μL of electrolyte are placed over the drilled hole. A slight level of vacuum is applied in order remove the air from the cavity over the TiO_2 layer and subsequently the atmospheric pressure is gently restored filling the device with the electrolyte. The area near the drilled hole is then cleaned with acetone and sealed using Surlyn® which is finally covered with Aluminium foil.

Electrical contacts are attached melting a Tin wire (Cerasolz CS186) at 220°C, covering the exposed FTO area, using an ultrasonic soldering iron (Frequency 60 kHz).

5.2 Instrumentation used at the UoW/IPRI

5.2.1 Solar simulator

Most of the J-V curves are obtained using a solar simulator (Newport) with AM1.5G filter calibrated to 100 mW/cm^2, for some devices a Peccel solar simulator (AM1.5G - 100mW/cm^2), in both cases the instrument was coupled with a Keithley 2400 source meter.

5.2.2 Incident photon to current efficiency (IPCE) measurements

The IPCE spectrum is obtained using a Xenon lamp (Power 300 W) with a monochromator and a long pass filter, the measurement area is 0.5 cm^2. A Si reference diode is used for calibration, before measurements. The photocurrent value is measured using a Keithley 2400 source meter, with 5 nm steps, driven by a custom made Labview program.

5.2.3 Electrochemical impedance spectroscopy (EIS)

A Zhaner (IM6) electrochemical workstation is used to measure the frequency dependant current and voltage response of the cell, while a secondary potentiostat (P211) is used to drive a calibrated white high intensity LED light (Maximum light intensity 220 W/cm^2) which is continuosly controlled using a reference Si photodiode (TLS-02), connected to the IM6 workstation, by a feedback loop assuring that no drift in the light intensity is present. Measurements are performed under irradiation, at the open circuit potential corresponding to 5 different light intensities (20, 60, 100, 140, 220 W/ cm^2) with a modulation of +/- 5 mV and frequency range from 1 MHz to 0.1 Hz.

5.2.4 Controlled intensity modulated photovoltage/photocurrent spectroscopy (IMVS/IMPS)

The instrumental setup is the same as for EIS measurements. The cell is aligned and centered in the light path. A small modulation (+/- 10 mV - frequency range 100kHz - 0.1 Hz) is applied by the P211 potentiostat to the voltage which drives the high intensity

LED, causing a small modulation in the light intensity. The voltage (IMVS) and current (IMPS) frequency response of the DSSC is measured with the Zahner IM6 electrochemical workstation.

5.3 Procedures for Dye-Sensitized Solar Cells assembly and characterization - UniPD - DiSC

5.3.1 Conductive glass cutting and cleaning

The procedure is the same as reported previously (see section 5.1.1) with the only exeption of the FTO which is obtained from Solaronix (TCO22-15 - 15 Ohm/cm^2). The electrodes are cutted with dimensions of 16.5 x 12.5 mm prior of the washing procedure.

5.3.2 Counter-electrode preparation

A platinized commercially available counter electrode (Dyesol Pt-Electrode) is drilled using a dremmel with a 1mm diamond tip. The FTO has to be kept under water while drilling in order to cool the temperature of the tip and to prevent glass dust to be breathed.

5.3.3 Photoanode preparation

A 4 x 4 mm adesive tape (3M - 60μm thick) mask is sticked on the FTO (Solaronix TCO22-15 - 2 mm thick), placing the active area 2 mm far from the edges of the FTO glass. Some pressure is applied with a glass rod in order to remove air bubbles creating an homogeneus thickness. A drop of 0.01 M $Ti(OBu)_4$ (Sigma-Aldrich - CAS 5593-70-4) solution in isopropanol (Sigma-Aldrich) is deposited into the 4 x 4 area created by the mask and allowed to dry. A TiO_2 paste (Solaronix - Ti-Nanoxide HT) is sonicated 5 minutes then a small amount is placed near one of the edges of the mask and it is spread by doctor blading sliding the glass rod. After 5 minutes the mask is carefully removed and the photoanodes are sintered at 500°C for 1 hour using a ceramic hot plate, then they are allowed to cool at 110°C if sensitization will be carried out by dipping or to room temperature if they will be stored or assembled in the flow device.

5.3.3.1 General dye sensitization technique by impregnation

When complete dye uptake is required, a freshly prepared photo anode, still hot (around 80°C), is dipped into a 0.2 mM solution of dye (TFAT or ZnTMCP) in methanol or

ethanol respectively (Sigma-Aldrich) for 17 hours (overnight). When removed from the solution it is quickly rinsed by squeezing for 2 times a Pasteur pipette with acetonitrile.

5.3.3.2 Cyclodextrins co-adsorption on photoanodes

When the photoanode is treated with with a co-adsorbate (cyclodextrins C1 or C2) prior to dye uptake, it is dipped into a 1 mM solution in milieu water overnight. Partial co-adsorbate coverage is obtained by shortened dipping time in the cyclodextrins solutions (1, 2, 5, 17 hours). The same rinsing procedure is performed also for co-adsorbates loading.

5.3.3.3 Flow sensitization

This system is similar to the one described in chapter 5.1.3, it has been developped during my master thesis and succesfully used for the monitoring of N3 and N719 dye uptake on 6 µm transparent TiO_2 photoanodes[15]. Some improvements in the flow cell setup have been introduced since then, hence I will describe it in this section.

Two polypropylene (PP - thickness 1 cm) supports are adapted to accommodate fittings for the fluidic part connections, collimating lens for linking the optic fibers and the screws needed to keep every piece in place. The TiO_2 photoanode is placed on the support (Figure 51) with the semiconductor layer facing up, a previously custom adapted gasket which act both as spacer and sealer (Kalrez® - thickness 0.5 mm) is put onto the photoanode being careful to do not cover the active area, then a drilled microscope glass, with two holes for allowing to flux the dye, is put on top of the spacer, creating a sealed cavity adapted for the fluidic connection. The second PP support, hosting the PTFE tubing which will be connected to the syringe pump, is carefully aligned with the drilled holes of the glass slide, and the flow cell is then tightened with screws to prevent leakage.

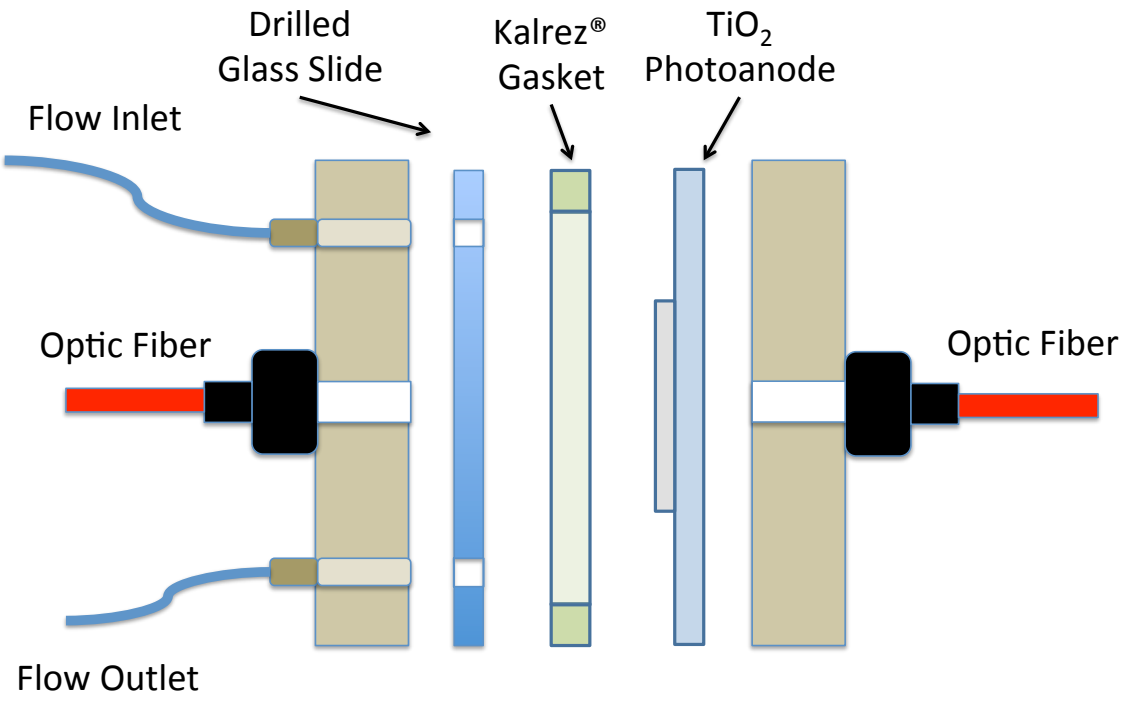

Figure 51: flow cell used in Padova for the flow experiments

The inlet tube is connected to the syringe pump (New era pump systems - NE300) set to a flow rate of 200 µL/min, and the outlet tube is place into a vial for waste collection. The optic fiber facing the TiO_2 side is connected to the light source (halogen lamp - Avantes HL-2000-LL) and the remaining optic fiber brings the signal to the UV-Vis spectrophotometer (Avantes Avaspec-2048). The data is acquired in real-time at the most suitable wavelenght (558 nm for ZnTMCP; 450 nm for TFAT) by a computer linked to the spectrophotometer. Initially, pure solvent is fluxed into the flow cell and the baseline is acquired, then the syringe is swapped with a new one, containing the sensitizer and the data acquisition is continued until desired. When a flow rinsing procedure is present, after the sensitization another syring with only solvent is mounted on the syringe pump after sensitization and rinsing last for 10 seconds in flow.

5.3.4 Device assembly

A 6 x 6 mm (Meltonix 1170-25 - 25 µm - DuPont Surlyn®) is positioned on a freshly sensitized photoanode and is heated for few seconds to 120°C in order to partially melt it assuring adhesion on the FTO. The protective foil is removed and the counter-electrode is carefully placed over the photoanode. In particular it is important to center the platinized area over the TiO_2 and avoid to block the drilled hole mistakenly placing it over the Surlyn®. The DSSC is placed on the hot plate at 120°C from the counter-

electrode side and some pressure is applied in order to ensure that the electrodes are perferctly glued together with no leakage.

The partially assembled devices are placed into a vacuum proof glass jar with connected to a vacuum pump, the drilled holes are facing up, a drop of electrolyte is deposited onto the hole, and vacuum is applied for few seconds in order to remove the air from the inside of the DSSC which will be replaced by the electrolyte when atmospheric pressure is slowly restored. The counterelectrode is cleaned with acetone and the hole is sealed using Surlyn (4 x 4 mm) covered with an Aluminium foil.

5.4 Instrumentation used for DSSC characterization at UniPD and UniFE

DSSC characterization was done in collaboration with the University of Ferrara which owns the following intruments described below.

5.4.1 Solar Simulator - UniFE

A Luxtel Xenon lamp (100 mW/cm2, AM1.5G - Power 175 W) is used to simulate the sunlight spectrum.

5.4.2 Incident photon to current efficiency (IPCE) - UniFE

IPCE is measured using a Xenon lamp (Luxtel - Power 175 W) coupled with a manual monochromator. The curent value is recorder, using PGSTAT 30 electrochemical workstation, with steps of 20 nm in wavelenght between 390 - 710 nm. The system was calibrated using a Si photodiode (Centronic ASD100-7Q).

5.4.3 Electrochemical impedance spectroscopy (EIS) - UniFE

Impedance spectroscopy measurements are perfomed under illumination (100 mW/cm^2 - AM1.5G) at the Voc of the device. A Frequency response analyzer (FRA2.v10) driven by NOVA 1.10 software is used. Frequency range goes from 1 MHz to 0.1 Hz. The equivalent circuit used for the data fittin takes into account the series resistance of the FTO, and two main interfaces between TiO2/electrolyte and electrolyte/counter-electrode [$R_s(QR_{ct})(QR_{ce})$]. Q represent a costant phase element (CPE) which model the non ideal behaviour of the capacitance of real interfaces.

5.5 Instrumentation description - UniPD

5.5.1 UV-Visible spectrophotometer

UV-Visible spectrum were acquired with a UV-Vis NIR spectrophotometer (Varian - Cary 5000). Calibration curves of dyes are obtained by TGA precise weighting of increasing amounts of dye which is diluted in an exact amount of the correspondent solvent.For Dye loading measurements, the molar extinction coefficient of the dyes were calculated again using a freshly prepared NaOH 0.1 M solution in THF:H2O (1:1 ratio).Absorbance of dyes on sensitized photoanodes has been measured by directly attaching the glass on the cuvette support carefully placing the mesoporous oxide in the light path. (Baseline was acquired before every set of experiments using a photoanode which has not been sensitized).

5.5.2 NMR analysis

NMR spectra have been acq uired with a Bruker AV 300 (300 MHz).

5.5.3 Mass analysis

Mass analysis have performed using 4800 Plus MALDI TOF/TOF™ Analyzer.

5.5.4 Thermogravimetric analysis

Thermogravimetric analysis has been executed using a thermogravimetric analyzer TGA Q5000 (TA instruments) using standard Platinum pan (100µL) with
the following heating program:

Command	Description
Temperature increase rate	10°C*min^{-1}
Maximum Temperature	700°C (Hold for 2 minutes)
Gas	Air

5.5.4.1 TGA experiment description

Thermogravimetry has been used as a tool for estimating the loading of both cyclodextrins and dyes on the TiO_2 surface.

At least three photoanodes of each type have been measured. The output of the analysis represent a weight loss due to the organic molecules bound on the surface. Since a small variability of active TiO_2 area deposited on the FTO may be present (because photoanodes are manually assembled), the weight losses have been normalized to 1 mg of mesoporous TiO_2 and converted to moles ($mol*mg^{-1}_{TiO2}$). Initially, the weight losses of TiO_2 substrates functionalized only with cyclodextrins have been investigated, obtaining their average value of functionalization on the semiconductor surface.

The average value of CD loading was subtracted from the normalized weight loss calculated from CD + Dye sensitized photoanodes, obtaining the amounts of dye loading.

In Table 11 below is reported the average weight loss based on multiple TGA analys of at least three photoanodes sensitized with:

	Average value ($mol*mg^{-1}_{TIO2}$)	**Error ($mol*mg^{-1}_{TIO2}$)**	**Comments**
βCD1	5,48E-08	3,50E-09	Amount of **βCD1** on 1 mg of TiO_2
βCD2	4,64E-08	3,01E-09	Amount of **βCD2** on 1 mg of TiO_2
ZnTMCP	8,09E-08	9,07E-09	Amount of **ZnTMCP** on 1 mg of TiO_2
TFAT	2,27E-07	2,30E-08	Amount of **TFAT** on 1 mg of TiO_2
βCD1/ZnTMCP	3,04E-08	9,46E-09	Amount of **ZnTMCP** on 1 mg of **βCD1** functionalized TiO_2
βCD1/TFAT	8,37E-08	6,21E-09	Amount of **TFAT** on 1 mg of **βCD1** functionalized TiO_2

	Average value ($mol*mg^{-1}_{TIO2}$)	Error ($mol*mg^{-1}_{TIO2}$)	Comments
βCD2/ZnTMCP	1,20E-08	4,50E-09	Amount of **ZnTMCP** on 1 mg of **βCD2** functionalized TiO_2
βCD2/TFAT	4,26E-08	4,28E-10	Amount of **TFAT** on 1 mg of **βCD2** functionalized TiO_2

Table 11: average loading of cyclodextrins and dyes normalized to 1 mg of TiO_2

5.5.3 Calibration curves

Reported calibration curves are calculated from solution obtained weighting exact amounts of dye with the TGA and are measured in the same solution used for dye desorption (NaOH 0.1 M in THF:H_2O 1:1).

5.5.3.1 Calibration curve of TFAT

Diluted solutions concentrations (M)	Abs 416 nm
5,76E-06	0,1395
1,10E-05	0,2589
2,20E-05	0,4728
3,30E-05	0,6529
5,50E-05	0,8442

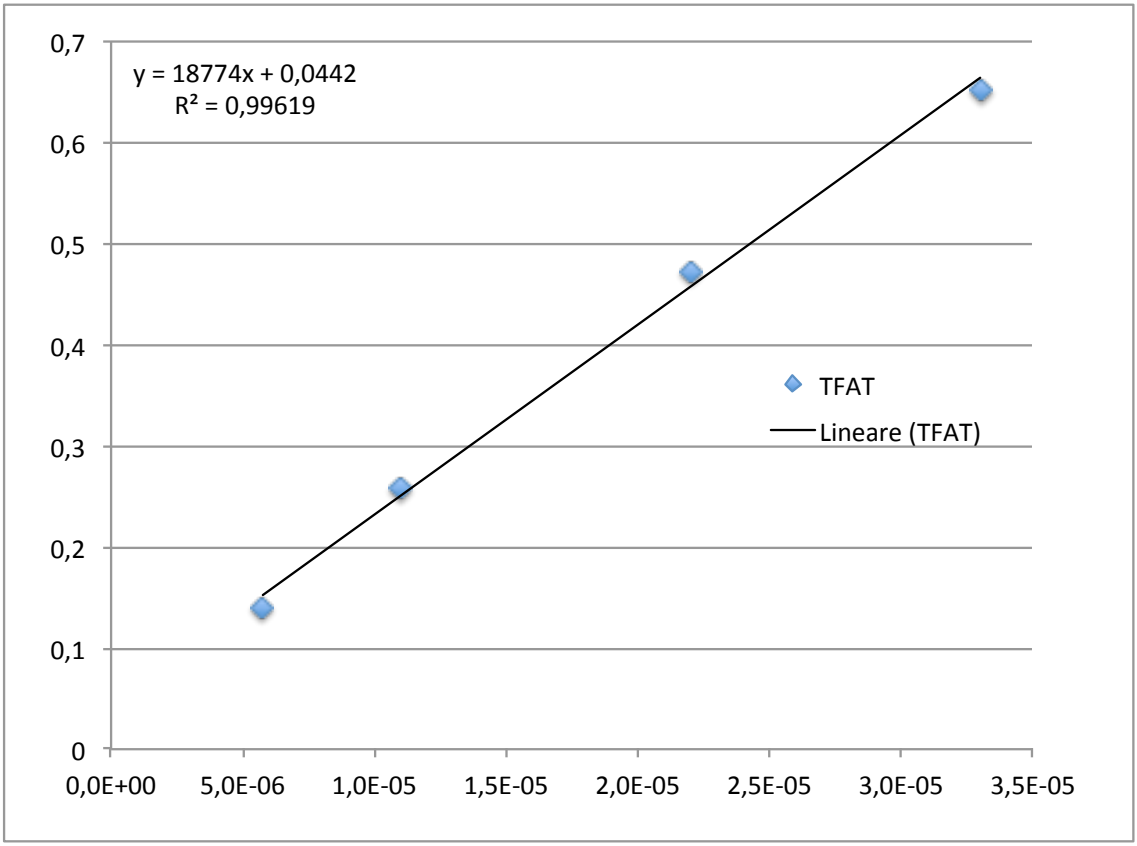

5.5.3.2 Calibration curve ZnTMCP

Diluted solutions concentrations (M)	Abs 558 nm
1,13E-04	0,3971
5,66E-05	0,1998
2,83E-05	0,1000
1,41E-05	0,0536
7,07E-06	0,0247
3,54E-06	0,0139

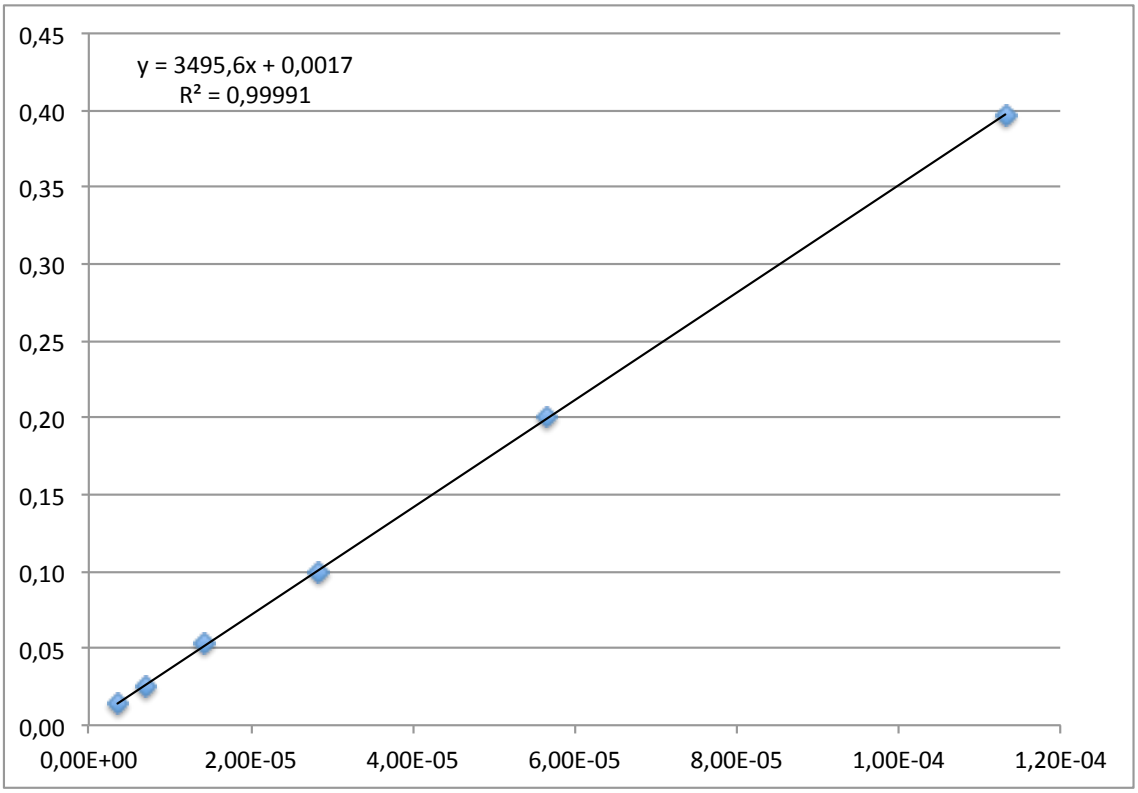

5.6 Spectrophotometric dye loading evaluation

In order to obtain the dye loading on photoanodes treated with cyclodextrins, the following working scheme applies. Five freshly prepared TiO_2 photoanodes are dipped into different solutions of CD (CD1 or C2) for different periods of time (from 1 to 17 hours). They are then removed from the solution, rinsed and dried, then they are dipped into a 0.2 mM sensitized solution overnight (17h). The next day, they are removed from the solution, rinsed and dried, then store in the dark until they are analized within 1 hour. One photoanode is also directly dipped into the dye solution.

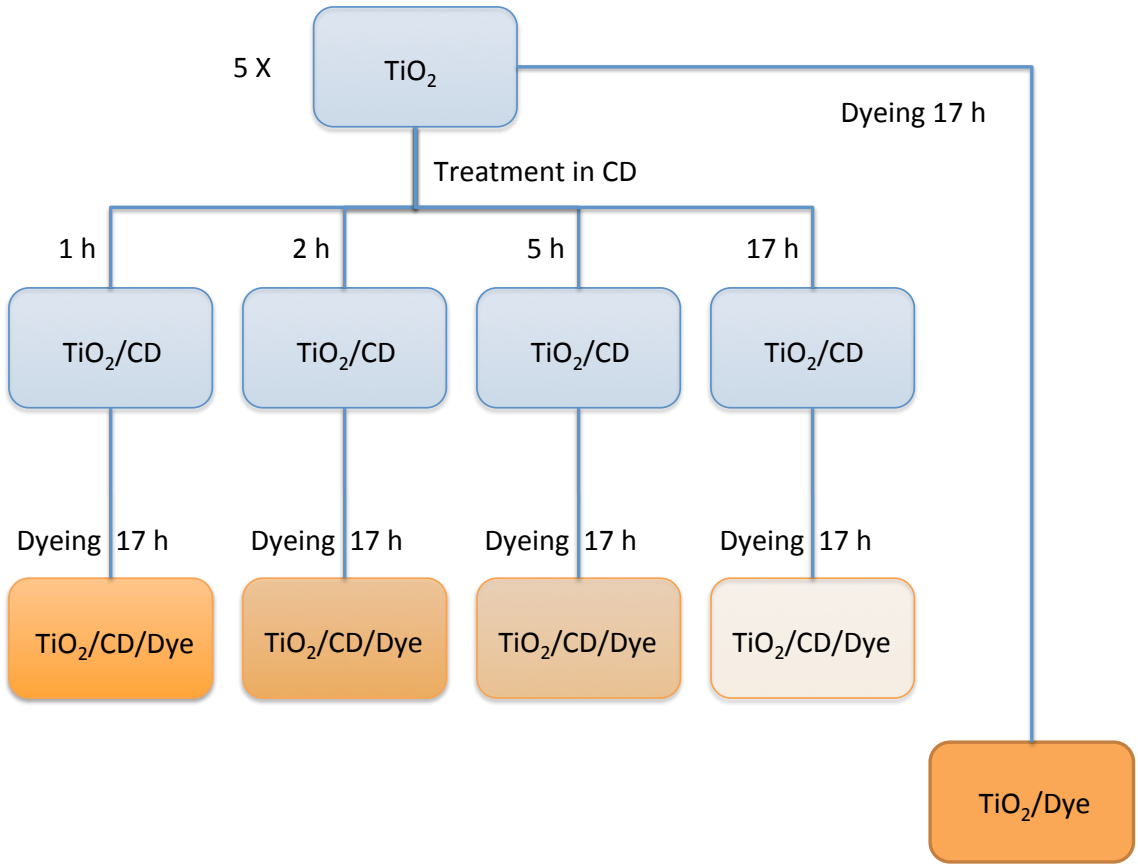

Figure 52: scheme of the working schedule for the preparation of cyclodextrin functionalized photoanodes.

Desorption of the dye occur by dipping the sensitized photoanodes into a vial containing an exact amount of 0.1 M NaOH solution in THF:H_2O (1:1 ratio) for 30 minutes. The solution is transfered into a quartz cuvette just before the spectrum is acquired and the solution concentration is obtained through the molar extinction coefficient. The moles of dye are calculated and, since the amount of TiO_2 on the photoanode has been

weighted, they can be normalized to 1 mg of mesoporous TiO_2 (mol*mg$^{-1}_{TiO2}$) in order to ease the dye loading comparison among different photoanodes.

5.6.1 Dye loading of TFAT

Calculation of TFAT concentration from desorbed photoanodes						
Epsilon 416 nm = 18800						
Photoanode name	Abs. Of Solution (A.U.)	Calculated Concentration (mol^{-1}*cm^{-1})	V solution (L)	mol TFAT	TiO_2 weight (mg)	**mol*mg^{-1}**
TFAT	0,8759	4,66E-05	0,004	1,86E-07	1,1	**1,69E-07**
1h in bCD-TFAT	0,7424	3,95E-05	0,002	7,90E-08	1,2	**6,58E-08**
2h in bCD-TFAT	0,4764	2,53E-05	0,002	5,07E-08	1,2	**4,22E-08**
5h in bCD-TFAT	0,3636	1,93E-05	0,002	3,87E-08	1,2	**3,22E-08**
17h in bCD-TFAT	0,2965	1,58E-05	0,002	3,15E-08	1	**3,15E-08**
1h HOOC-bCD-Me-TFAT	0,2513	1,34E-05	0,002	2,67E-08	1,7	**1,57E-08**
2h HOOC-bCD-Me-TFAT	0,1905	1,01E-05	0,002	2,03E-08	1,1	**1,84E-08**
5h HOOC-bCD-Me-TFAT	0,1159	6,17E-06	0,002	1,23E-08	0,7	**1,76E-08**
17h HOOC-bCD-Me-TFAT	0,0863	4,59E-06	0,002	9,18E-09	0,9	**1,02E-08**

Table 12: values of dye loading of TFAT obtained by UV-Vis spectroscopy.

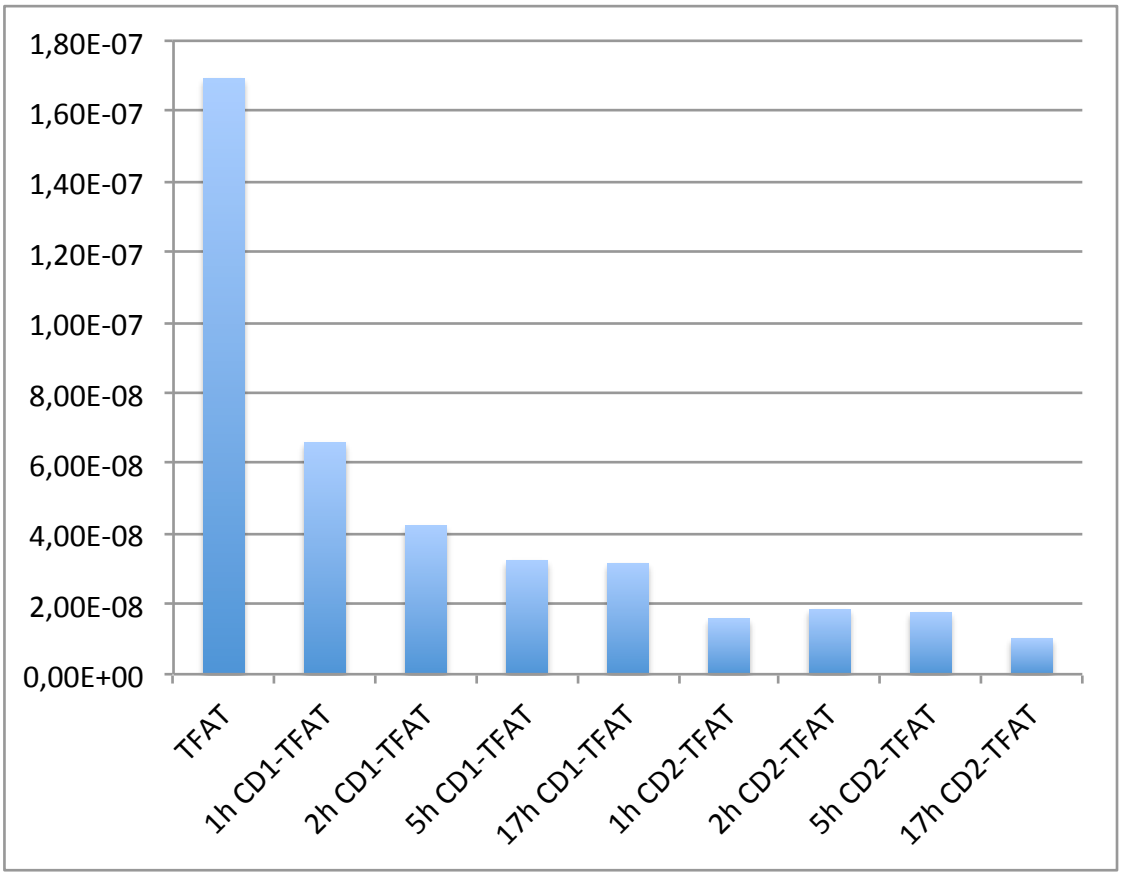
1,80E-07
1,60E-07
1,40E-07
1,20E-07
1,00E-07
8,00E-08
6,00E-08
4,00E-08
2,00E-08
0,00E+00
TFAT
1h CD1-TFAT
2h CD1-TFAT
5h CD1-TFAT
17h CD1-TFAT
1h CD2-TFAT
2h CD2-TFAT
5h CD2-TFAT
17h CD2-TFAT

5.6.2 Dye loading of ZnTMCP

Calculation of ZnTMCP concentration from desorbed photoanodes							
Epsilon 425nm = 82000 - Epsilon 558nm = 3500							
Device number	Photoanode name	Abs. Of Solution (A.U.)	Calculated Conc ($mol^{-1}*cm^{-1}$)	V solution (L)	mol ZnTMCP	TiO_2 weight (mg)	**$mol*mg^{-1}$**
7	ZnTMCP	0,367	1,05E-04	0,002	2,10E-07	1,2	**1,75E-07**
13	1h in bCD-ZnTMCP	0,147	4,20E-05	0,002	8,40E-08	1,0	**8,40E-08**
6	2h in bCD-ZnTMCP	0,101	2,89E-05	0,002	5,79E-08	1,0	**5,79E-08**
5	5h in bCD-ZnTMCP	0,108	3,09E-05	0,002	6,19E-08	1,3	**4,76E-08**
1	17h in bCD-ZnTMCP	0,060	1,71E-05	0,002	3,43E-08	1,3	**2,64E-08**
15	1h HOOC-bCD-Me-ZnTMCP	0,156	1,91E-06	0,002	3,81E-09	0,6	**6,35E-09**
9	2h HOOC-bCD-Me-ZnTMCP	0,183	2,23E-06	0,002	4,46E-09	1,4	**3,19E-09**
8	5h HOOC-bCD-Me-ZnTMCP	0,145	1,77E-06	0,002	3,54E-09	1,4	**2,53E-09**
4	17h HOOC-bCD-Me-ZnTMCP	0,106	1,30E-06	0,002	2,59E-09	1,0	**2,59E-09**

Table 12: values of dye loading of TFAT obtained by UV-Vis spectroscopy.

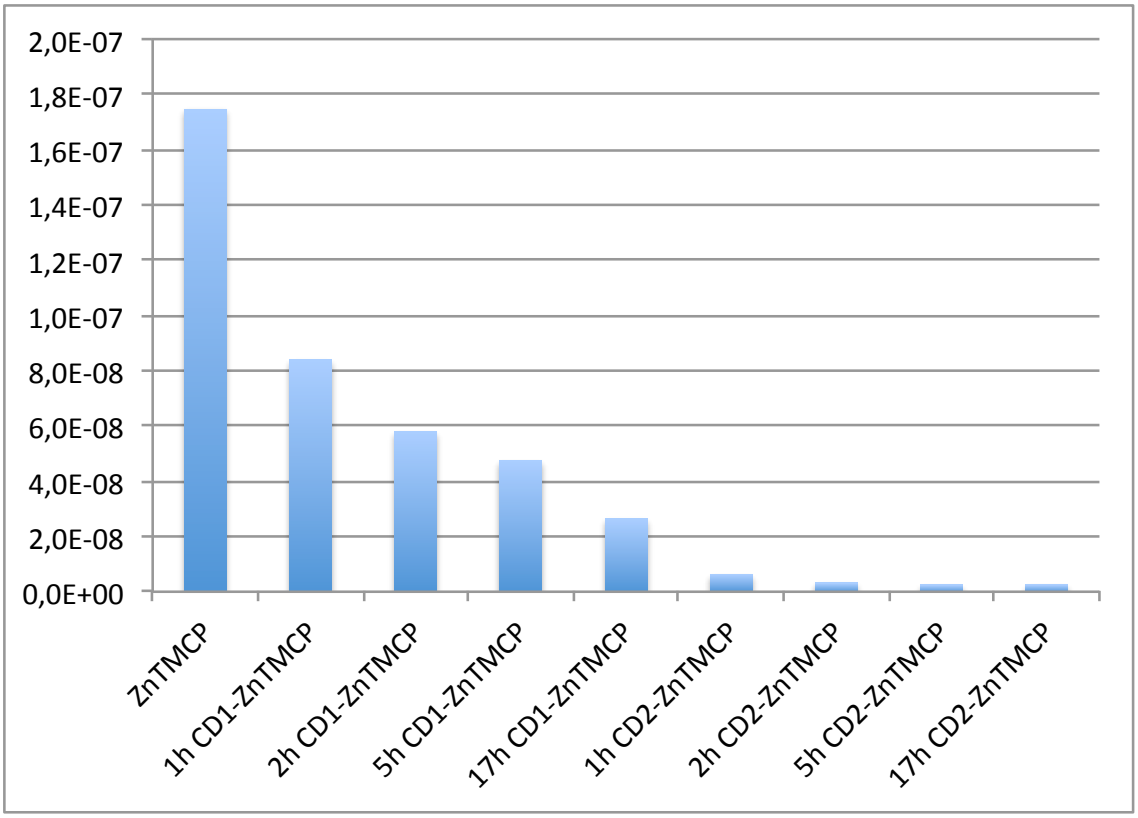
2,0E-07
1,8E-07
1,6E-07
1,4E-07
1,2E-07
1,0E-07
8,0E-08
6,0E-08
4,0E-08
2,0E-08
0,0E+00
ZnTMCP
1h CD1-ZnTMCP
2h CD1-ZnTMCP
5h CD1-ZnTMCP
17h CD1-ZnTMCP
1h CD2-ZnTMCP
2h CD2-ZnTMCP
5h CD2-ZnTMCP
17h CD2-ZnTMCP

5.7 Synthesis of cyclodextrin derivatives

5.7.1 Synthesis of (1)

Heptakis(6-O-*tert*-butylmethylsilyl)cyclomaltoheptaose

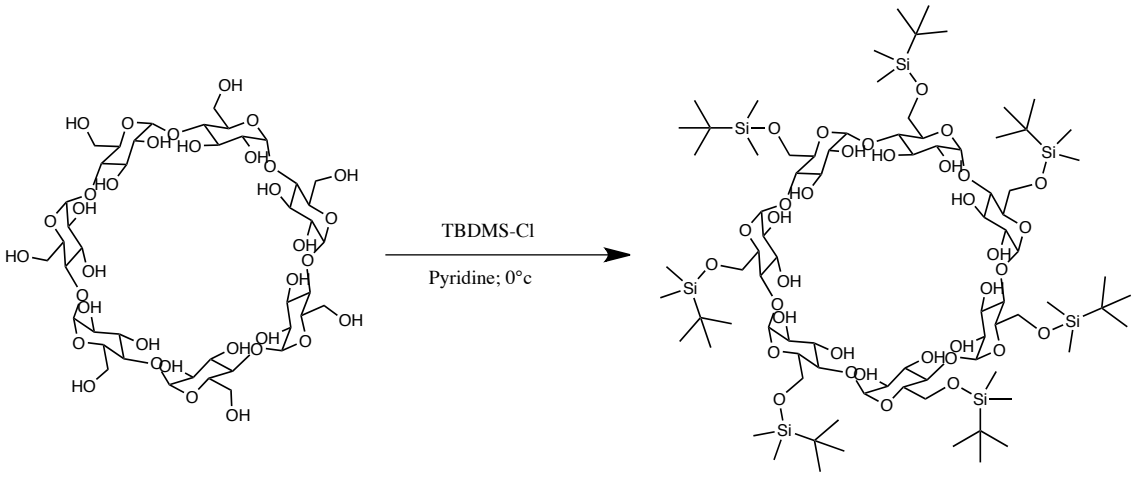

βCD **1**

Following a literature procedure[31], dried **βCD** (15.00 g, 13.2 mmol) is dissolved in 152 mL of dry pyridine in a 500 mL round bottom flask at room temperature. The solution is cooled to 0°C using an ice bath and TBDMS-Cl (15.94 g, 105.7 mmol) is added. The reaction is monitored by TLC (silica gel, eluent $CHCl_3$/MeOH/H_2O, 40:10:1v/v). When the reaction is judgec completed, distilled water (1.64 l) is added and compound **1** precipitate. It is then recovered by filtration on filtering paper and washed with water (2 x 130 mL) and acetone (150 mL).

The product was recrystallized twice from CH_2Cl_2 (25 mL) and MeOH (200 mL) and once from CH_2Cl_2(16.5 mL) and acetone (132 mL) obtaining 8.7 g of compound 1 (yeald 34%). MALDI-MS obsd 1955.49 m/z [M + Na^+]; calcd 1955.97 m/z; $C_{84}H_{168}O_{35}Si_7$. ^{1}H-NMR (CD_3Cl, 300 MHz) 4.90 (d, 7H), 4.04 (t, 7H), 3.9 (m, 7H), 3.73-3.53 (m, 28H), 0.87 (s, 63H), 0.03 (d, 42H).

5.7.2 Synthesis of (2)

Heptakis(6-O-tert-butyldimethylsilyl-2,3-di-O- methyl)cyclomaltoheptaose

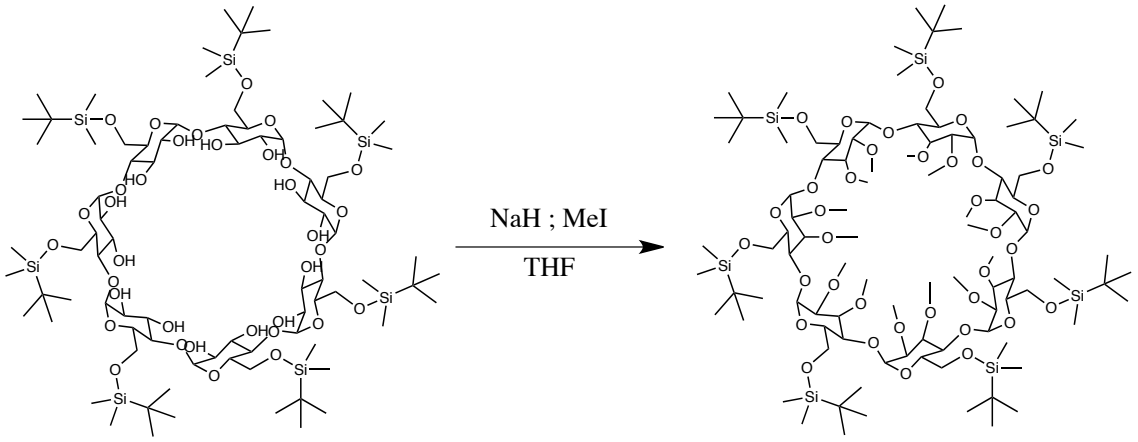

1 **2**

NaH (2.8 g, 70 mmol) is suspended in dry THF (24 mL) under nitrogen atmosphere in a cooling bath at 0°C. Compound **1** (4.0 g, 2.07 mmol) is dissolved into the mixture. CH_3I (5.0 mL, 80.3 mmol) is carefully added to the heated solution (40°C, 30 minutes), stirring at room temperature overnight. MeOH (20 mL) is carefully added in small portions. Solvent is evaporated and the crude product is re-suspended in hexane (60 mL) and filtered. After removing the solvent, 2.46 g (yeald 56%) of compound **2** are obtained. MALDI-MS obsd2151.66 m/z $[M + Na]^+$; calcd 2152.17 m/z; $C_{98}H_{196}O_{35}Si_7$. ^{1}H-NMR (CD_3Cl, 300 MHz) 5.19 (d, 7H), 4.12 (m, 7H), 3.9 (m, 7H), 3.75-3.46 (m, 35H), 3.66 (s, 21H), 3.50 (s, 21H), 3.05 (dd, 7H), 0.87 (s, 63H), 0.01 (d, 42H)

5.7.3 Synthesis of (3)

Heptakis(2,3-di-O-methyl)cyclomaltoheptaose

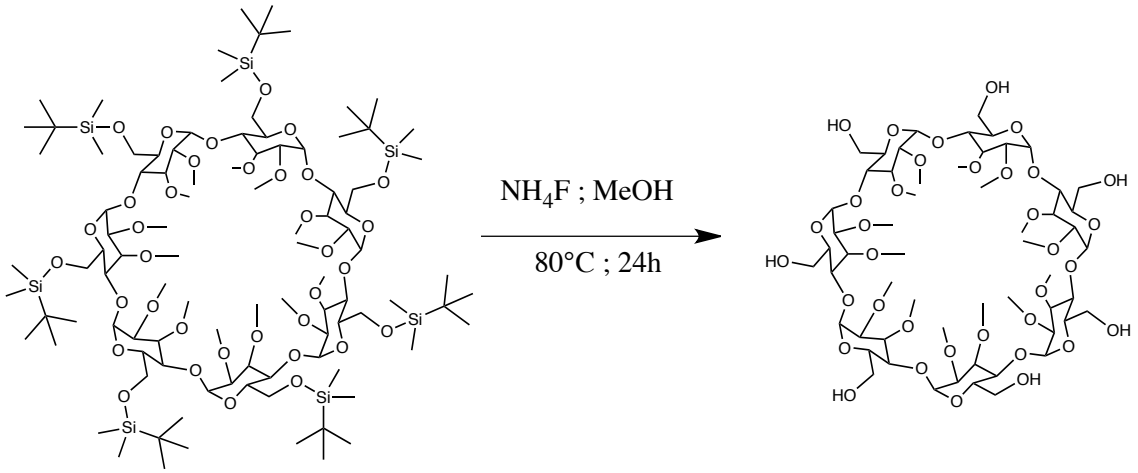

2 **3**

Compound **2** (2.26 g, 1,06 mmol) is dissolved in MeOH (80 mL) in a 250 mL round-bottom flask. NH_4F (2.49 g, 67.22 mmol) is added and the solution is heated (80°C) for 24 hours. MeOH is removed by vacuum evaporation and the solid is dissolved in CH_2Cl_2 (200 mL) and washed with brine (3 x 70 mL). The solution is dried filtering through Na_2SO_4 and the solvent is removed under vacuum. 1.6 g (yeald 100%) of compound **3** is obtained. MALDI-MS obsd 1353.24 m/z $[M + Na]^+$; calcd 1353,59 m/z. ^{1}H-NMR (CD_3Cl, 300 MHz) 5.08 (d, 7H), 4.20 (br, 7H), 3.95 (m, 7H), 3.80 (m, 21H), 3.62 (s, 21H), 3.50 (s, 21H), 3.19 (m, 7H).

5.7.4 Synthesis of βCD2

Per(5-carboxy-5-dehydroxy-2,3-di-O-methyl)cyclomaltoheptaose

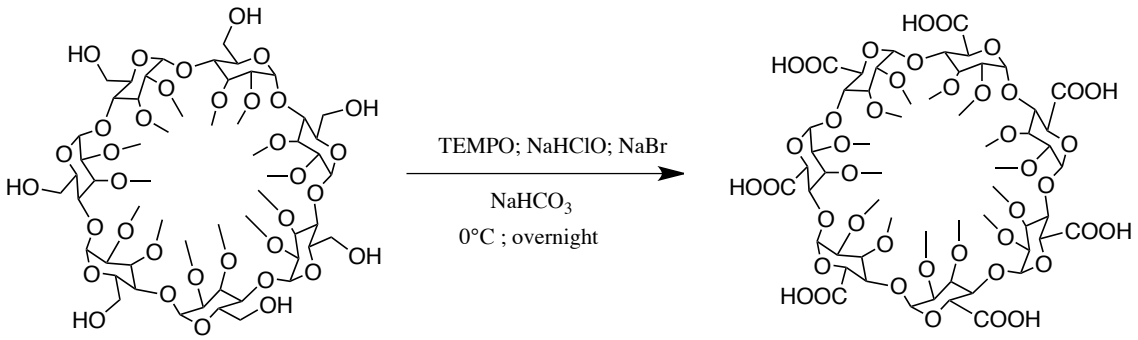

3 **βCD2**

Compound **3** (0.8 g, 0.60 mmol) is dissolved in H_2O (100 mL) in a 500 mL round bottom flask, cooled at 0°C. An aceonitrile solution (25 mL) of NaBr (0.46 g, 4.43 mmol) and TEMPO (0.70 g, 4.51 mmol) is added the solution of compound **3**. An aqueous solution of $NaHCO_3$ (25 mL, 0.5 M) and NaClO (12.5 mL, 6 - 14 %) is added to the reaction vesses, the pH is quickly adjusted to 10 with NaOH (1 M). The reaction is monitored by MALDI-TOF/TOF and left overnight. TEMPO is quenche with MeOH (1M) drop by drop until coloration disappears. Solvent is removed under vacuo, and the remaining TEMPO is exctracted with ether (3 x 50 mL) and solvent is evaporated. The solid is dissolved into the smallest amount ho MeOH an purified by re-crystallization from MeOH/Acetone. Acidification with a strongly acidic exchange resin (Amberlite IRA-120, 40 mL) is performed and **βCD2** is obtained and dried by lyophilization overnight. MALDI-MS obsd 1451.35 m/z $[M + Na]^+$; calcd 1451.43 m/z. ^{1}H-NMR (D_2O, 300 MHz) 5.41 (d, 7H), 4.35 (m, 7H), 3.90 (t, 7H), 3.79 (t, 7H), 3.67 (s, 21H), 3.46 (dd, 7H).

5.8 Synthesis of ZnTMCP

5.8.1 Synthesis of TMCP1

5-(4-methoxycarbonylphenyl)-10,15,20-tris(2,4,6-trimethylphenyl)porphyrin

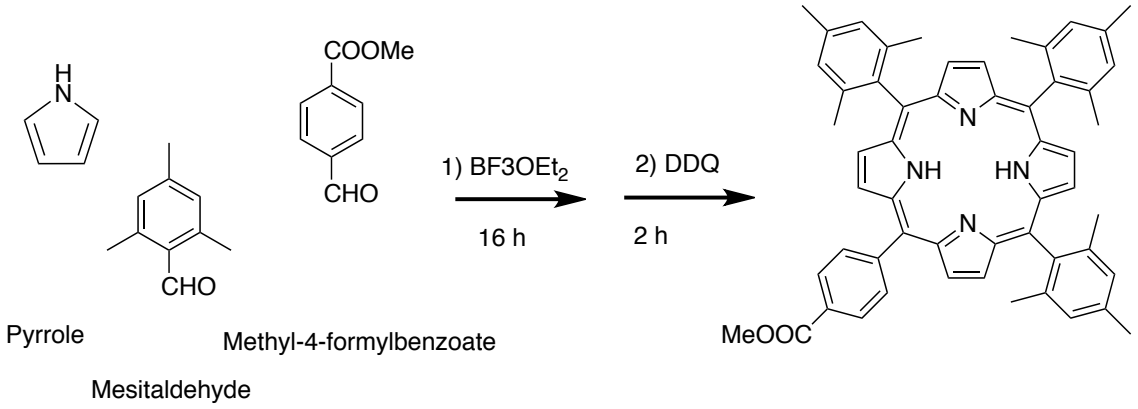

Following a procedure found in literature[30] a mixture of mesitaldehyde (1.0 g, 6.8 mmol) previously filtered on Al_2O_3, methyl-4-formylbenzoate (381 mg, 2.3 mmol), and pyrrole (629 mg, 9.4 mmol) in $CHCl_3$ (1.0 L) was treated with BF_3xOEt_2 (370 μL, 3.0 mmol). The mixture was stirred at room temperature 16 h, then (2,3-dichloro-5,6-dicyano-p-benzoquinone) DDQ (1.50 g, 6.6 mmol) was added and stirring was continued for 2 h. The residue was chromatographed using CHCL3 as eluent obtaining **TMCP1** as a purple solid (353 mg, 0.44 mmol, 5.2%). MALDI-MS 799 m/z $[MH]^+$. ^{1}H-NMR ($CDCl_3$, 300 MHz) 8.72 (q, 4H), 8.66 (s, 4H), 8.39 (d, 2H), 8.30 (d, 2H), 7.30 (s, 6H), 4.14 (s, 3H), 2,65 (s, 9H), 1.88 (m, 18H), -2.55 (s, 2H).

5.9 Synthesis of TMCP

5-(4-Carboxyphenyl)-10,15,20-tris(2,4,6-trimethylphenyl)porphyrin

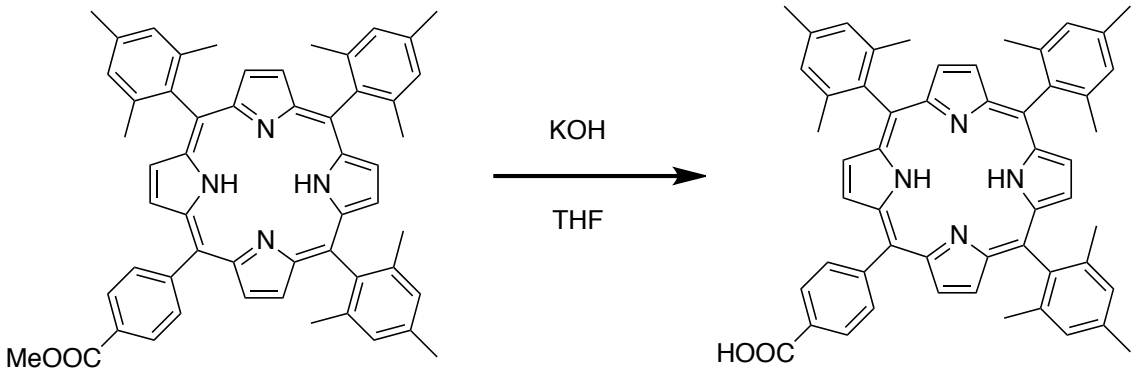

A solution of 5 mL KOH (0.37 g) in H_2O is added to **TMCP1** (91 mg) in 10 mL of THF and stirred at 50°C for 28 h. The mixture was cooled at room temperature and pH was adjusted to 7 adding HCl 3 M. **TMCP** was extracted with CH_2Cl_2, washed with H_2O and dried over Na_2SO_4. Solvent was removed and the product was recrystallized from CH2Cl2/MeOH obtaining 63 mg of **TMCP** (Yeald 70%). MALDI-MS 786 m/z $[MH]^+$. ^{1}H-NMR ($CDCl_3$, 300 MHz) 8.74 (q, 4H), 8.67 (s, 4H), 8.53 (d, 2H), 8.40 (d, 2H), 7.30 (s, 6H), 4.14 (s, 3H), 2,65 (s, 9H), 1.88 (m, 18H), -2.55 (s, 2H).

5.10 Synthesis of ZnTMCP

5-(4-Carboxyphenyl)-10,15,20-tris(2,4,6-trimethylphenyl)porphyrinatozinc(II)

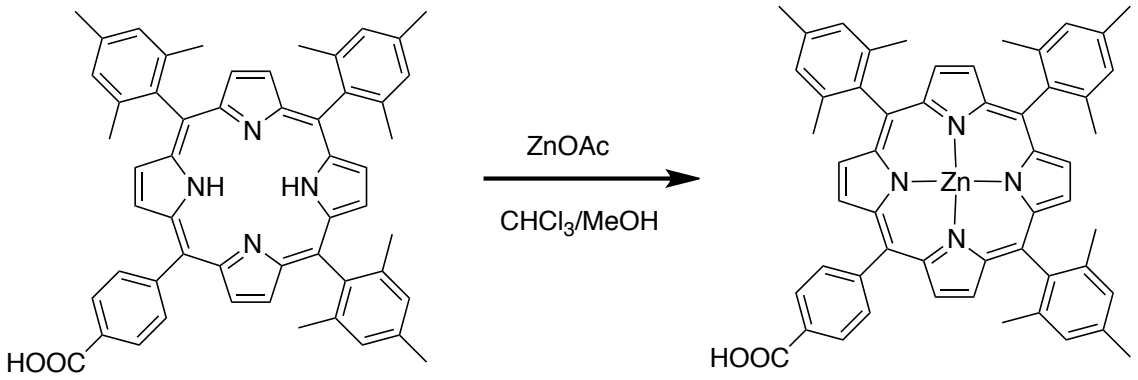

To a solution of **TMCP** (63 mg, 0.081 mmol) in CH_3Cl (10 mL) was added a saturated methanol solution of zinc acetate (4.0 mL) and refluxed 1h. The product is dissolved in CH_2Cl_2 and washed with with water to remove residual zinc acetate. The crude of reaction was dried over Na_2SO_4, filtered and the solvent evaporate, obtaining **ZnTMCP** (53 mg, 0.062 mmol, yeald 75%). MALDI-MS 847 m/z $[MH]^+$. 1H-NMR ($CDCl_3$, 300 MHz) 8.79 (q, 4H), 8.70 (s, 4H), 8.59 (d, 2H), 8.41 (d, 2H), 7.33 (s, 6H), 2.68 (s, 9H), 1.91 (s, 18H)

5.11 Synthesis of TFAT

2-Cyano-3-(5-((4-(diphenylamino)phenyl)ethynyl)thiophen-2-yl)acrylic acid

TFAT has been synthesised by Dott. Marco D'Acunzo in fullfillment of his master thesis, and it has been performed following a literature method. Here below I report a schematic representation of the synthesis:

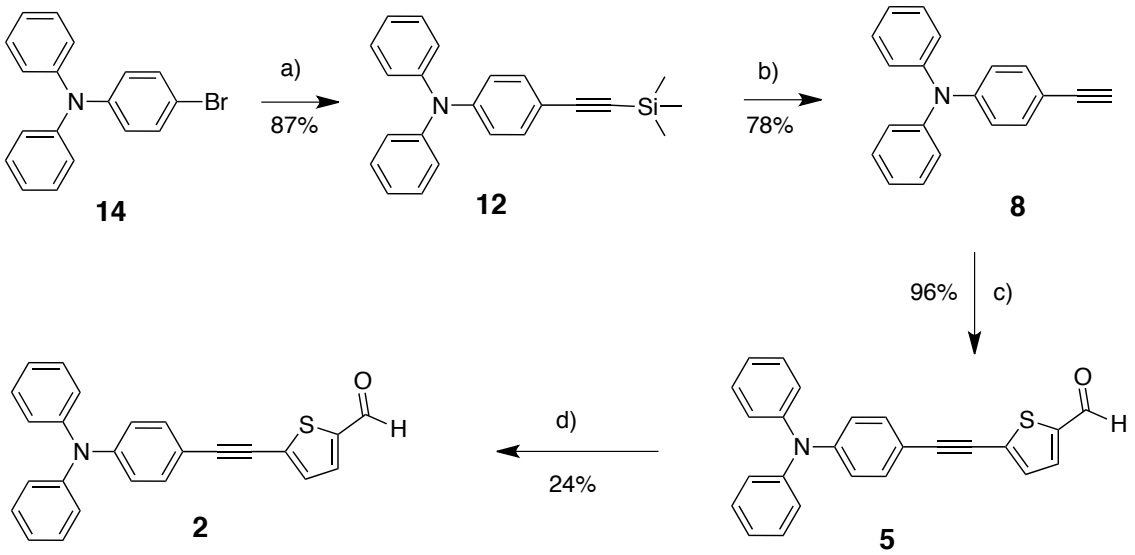

a) 1.5 eq trimetilsililacetilene, 3 %[PdCl2(PPh3)2], 1.6 % PPh3, 1.6 % CuI, NEt3, N2, 90 °C, 6 h b) K2CO3, MeOH, 4 h, t.a.
c) 1.1 eq. 5-bromotiofene-2-carbossaldeide 3 %[PdCl2(PPh3)2], 1.5 % PPh3, 1.5 % CuI, NEt3/ THF, N2, 80 °C, 15h d) acido cianoacetico, piperidina, CH3CN, 3h, riflusso.

Bibliography

1. *BP Statistical Review of World Energy 2014*. 2014.

2. Feldman, D.; Barbose, G.; Margolis, R.; James, T.; Weaver, S.; Darghouth, N.; Fu, R.; Davidson, C.; Booth, S.; Wiser, R., Photovoltaic System Pricing Trends. NREL: 2014.

3. O'Regan, B.; Graetzel, M., A low-cost, high-efficicency solar cell based on dye-sensitized colloidal TiO2 films. *Nature* **1991,** *353*.

4. (a) Law, M.; Greene, L. E.; Johnson, J. C.; Saykally, R.; Yang, P., Nanowire dye-sensitized solar cells. *Nature materials* **2005,** *4*, 5; (b) JuanA.Anta; ElenaGuillén; Tena-Zaera, R., ZnO-Based Dye-Sensitized Solar Cells. *J. Phys. Chem. C* **2012,** *116*, 13; (c) Saarenpää, H.; Sariola-Leikas, E.; Pyymaki Perros, A.; Kontio, J. M.; Efimov, A.; Hayashi, H.; Lipsanen, H.; Imahori, H.; Lemmetyinen, H.; Tkachenko, N. V., Self-Assembled Porphyrins on Modified Zinc Oxide Nanorods: Development of Model Systems for Inorganic–Organic Semiconductor Interface Studies. *The Journal of Physical Chemistry C* **2012,** *116* (3), 2336-2343.

5. Prasittichai, C.; Hupp, J. T., Surface Modification of SnO2 Photoelectrodes in Dye-Sensitized Solar Cells: Significant Improvements in Photovoltage via Al2O3 Atomic Layer Deposition. *J. Phys. Chem. Lett.* **2010,** *1* (10), 5.

6. (a) Hagfeldt, A.; Graetzel, M., Molecular photovoltaic. *Accounts of Chemical Research* **2000,** *33*, 9; (b) Wagner, K.; Griffith, M.; James, M.; Mozer, A.; Wagner, P.; Triani, G.; Officer, D.; Wallace, G., Significant performance improvement of porphyrin-sensitized TiO2 solar cells under white light illumination. *The journal of physical chemistry. C, Nanomaterials and interfaces* **2011,** *115* (1), 317.

7. Ito, S.; Murakami, T. N.; Comte, P.; Liska, P.; Grätzel, C.; Nazeeruddin, M. K.; Grätzel, M., Fabrication of thin film dye sensitized solar cells with solar to electric power conversion efficiency over 10%. *Thin Solid Films* **2008,** *516* (14), 4613-4619.

8. Feldt, S. M.; Wang, G.; Boschloo, G.; Hagfeldt, A., Effects of Driving Forces for Recombination and Regeneration on the Photovoltaic Performance of Dye-Sensitized Solar Cells using Cobalt Polypyridine Redox Couples. *J. Phys. Chem. C* **2011,** *115*, 8.

9. Yella, A.; Lee, H. W.; Tsao, H. N.; Yi, C.; Chandiran, A. K.; Nazeeruddin, M. K.; Diau, E. W. G.; Yeh, C. Y.; Zakeeruddin, S. M.; Gratzel, M., Porphyrin-Sensitized Solar Cells with Cobalt (II/III)-Based Redox Electrolyte Exceed 12 Percent Efficiency. *Science* **2011,** *334* (6056), 629-634.

10. (a) Campbell, W. M.; Burrell, A. K.; Officer, D. L.; Jolley, K. W., Porphyrins as light harvesters in the dye-sensitised TiO2 solar cell. *Coordination Chemistry Reviews* **2004,** *248* (13-14), 1363-1379; (b) Campbell, W. M.; Jolley, K. W.; Wagner, P.; Wagner, K.; Walsh, P. J.; Gordon, K. C.; Schmidt-Mende, L.; Nazeeruddin, M. K.; Wang, Q.; Graetzel, M.; Officer, D. L., Highly Efficient Porphyrin Sensitizers for Dye-Sensitized Solar Cells. *The Journal of Physical Chemistry C* **2007,** *111* (32), 11760-11762.

11. Rawolle, M.; Niedermeier, M. A.; Kaune, G.; Perlich, J.; Lellig, P.; Memesa, M.; Cheng, Y.-J.; Gutmann, J. S.; Müller-Buschbaum, P., Fabrication and characterization of nanostructured titania films with integrated function from inorganic–organic hybrid materials. *Chemical Society Reviews* **2012**.

12. Griffith, M. J.; Sunahara, K.; Wagner, P.; Wagner, K.; Wallace, G. G.; Officer, D. L.; Furube, A.; Katoh, R.; Mori, S.; Mozer, A. J., Porphyrins for dye-sensitised solar cells: new insights into efficiency-determining electron transfer steps. *Chemical Communications* **2012,** *48* (35), 4145-4162.

13. (a) Su, J.-Y.; Tsai, C.-H.; Wang, S.-A.; Huang, T.-W.; Wu, C.-C.; Wong, K.-T., Functionalizing organic dye with cross-linked electrolyte-blocking shell as a new strategy for improving DSSC efficiency. *RSC Adv.* **2012,** *2* (Copyright (C) 2012 American Chemical Society (ACS). All Rights Reserved.), 3722-3728; (b) Gao, F.; Wang, Y.; Shi, D.; Zhang, J.; Wang, M.; Jing, X.; Humphry-Baker, R.; Wang, P.; Zakeeruddin, S. M.; Graetzel, M., Enhance the Optical Absorptivity of Nanocrystalline TiO2 Film with High Molar Extinction Coefficient Ruthenium Sensitizers for High Performance Dye-Sensitized Solar Cells. *J. Am. Chem. Soc.* **2008,** *130*, 9.

14. Allegrucci, A.; Lewcenko, N. A.; Mozer, A. J.; Dennany, L.; Wagner, P.; Officer, D. L.; Sunahara, K.; Mori, S.; Spiccia, L., Improved performance of porphyrin-based

dye sensitized solar cells by phosphinic acid surface treatment. *Energy & Environmental Science* **2009,** *2*.

15. Concina, I.; Frison, E.; Braga, A.; Silvestrini, S.; Maggini, M.; Sberveglieri, G.; Vomiero, A.; Carofiglio, T., On-line monitoring and active control of dye uptake in dye-sensitised solar cells. *Chem. Commun. (Cambridge, U. K.)* **2011,** *47*, 11656-11658.

16. Li, L.-L.; Diau, E. W.-G., Porphyrin-sensitized solar cells. *Chemical Society Reviews* **2013,** *42* (1), 291-304.

17. Wagner, K.; Griffith, M. J.; James, M.; Mozer, A. J.; Wagner, P.; Triani, G.; Officer, D.; Wallace, G. G., Significant Performance Improvement of Porphyrin-Sensitized TiO2 Solar Cells under Illumination. *J. Phys. Chem. C* **2011,** *115*.

18. (a) Grätzel, M.; Ko, J.; Choi, H.; Kang, S. O.; Gao, G.; Kang, H. S.; Kang, M.-S.; Nazeeruddin, M. K., An Efficient Dye-Sensitized Solar Cell with an Organic Sensitizer Encapsulated in a Cyclodextrin Cavity. *Angewandte Chemie International Edition* **2009,** *48* (32), 5938-5941; (b) Toma, S. H.; Bonacin, J. A.; Araki, K.; Toma, H. E., Selective host–guest interactions on mesoporous TiO2 films modified with carboxymethyl-β-cyclodextrin. *Surface Science* **2006,** *600* (19), 4591-4597.

19. Cai, M.; Pan, X.; Liu, W.; Sheng, J.; Fang, X.; Zhang, C.; Huo, Z.; Tian, H.; Xiao, S.; Dai, S., Multiple adsorption of tributyl phosphate molecule at the dyed-TiO2/ electrolyte interface to suppress the charge recombination in dye-sensitized solar cell. *Journal of Materials Chemistry A* **2013,** *1* (15), 4885.

20. Miyashita, M.; Sunahara, K.; Nishikawa, T.; Uemura, Y.; Koumura, N.; Hara, K.; Mori, A.; Abe, T.; Suzuki, E.; Mori, S., Interfacial Electron-Transfer Kinetics in Metal-Free Organic Dye-Sensitized Solar Cells: Combined Effects of Molecular Structure of Dyes and Electrolytes. *J. Am. Chem. Soc.* **2008,** *130*, 8.

21. O'Regan, B.; Xiaoe, L.; Ghaddar, T., Dye adsorption, desorption, and distribution in mesoporous TiO2 films, and its effects on recombination losses in dye sensitized solar cells. *Energy & Environmental Science* **2012,** *5* (5), 7203-7215.

22. Pazoki, M.; Lohse, P. W.; Taghavinia, N.; Hagfeldt, A.; Boschloo, G., The effect of dye coverage on the performance of dye-sensitized solar cells with a cobalt-based electrolyte. *Phys. Chem. Chem. Phys.* **2014,** *16*, 6.

23. Dell'Orto, E.; Raimondo, L.; Sassella, A.; Abbotto, A., Dye-sensitized solar cells: spectroscopic evaluation of dye loading on TiO2. *J. Mater. Chem.* **2012,** *22*, 6.

24. Chou, T. P.; Zhang, Q.; Cao, G., Effects of Dye Loading Conditions on the Energy Conversion Efficiency of ZnO and TiO2 Dye-Sensitized Solar Cells. *J. Phys. Chem. C* **2007,** *111*, 8.

25. Mori, S.; Nagata, M.; Nakahata, Y.; Yasuta, K.; Goto, R.; Kimura, M.; Taya, M., Enhancement of Incident Photon-to-Current Conversion Efficiency for Phthalocyanine-Sensitized Solar Cells by 3D Molecular Structuralization. *J. Am. Chem. Soc.* **2010,** *132*, 3.

26. Freitag, M.; Galoppini, E., Molecular host-guest complexes: Shielding of guests on semiconductors. *Energy & Environmental Science* **2011,** *4*, 13.

27. Szejtli, J., Introduction and General Overview of Cyclodextrin Chemistry. *Chem. Rev.* **1998,** *98*, 11.

28. Saif A. Haque, J. S. P., Mohan Srinivasarao, James R. Durrant, Molecular-Level Insulation: An Approach to Controlling Interfacial Charge Transfer. *Advanced Material* **2004,** *16* (14), 1177-1181.

29. Teng, C.; Yang, X.; Yang, C.; Tian, H.; Li, S.; Wang, X.; Hagfeldt, A.; Sun, L., Influence of Triple Bonds as π-Spacer Units in Metal-Free Organic Dyes for Dye-Sensitized Solar Cells. *J. Phys. Chem. C* **2010,** *114*, 9.

30. Hiroshi Imahori, S. Y., Comparison of Electrode Structures and Photovoltaic Properties of Porphyrin-Sensitized Solar Cells with TiO2 and Nb, Ge, Zr-Added TiO2 Composite Electrodes. *Langmuir* **2006,** *22*, 11405-11411.

31. Carofiglio, T.; Cordioli, M.; Fornasier, R.; Jicsinszky, L.; Tonellato, U., Synthesis of 6-amino-6deoxy-2,3-tetradeca-O-methyl-cyclomaltoheptaose. *Carbohydrate Research* **2004,** *339*.

32. Panda, S.; Panda, G., A new example of a steroid–amino acid hybrid: construction of constrained nine membered D-ring steroids. *Organic & Biomolecular Chemistry* **2007,** *5*, 7.

33. Jiri, Z.; Milos, B.; Tomas, K., Synthesis of Per(5-carboxy-5-dehydroxymethyl)-α- and β-Cyclodextrins - Self-Assembly of the Per(2,3-di-O-methyl)-Protected Homologues into Highly Stable Dimers, Driven by Multiple Hydrogen Bonds. *Eur. J. Org. Chem.* **2000,** *2000* (18).